From DEPARTMENT OF LABORATORY MEDICINE
Karolinska Institutet, Stockholm, Sweden

CARBON NANOTUBES IN NANOMEDICINE

Ramy El-Sayed

Karolinska Institutet

Stockholm 2016

Published by Karolinska Institutet.
Printed by E-PRINT AB

ISBN 978-91-7676-216-5

Karolinska Institutet

Department of Laboratory Medicine
Clinical Research Center

Carbon Nanotubes in Nanomedicine

DOCTORAL DISSERTATION
Thesis for Doctoral Degree (Ph.D.) at Karolinska Institutet publically defended in C1:87 lecture hall, Karolinska University hospital, Huddinge, Sweden.

Friday march 18th, 2016; 09:30

By

Ramy El-Sayed
M.Sc.

Principal Supervisor:
Professor Moustapha Hassan
Karolinska Institutet
Department of Laboratory Medicine
Clinical Research Center

Co-supervisor(s):
Professor Mamoun Muhammed
Royal Institute of Technology
Department of Materials and Nano Physics
Division of Functional Nanomaterials

Dr. Fei Ye
Karolinska Institutet
Department of Laboratory Medicine
Clinical Research Center

Opponent:
Professor Heinrich Hofmann
Ecole Polytechnique Fédérale de Lausanne
Institute of Materials, Powder Technology Laboratory

Examination Board:
Professor Lars Österlund
Uppsala University
Department of Engineering Sciences
Division of Solid State Physics

Professor Sherif Kandil
Alexandria University
Department of Materials Science

Associate Professor Tommy Cedervall
Lund University
Department of Chemistry
Division of Biochemistry and Structural biology

This thesis is dedicated to my parents, brothers & in the loving memory of my grandmother

Aida Al-Mazini (1930-2015)

"***Risk the fall, just to know how it feels to fly***"

DAVE MIRRA

"***The true sign of intelligence is not knowledge but imagination***"

ALBERT EINSTEIN

KEY WORDS

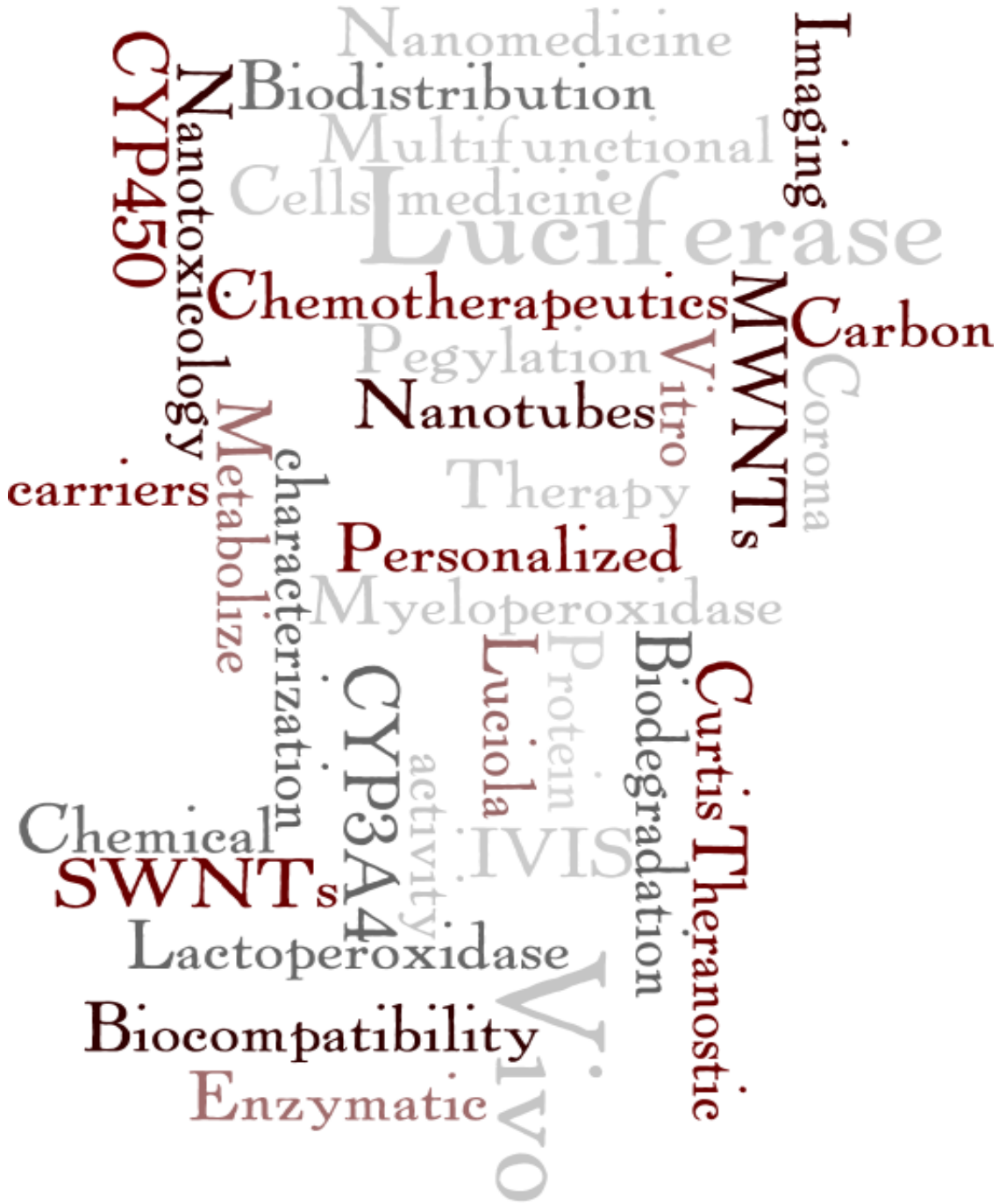

*The graph was created using online word cloud tool (http://wordle.net). It was based on the text content of the thesis.

ABSTRACT

The development of nanomedicine is based primarily on the development of smart and multifunctional nanomaterials that can serve under the different clusters including drug delivery systems, diagnostics, and regenerative medicine. Recently, carbon nanotubes (CNTs) have received enormous attention due to their extraordinary properties. CNTs have a wide range of applications and are used in a variety of products thus exposure to CNTs has become unavoidable, which may prompt an inflammatory response. The present Thesis is focused on studying CNTs especially addressing the key challenges highlighted by the Food and Drug Administration and the Alliance for Nano-Health, including imaging, biodistribution, interaction with biological environment, and predictive modeling.

For imaging in order to evaluate biodistribution we were able, for the first time, to use thermostable Luciferase from Luciola cruciate (LcL) as a qualitative imaging modality. LcL offers an alternative approach for following the biodistribution of CNTs over time. The biodistribution profile of CNTs was found to be similar to the majority of nanoparticles, falling in the same size criteria, and predominantly accumulate in the liver. This raised the question whether CNTs could interfere with the liver functionality explicitly the metabolizing activity of drugs and other xenobiotics by phase I metabolizing enzymes CYP450.

We therefore studied the ability of single wall carbon nanotubes (oxSWNTs) on inhibiting enzymatic capacity of CYP3A4. We found that oxSWNTs inhibit mediated conversion of testosterone (as a model compound), to its major metabolite 6β-hydroxy testosterone in a dose dependent manner. When oxSWNTs is pre-coated with bovine serum albumin, the enzymatic activity of CYP3A4 was restored. Also, the covalent functionalization of oxSWNTs with polyethylene glycol (PEG) has shown to have no influence on the enzymatic activity of CYP3A4. Further understanding of the molecular interactions was obtained by computational modeling and simulations (MD). MD simulations revealed that the inhibition of CYP3A4 catalytic activity is mainly due to blocking of the exit channel for substrate/products through a complex binding mechanism. CYP3A4 is a well-recognized isozyme accountable for the metabolization of various endogenous and exogenous xenobiotics by means of the monooxygenase cycle.

In the Thesis, we also studied the degradation of pristine and oxidized SWNTs (p-SWNTs, oxSWNTs) by CYP3A4, by Raman spectroscopy. We found that both p-SWNTs and oxSWNTs were degraded as evidenced by the increase of D-band, which corresponds to the increase of the structural defects. Surprisingly, CYP3A4 bactosomes were more proficient in degrading p-SWNTs more than oxSWNTs under similar incubation conditions. MD simulations suggested that CYP3A4 has a higher affinity for p-SWNTs (minimal MolDock Score of −186.34 kcal/mol) compared to oxSWNTs which bind in a weaker manner (MolDock Score = −111.47 kcal/mol).

Pulmonary accumulation of CNTs has shown to be critical. We therefore studied the biodegradation of oxSWNTs by Lactoperoxidase (LPO), a secreted peroxidase enzyme present in the mucus of the airways. We also investigated whether pulmonary surfactants can play a role in the biodegradation of oxSWNTs. Biodegradation was monitored using Raman spectroscopy, scanning electron microscopy, and UV–Vis–NIR spectroscopy. The biodegradation of oxSWNTs was not impeded by the formation of protein corona formed in the presence of lung surfactant (Curosurf®). Moreover, cell-free digestion of oxSWNTs was observed *ex vivo* in murine bronchoalveolar lavage fluid in the presence of peroxidase cofactors.

Since CNTs is studied as a theranostic agent, we therefore studied the biodegradation of PEGylated oxSWNTs. PEG is acknowledged as the gold standard for extending blood circulation times for many biological molecules. OxSWNTs functionalized with PEG of different molecular weight (MW) were incubated with myeloperoxidase (MPO). Biodegradation was noted only for oxSWNTs chemically functionalized with PEG. There was no sign of degradation of oxSWNTs with physically adsorbed PEG, nor for p-SWNTs. The extent of oxSWNT biodegradation by MPO was inversely proportional to the molecular weight of the PEG chains. *Ex vivo* biodegradation using isolated primary human neutrophils revealed that both chemically and physically PEGylated oxSWNTs undergo biodegradation independently of the PEG chain MW. These *ex vivo* findings suggest that, in a cell system, a combined process of stripping and biodegradation of PEGylated oxSWNTs might occur.

LIST OF SCIENTIFIC PAPERS

I. **Ramy El-Sayed** , Mohamed Eita , Åsa Barrefelt , Fei Ye , Himanshu Jain , Mona Fares, Arne Lundin , Mikael Crona , Khalid Abu-Salah , Mamoun Muhammed , and Moustapha Hassan, "Thermostable Luciferase from Luciola cruciate for Imaging of Carbon Nanotubes and Carbon Nanotubes Carrying Doxorubicin Using in Vivo Imaging System"
Nano Letters, **2013**, *13* (4), pp 1393–1398

II. **Ramy El-Sayed**, Zonglin Gu, Zaixing Yang, Jeffrey K. Weber, Hu Li, Klaus Leifer, Yichen Zhao, Muhammet S. Toprak, Ruhong Zhou, and Bengt Fadeel, "Single-Walled Carbon Nanotubes Inhibit the Cytochrome P450 Enzyme, CYP3A4"
Accepted Nature Scientific Reports (2016)

III. **Ramy EL-Sayed**, kariem Ezzat, Sergey Shityakov, Birgit Brandner, Mamoun Muhammed, and Moustapha Hassan, "Degredation of pristine and oxidised single wall carbon nanotubes by cytochrome P450; CYP 3A4"
Manuscript

IV. Kunal Bhattacharyaa, **Ramy El-Sayed**, Fernando T. Andóna, Sourav P. Mukherjeea, Joshua Gregoryb, Hu Lid, Yinchen Zhaoe, Wanji Seof, Andrea Fornara, Birgit Brandner, Muhammet S. Toprak, Klaus Leifer, Alexander Star, and Bengt Fadeel "Lactoperoxidase-mediated degradation of single-walled carbon nanotubes in the presence of pulmonary surfactant"
Carbon, **2015**, *91*, pp 506-517

V. Kunal Bhattachary, Cristiano Sacchetti, **Ramy El-Sayed**, Andrea Fornara, Gregg P. Kotchey, James A. Gaugler, Alexander Star,Massimo Bottinib,and Bengt Fadel, "Enzymatic 'stripping' and degradation of PEGylated carbon nanotubes"
Nanoscale, **2014**, *6*, pp 14686-14690

SCIENTIFIC PAPERS NOT INCLUDED IN THE THESIS

I. Kunal Bhattacharya, Fernando Torres Andón, **Ramy El-Sayed**, and Bengt Fadeel, "Mechanisms of carbon nanotube-induced toxicity: Focus on pulmonary inflammation"
Advanced Drug Delivery Reviews **2013**, *65* (15), pp 2087-2097

II. Kariem Ezzat, Eman M. Zaghloul, Samir EL Andaloussi, Taavi Lehto, **Ramy El-Sayed**, Tarek Magdy, C.I. Edvard Smith, and Ülo Langel, " Solid formulation of cell-penetrating peptide nanocomplexes with siRNA and their stability in simulated gastric conditions"
Journal of Controlled Release, **2012**, *162* (1), pp 1-8

III. Robina Shahid, Mikhail Gorlov, **Ramy El-Sayed**, Muhammet S. Toprak, Abhilash Sugunan, Lars Kloo, and Mamoun Muhammed, " Microwave assisted synthesis of ZnS quantum dots using ionic liquids"
Material letters, **2012**, 89, pp 316-319

IV. Mohamed Eita, **Ramy El-Sayed**, and Mamoun Muhammed " Optical properties of thin films of zinc oxide quantum dots and polydimethylsiloxane: UV-blocking and the effect of cross-linking"
Journal of Colloid and Interface Science **2012**, 387 (1), pp135-140

V. Fei Ye*, **Ramy El Sayed***, Ying Zhao, Torkel Brismar, Sergei Popov, Mamoun Muhammed, and Moustapha Hassan "Gold Nanorod/Mesoporous Silica/ Gadolinium oxide Carbonate Hydrate Core/shell Nanoparticles: A multimodal Contrast Agent for MRI/ CT and Fluorescence imaging "
Manuscript
*Equal Contribution

VI. Alaa Mohamed, **Ramy El-Sayed**, Tarek Osman, Muhammed Toprak, Mamoun Muhammed, and Abdusalam Uheida "Composite nanofibers for highly efficient photocatalytic degradation of organic dyes from contaminated water"
Enviromental research **2015**, 145, pp18-25

VII. Heba Asem, Ying Zhao, Fei Yei, Åsa Barrefelt, Manuchehr Abedi-Valugerdi, **Ramy El-Sayed**, Ibrahim El Serafi, Svetlana Pavlova, Jorg.Hamm, Mamoun Muhammed, and Moustapha Hassan" Biodistribution of Busulphan Loaded Biodegradable Nano-carrier Designed for Multimodal Imaging"
submitted toMolecular Pharmaceutics

CONTENTS

LIST OF ABBREVIATIONS

SWNT	Single wall carbon nanotubes
P-SWNT	Pristine single wall carbon nanotubes
OxSWNT	Oxidized carbon nanotubes
C-SWNT	Carboxylated carbon nanotubes
F-SWNT	Covalently functionalized SWNT
A-SWNT	Non-covalent functionalized SWNT
DWNT	Double wall carbon nanotubes
CNTs	Carbon nanotubes
I.V.	Intravenous
I.P.	Intraperitoneal
PL	Phospholipids
PEG	Polyethylene glycol
RES	Reticuloendothelial system
NIR	Near infra-red
TEM	Transmission electron microscopy
SEM	Scanning electron microscopy
FTIR	Fourier transform infrared spectroscopy
EMSA	Electrophoretic mobility shift assay
LcL	Luciola cruciata luciferase
MPO	Myeloperoxidase
ESO	Eosinophil peroxidase
LPO	Lactoperoxidase
DTPA	Diethylene tri-amine pentaacetic acid
BSA	Bovine serum albumin
EDC	1-Ethyl-3-(3-dimethylaminopropyl)carbodiimide
NHS	N-hydroxysuccinimide esters
HPLC	High performance liquid chromatography
BALF	Bronchoalveolar lavage fluid

1 INTRODUCTION

1.1 NANOPARTICLES AND NANOTECHNOLOGY

Nanoparticles are the basic fundamental building units of nanomaterials. The physical, chemical and biological properties of the nanostructured materials differ substantially from their micron and bulk counterparts [1]. The definition of a nanoparticle varies according to specific application. Various organizations for standardization have issued a strict definition [2]. Table 1.1 reviews the different size definitions of nanoparticles. In 2011, the European commission endorsed a broader yet more nominal definition stating that *"a natural, incidental or manufactured material containing particles in an unbound state or as agglomerate or as an aggregate and where for 50% or more of the particles in the number size distribution, one or more external dimensions in the size range 1nm-100nm"[3]*.

International organizations for standardization	***Definition***
❖ Federal institute for occupational safety and health (BAuA)	All the dimensions or diameters are in the nanoscale range
❖ Scientific Committee on Consumer Products (SCCP)	At least one dimension is in the nanoscale range.
❖ National Institute of Occupational Safety and Health (NIOSH)	A particle with diameter between 1 and 100 nm, or a fiber spanning the range 1–100 nm
❖ International Organization for Standardization (ISO)	A material confined in 1 or more dimensions at the nanoscale (ca. 1-100nm)
❖ British Standards Institution (BSI)	All the fields or diameters are in the nanoscale range

Table 1.1 Definitions of nanoparticles by various organizations

Nanoparticles have an astonishingly long antiquity; the earliest evidence belongs to the 4th century so called Lycurgus cup [4]. The extraordinary cup, held by the British museum, contains gold and silver nanoparticles that amend the color of the glass depending on the position of the observer due to the quantum size effect of the nanoparticles [5]. Another amazing discovery was the existence of gold nanoparticles in the stained glass present in the medieval European churches purifying the air and also adding a glimpse of luster to the decoration [6, 7]. Moreover, nearly a decade ago researchers reported that ancient Egyptians utilized lead sulfide nanocrystals as a hair dyeing recipe [8]. With numerous references to

nanoparticle application from ancient times, there is no uncertainty that nanoscience was pioneered centuries ago yet the lack of technology (i.e. electron microscopy) for visualization of such small entities made it impossible to further develop this marvelous technology.

With the invention of transmission electron microscopy in the early 19th century [9], an innovative era was inaugurated, the era of "Nanotechnology". Nanotechnology emerged as an invincible giant changing the course of science in all fields utilizing nanoparticles as building components. Nanotechnology contributed significantly to interdisciplinary fields including medicine, materials, chemical catalysis, and micro-wiring. Given the broad-reaching prospective of nanotechnology, the world acquired a commensurate action in terms of global research and development. It is estimated that the world governments, private sectors and corporates have financed nanotechnology applications with approximately € 0.23 trillion by 2015 [10].

1.2 DEVELOPMENT OF NANOMEDICINE

The idea was originally inspired by Paul Ehrlich, who perceived that the creation of a therapy called "Zauberkugeln" (Magic Bullets) would alter the course of medical treatment; being a great immunologist he had antibodies in mind [11]. The concept was revolutionized in the 1950's to include therapeutic loaded nanoparticles as a potential targeting moiety. Although it seems like a simple approach, it required the adaptation of a new thinking and research methodology to realize the full potential of nanoparticles.

In 2005 the European commission initialized nanomedicine strategic research, which was defined as "*the application of Nanotechnology to Health. It exploits the improved and often novel physical, chemical, and biological properties of materials at the nanometric scale. NanoMedicine has potential impact on the prevention, early and reliable diagnosis and treatment of diseases*" [12]. The field was divided into three main clusters 1) targeted drug delivery, 2) regenerative medicine, 3) diagnosis [13, 14]. To aid the rapid development in any of these biological clusters, multifunctional nanomaterials were demanded.

1.3 MULTIFUNCTIONAL NANOMATERIALS

Multifunctional nanomaterials known also as theranostic agents are a distinctive breed of nanoparticles/materials that perform multiple tasks simultaneously, such as biological imaging, biosensing, drug delivery, targeting special organelles [15], controlled release and dual therapeutic effect. In addition, the nano magnitude of these carriers offers a high surface area-to-volume ratio, permitting high loading capacity of therapeutic drugs.

Theranostic agents can be physically, chemically and morphologically tailored to fulfill the requirements of a predefined application [16].

Several classes of multifunctional nano-carriers have been developed; they can be categorized according to their dimensions as 0D (quantum dots, nanoparticles, nanospheres), 1D (nanorods, nanotubes, nanowires), 2D (nanofilms, nanosheets), or 3D (bulk materials with nanoscale structure, nanocomposites and mesoporous materials) [17]. The chemical nature of the nanomaterials can be also used as a classification category. Figure 1 shows the arsenal of organic, inorganic and hybrid multifunction nanosystems. The most extensively investigated class is the polymeric nanoparticles, predominantly the liposomes subcategory. Some of these theranostic agents have been approved by regulatory authorities and translated to clinical use, while others are still in clinical trials [18]. Some of the theranostic agents that have successfully entered the market are Doxil, Myocet, Abraxane, Endorem, Resovist and ThermoDox.

With basic nanoparticle synthesis becoming a routine and driven by the growing medical need for novel tools, carbon based nanomaterials emerged as a lucrative nanomaterial as they offer a hybrid advantage compared to other nano-carrier classes.

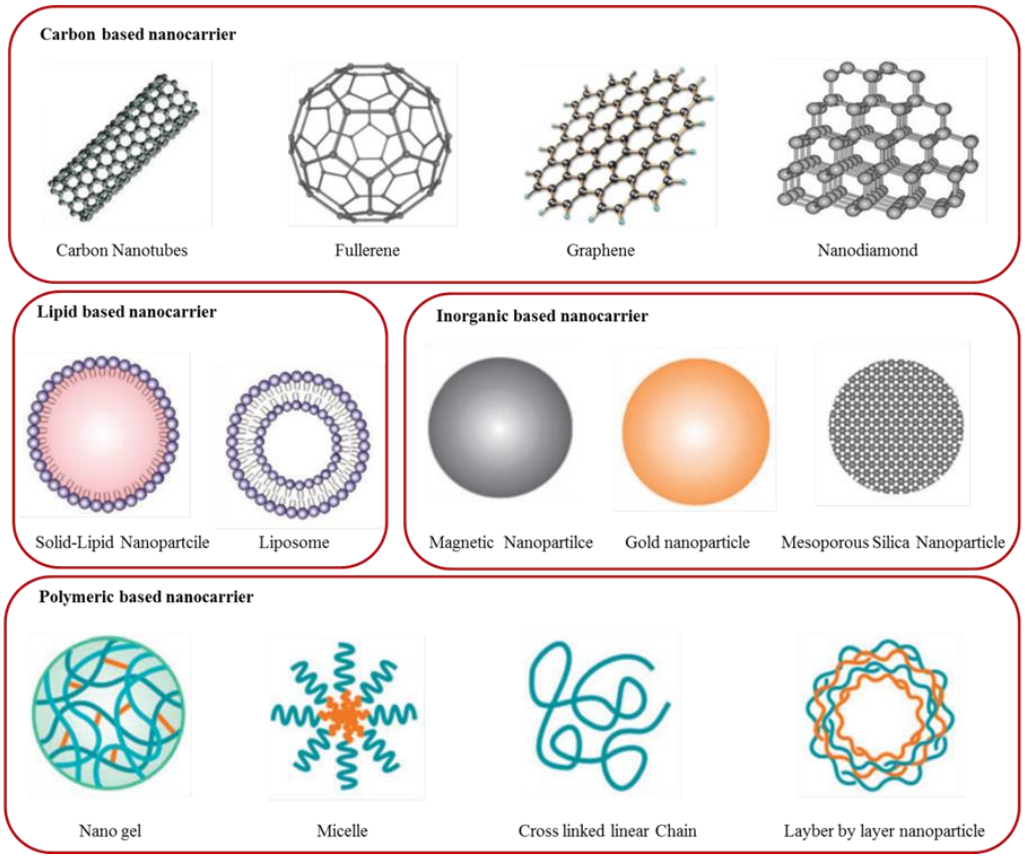

Figure 1. The arsenal of organic, inorganic and hybrid multifunctional drug delivery carriers. Adapted from ref. [19] with permission of The Royal Society of Chemistry.

2 CARBON NANOTUBES

Carbon nanotubes (CNTs) are seamless cylinders of graphene sheets. The ends of the CNTs are concealed by a hemispherical buckyball [20]. Ideally, pristine CNTs (p-CNTs) have all carbons bonded in a hexagonal lattice (sp2 conjugated lattice) [21, 22]. Nevertheless, in reality, pristine mass produced CNTs contain topological defects in their atomic structure (octagon, pentagon, heptagon) [23-25], rehybridization defects depending on the chirality [26, 27], and incomplete bonding [28]. Depending on the number of the graphene sheet layers the CNTs are composed of, CNTs are divided in to single wall (SWNTs) [29], double wall (DWNTs) [30-33], triple wall (TWNTs) [34-37] and multiwall (MWNTs) [38]. Concurrently, the diameter varies from 3 Å for SWNTs [39, 40] up to 200 nm for MWNTs [41].

The commencement of widespread CNT research in the 1990s as an essential contributor to nanotechnology advancement, as well as to fulfill nanotube structure-property relations, demanded the development of controlled mass production of CNTs with desired properties and structure.

2.1 CNTS SYNTHESIS CONCEPT

The building of CNTs requires exquisite control at the atomic level. With such precise atomic structural arrangement, infinite possible chiralities (the chiral angle between the CNT axis and hexagons) can be constructed. There are 3 defined structures known as armchair, zigzag and chiral [42]. Regardless of the simple atomic bonding configuration and chemical composition of CNTs, the different chiralities play a vital role in their biological [43], chemical [44], and physical properties [45-47]. Dependent on the helicity of the structure, SWNTs can be either metals or semiconductors [48-51]. Understanding the nucleation and controlling the growth mechanism to achieve desirable characteristics is a key goal for material scientists [52-54].

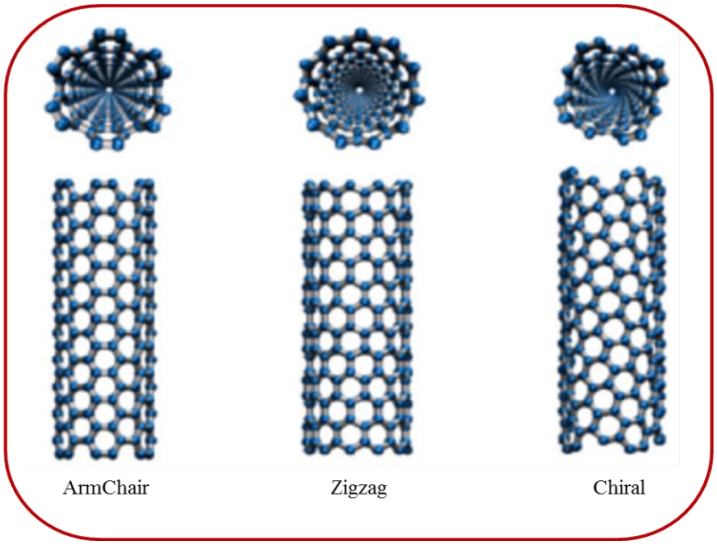

Figure 2. Carbon nanotubes of different structural configurations.

Several techniques have been developed to fabricate CNTs. Chemical vapor deposition (CVD), laser ablation, and arc discharge are the most established methodologies for successful growth based on gas phase processes [53, 55]. Other methods are the electrolysis [56, 57] and sonochemical [58-60]. Among these approaches, CVD is the cheapest, most controllable and highly productive method offering the best control of nanotube diameter, length, alignment and purity [61, 62].

2.2 FUNCTIONALIZATION OF CARBON NANOTUBES

Flawless p-CNTs formed of defect free hexagonally arranged aromatic rings are chemically inert [63]. p-CNTs have a pronounced tendency to agglomerate and are known to be aqua insoluble or have limited solubility in any known solvent. To facilitate the processing and transformation of CNTs to the application phase, functionalization strategies have been introduced. Functionalization stands for creating active functional moieties on the surface of the CNTs. Functionalization categories includes defect-site functionalization, covalent functionalization, and non-covalent functionalization.

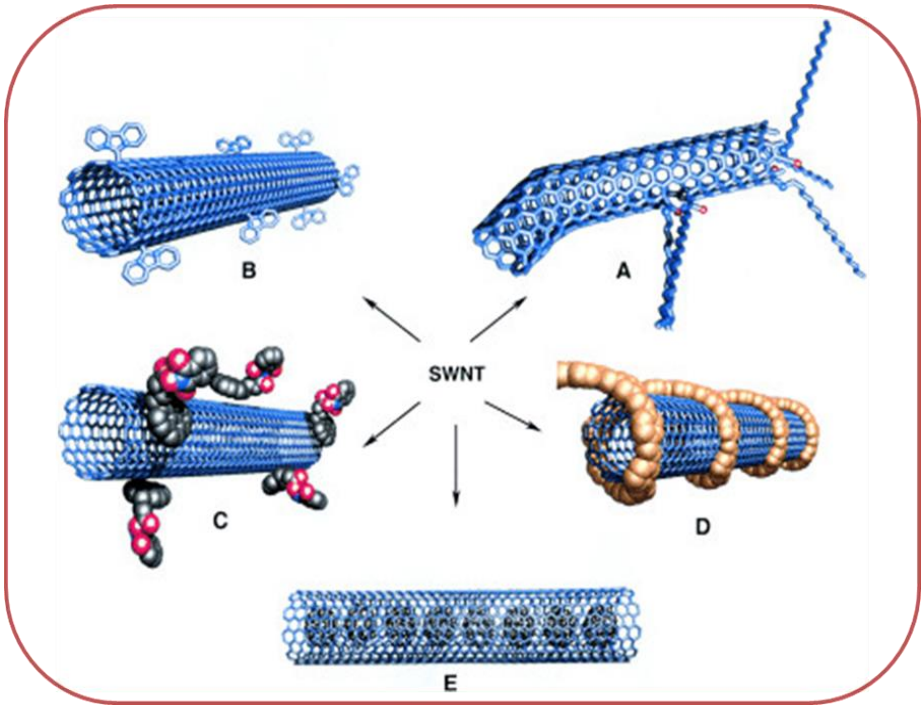

Figure 3. Different functionalization strategies for carbon nanotubes A) defect-site functionalization, B) covalent functionalization, C) non-covalent exohedral functionalization with surfactants, D) non-covalent exohedral functionalization with polymers, and E) endohedral functionalization. Reproduced from ref. [64] with permission from John Wiley and Sons.

2.2.1 Defect site functionalization

The most common functionalization approach is the "*oxidative purification*" of CNTs, which can be achieved through a liquid phase or gas phase [65]. The most utilized oxidative agents are nitric acid, sulfuric acid, hydrogen peroxide, ozone, air or a combination of these phases [65, 66]. Oxidative treatment introduces oxygen bearing groups at the side walls and the end

of the CNTs such as carboxylic, phenolic and lactone. The ratio of oxygen moieties can also be controlled by adjusting the acid/CNT ratios [67-69]. This method also serves as a purification method eliminating the remaining catalyst used for the CNT growth and the amorphous carbon. In addition, oxidative protocols lead to the shortening/cutting of the raw CNT which is vital for some biomedical applications maneuvering through toxicity and biocompatibility [70-72]. The cutting can even result in ultra-short CNTs of ca. 5nm [73, 74]. On the other hand, it is a harsh treatment that leads to the loss of the electronic properties of the CNTs [75, 76].

Oxidative treatments are typically used as a pre-modification since the grafted functional oxygen groups can be exploited to introduce further chemical transformations or entities. Carboxamides can be derived from carboxylic acid groups facilitating decoration with aryl amines, aliphatic amines, and amino acid derivatives [65, 77]. Thiolation is another further transformation that carboxylic groups and hydroxyl groups can adapt [78, 79]. It is also common to use the oxygen functional groups to form ester bonds directly with macromolecules of interest.

2.2.2 Covalent functionalization of CNTs

The chemical reactivity of strained quasi-1D cylindrical aromatic CNTs to covalent addition reactions arises from its geometric topology. Local strain on the sidewalls of CNTs is prompted due to the wall curvature promoting two main factors, 1) π-orbital misalignment between adjacent carbons, and 2) pyramidalization at the carbon atom [80]. From a chemical point of view, it is essential to note that the chemistry of the sidewalls is completely different from the cap chemistry. The caps are composed of a semispherical fullerene with almost a perfect π orbital alignment and the high reactivity arises from the pyramidalization at the carbon atoms [81, 82]. This is not the case with the side walls, where the π orbital misalignment makes a greater contribution to the chemical reactivity [65, 83] .

Addition reactions are by far the most common organic reactions utilized for covalent functionalization. The chemical nature of CNTs comprised of carbon-carbon double bonds (alkenes), or with triple bonds (alkynes) in defected sites facilitates the utilization of addition reactions. Several modes for addition reactions exist including halogenation, chlorination, addition of radicals, addition of nucleophilic carbenes, as well as addition of carbenes or nitrenes [84-87]. It is worth mentioning that there is no method to date that can synthesize a defined nature of chiral tubes, and a discrepancy in reactivity of current CNTs depending on their diameters is expected; a smaller diameter CNT is anticipated to be more reactive [88].

Moreover, it is challenging to gain control over the regio-selectivity of such addition reactions [88].

2.2.3 Non-covalent functionalization of CNTs

Non-covalent functionalization is acknowledged owing to the noninvasive/nondestructive treatment. This mode of converting the hydrophobic characteristic of the CNTs to more hydrophilic ones preserves the chemical and structural nature of the pristine CNTs eradicating any altering in the optical and physicochemical properties. Non-covalent functionalization is a very attractive surface treatment for various applications that demand certain optical or electronic properties [65]. Non-covalent approaches utilize small aromatic molecules, macromolecules (surfactants [89-91] and synthetic or natural polymers [92-94]), or highly charged nanoparticles [95, 96] to adsorb on the surface of the CNT structures to achieve a stable suspension. The physical attachment/anchoring of such molecules is conceivable due to the π-π interactions [97-100], CH–π interactions [101, 102], OH-π interactions [103, 104], cation-π interactions [105-107] , and hydrophobic interactions [108-111].

The efficiency in obtaining high concentrations of CNT suspension is vastly sensitive to the dispersion parameters, like the initial concentrations of CNTs and the chosen dispersant, the composition [112, 113], diameter and the chirality [114] of the initial pristine material, sonication power and sonication time [115] interval. Environmental factors like pH [116] and temperature [117] also affect the quality of the suspension.

From a biological rationale, CNT surface modification is crucial to potential in *in vivo* applications. Different surface functional groups manipulate the surface charge and the surface density, and thus have different biological distribution, response and pharmacology.

2.3 CARBON NANOTUBES IN BIOLOGY AND MEDICINE

2.3.1 Biodistribution profile of pristine and functionalized CNTs

The pharmacokinetics and biodistribution of CNTs rely intensively on the administration route and physicochemical properties such as size, aggregation, shape, surface modification, and chemical compositions. With the pronounced promise CNTs exhibit, biodistribution becomes an imperative question that needs to be examined after systematic administration in an animal model. Various tracking and imaging methods have been applied for determining the biodistribution.

2.3.1.1 Radionuclide and fluorescent tagging-based imaging

McDevitt *et al.* [118] investigated the biodistribution of i.v. and i.p. administered radiolabeled (^{86}Y-DOTA or ^{111}ln-DOTA) SWNTs in mice. These SWNTs were covalently functionalized by 1,3-dipolar cycloaddition to bear amine groups. The PET/CT study showed that the major accumulation organs after 24 hours for both i.p. and i.v. administration were the liver, kidney and spleen and (to a much lesser extent) the bone. Controversially, Singh *et al.* [119] reported that radiolabeled (^{111}In-DTPA) SWNTs and MWNTs functionalized in the same manner showed rapid urinal clearance of the SWNT constructs, with the majority (>95%) cleared out within 3 hours. No uptake in reticuloendothelial organs such as the liver and spleen was observed. Both studies provide clear evidence that SWNTs constructed with such functionalization act like small molecules. They are most likely cleared via active secretion into the tubular lumen and via longitudinal filtration through the renal glomeruli evidenced by the accumulation of SWNT constructs in the renal cortex region where filtration takes place [118]. Similar observations were reported by Gao *et al.* [120] investigating the biodistribution of i.p. injected ^{99m}Tc-labeled acid oxidized MWNTs amended amine terminal through acyl chloride mediated reaction.

Liu *et al.* [121] studied the biodistribution of (^{64}Cu-DOTA) SWNTs surface modified through anchoring PL–PEG-NH_2 by hydrophobic interactions. The results revealed that SWNT constructs were prominently taken up in the liver and spleen after 24 hours (i.p. injection). More remarkable, Liu *et al.* [121] demonstrated that the high molecular weight PEG reduced the tendency of SWNT constructs to undergo RES uptake. RES uptake occurs through identification of phagocytes to the antibody that tags the SWNTs in the plasma. The minimization of antibody tagging enhanced the blood circulation time of the SWNT constructs [122]. These results demonstrate that both kinds of functionalized SWNTs follow a similar pattern for RES uptake compared to that of other nanomaterials with a size of ca.10-100 nm [123]. A similar pattern of RES accumulation was reported for radio tracer labelled MWNTs [124].

Another traditional modality to track the biodistribution of SWNTs is fluorescent tags. Kang *et al.* [125] studied the biodistribution of fluorescent tagged short SWNTs non-covalently functionalized by a chitosan. 3 hours after i.v. injection, the liver was found to have the highest share of accumulation followed by the spleen and kidney.

The radio-labeled and fluorescent tagging method is a convenient way that allows imaging of molecular and cellular events in the living system, offering qualitative and quantitative data.

Radio tracer offers a detection level down to picomolar. However, extreme caution should be taken to evaluate the results as excess free radioisotopes and tags may lead to misinterpretation. Also, radionuclide can be gradually released from the chelating complex, leading to deceptive results. Thus it might not be the ideal strategy for imaging over an extended period of time. To overcome the traditional tracking drawbacks, researchers have investigated the *in vivo* accumulation of functionalized SWNTs relying on their intrinsic properties.

2.3.1.2 SWNTs intrinsic property-based imaging

SWNTs exhibit distinct physical properties, which makes them more appealing for medical applications. Imaging SWNTs with no surface or minimum surface modification gives a vibrant proof regarding the actual biodistribution. Adding an external moiety to facilitate imaging induces chemical alterations to the CNTs and may lead to misleading results.

Liu *et al.* [126] utilized the unusual electronic and phonon properties as a direct long term detection of SWNT surface functionalized by PL–PEG. Another advantage is that Raman signals are stable against photobleaching. The robust Raman scattering showed superior accumulation of SWNT constructs in the liver, spleen, and intestine lysates 3 days post i.v. administration. Raman spectroscopy offers high sensitivity permitting the following of SWNT constructs up for 100 days. The results showed that only small fraction of SWNTs below the renal excretion threshold (ca. 5.5 nm) can be passed as urine, proposing that excretion occurs mainly via the biliary pathway ending up in feces [126, 127].

An intriguing study investigated the biodistribution of pristine SWNTs (p-SWNTs) synthesized to bare ^{13}C as a building unit in the tube structure [128]. The results show distribution to the whole body with major accumulation mainly in the lungs, followed by the spleen and liver. Lung accumulation is predictable due to the long length of the SWNTs (ca. 2-3 µm). It is worth emphasizing that long term accumulation is very different for pristine tubes compared to functionalized ones. p-SWNTs were not cleared by either the biliary pathway or renal excretion and remained in a high concentration 28 days after i.p. injection [128]. Consistent results were demonstrated by Faraj *et al.* [129] who reported the biodistribution of purified and raw p-SWNTs in a rat model using ^{3}He and ^{1}H magnetic resonance imaging by means of the metal catalyst impurities. This study concluded that ^{1}H MRI allowed detection of intravenously injected p-SWNTs, and that hyperpolarized ^{3}He can be used for the investigation of CNT pulmonary biodistribution.

Another intrinsic property is that individual SWNTs have small band gaps on the order of ~1 eV. The small band gaps permit monitoring through their NIR photoluminescence (900-1600 nm) which has high optical transparency of biological tissue, least interference from biological media and inherently low auto-fluorescence from tissue. Cherukuri *et al.* [130] showed that copolymer Pluronic F108-coated SWNTs accumulate in the liver mainly after jugular vein administration. The limitation of imaging by means of NIR fluorescence is that it only permits short time tracing of semiconductor SWNTs that maintain its electronic integrity [131]. Moreover, preparation of p-SWNTs by surfactants or polymers affects the quantum efficiency; thus quantitative data is hard to obtain [132]. Another drawback is that quantitative data is difficult to obtain using NIR fluorescence technique [133].

In summary, the different biodistribution studies of SWNTs functionalized by different methods show no organ specific affinity, which can be considered an advantage for the development of targeted complexes, because there is no distinctive tissue affinity to overcome.

2.3.2 Carbon nanotubes as therapeutic delivery carriers

2.3.2.1 Anti-cancer therapeutics delivery by CNTs

Regardless of the numerous advancements in the field of cancer therapeutics, there are still many barriers to conventional administration. The major hurdles are tissue selectivity by the treatment, poor distribution of the drug among cells, limited solubility of the therapeutic molecule, high interstitial fluid pressure and target resistance to the therapeutic drug in multidrug resistant cancers [134-136].

CNTs compared to other multifunctional nanocarriers possess many thrilling features that make them a potential candidate to overcoming the challenges of nanotechnology in cancer treatment. CNTs can cross the cellular membrane through multiple pathways: 1) energy dependent mechanisms, 2) energy independent mechanisms, or 3) direct translocation independent of method of functionalization of CNTs. Al-Jamal *et al.* [137] studied both phagocytic and non-phagocytic cell uptake of amine functionalized MWNTs by means of 3D electron tomography, showing that cellular translocation occurs through membrane wrapping, direct membrane translocation, and within vesicular compartments. Kostarelos and colleagues [138-140] showed that even under endocytosis inhibiting conditions, other mechanisms contributed to the intracellular trafficking of SWNTs and MWNTs if surface modified with various strategies. In addition, the needle shape of CNTs facilitates drug molecule intercellular accumulation in cells via transmembrane penetration independent of

method of functionalization of CNTs [138, 141-143]. Cellular trafficking for SWNTs depends on the size of nanotube, cell type and degree of bundling [144]. Changing the cellular translocation for small molecules from passive diffusion to endocytic mechanism offers an alternative strategy to overcoming cell resistance to the chemotherapeutic agent. The oxidized SWNTs (oxSWNTs) loaded with doxorubicin boosted cellular uptake by 23 fold and showed cytotoxicity against MDR P-glycoprotein overexpressing K562 human leukemia cells compared to free doxorubicin [145]. Another stimulating benefit of utilizing CNTs is their ability to accumulate at tumor sites through enhanced permeability and retention effect. The poorly formed structure of the lymphatic and tumor vasculature rapidly proliferating in tumor sites enable passive targeting of CNTs loaded with chemotherapeutic agents [146, 147]. Furthermore, CNTs offer a high aspect ratio and surface areas displaying a unique aptitude for multiple drugs with high loading capacity.

2.3.2.2 Delivery of small-molecule drugs by CNTs

Different categories of anticancer agents have been exploited as cargo for CNTs including topoisomerase I inhibitors (10-hydroxycamptothecin [148], camptothecin [149, 150], irinotecan [151]), topoisomerase II inhibitors (Etoposide [152]), Anthracyclines (doxorubicin [153-157], epirubicin [158], daunorubicin [159], pirarubicin [160], mitoxantrone [161]) platinum-based drugs (cisplatin [162, 163], platinum (IV) prodrug [164, 165], antifolates (Methotrexate [166, 167]), pyrimidine/purine antagonists (gemcitabine [168, 169], difluorodeoxycytidine [170]) and antimicrotubules (taxoid [171], docetaxel [172], paclitaxel [173, 174]). The aforementioned agents have been anchored to the side walls of the CNTs by means of covalent and non-covalent strategies as well as drug loading in the interior core of CNTs. The most studied agent is doxorubicin. Liu *et al.* [153] showed that exploiting the flat aromatic tetracyclic structure of doxorubicin facilitated strong π–π and hydrophobic interactions with the aromatic surfaces of CNTs reaching an ultrahigh loading capacity of around 400%. Furthermore, Wu *et al.* [175] showed that CNTs loaded with cytotoxic agents deliver comparable clinical efficacy at a 100-fold lower concentration compared to exogenous treatment.

2.3.2.3 Generic-material delivery by CNTs

Cancer gene therapy emerged as a promising method for treatment as an alternative approach to traditional chemotherapeutic agents [176]. Gene therapy is about the transfer of nucleic acids; most commonly plasmid siRNA, DNA, oligonucleotides and aptamers. Unlike small drug molecules that translocate to the cells by passive diffusion, biomacromolecules can hardly cross the cell membrane. These generic materials bypass the cellular barrier of

malignant cells by means of vectors. Genetic cargo facilitates cell death, immunomodulation or enforcing genetic corrections [177]. Nanocarriers have been introduced as vectors to overcome the hitches of viral vectors ranging from low transduction efficacy, low loading efficiency to possible host toxicity [177].

CNTs offered a new opportunity and the fact that the chemical nature of the CNT walls can be functionalized endorsed them as ideal candidates for the delivery of nucleic acids [178]. Surface modified CNTs have demonstrated improvement in the transfection efficiency of plasmid DNA [143, 179-181], oligonucleotides [182, 183], siRNA [184-187], miRNA [188] and aptamers [189, 190]. It is worth mentioning that not only cationic or anionic surface modified CNTs were applicable to generic material delivery, but also siRNA loaded pristine SWNTs showed a promise in suppressing tumor growth and minimal toxicity [191]. Nucleic acids and aromatic nucleobases interact with CNT aromatic walls through π-π stacking interactions, permitting the generic material to form a wrap-like structure exposing the phosphate and sugar groups, thus improving the colloidal stability of CNTs [192]. DNA in particular has a curvature that matches the tube morphology, facilitating maximal binding affinity [193, 194].

2.3.3 Stimuli-responsive CNT-based drug delivery systems

Environmentally sensitive drug delivery systems were introduced as smart structures that deploy the therapeutic cargo utilizing specific factors that are explicit in the unhealthy tissue. This concept was later realized to also serve in regulating the release behavior of single or multiple payloads in case of cocktail therapy. The controlled release prompts a higher synergistic effect with reduced side effects. With a prominent loading capacity of CNTs and to eliminate premature release in case of physical packing, the development of smart vesicles was further acknowledged.

Several CNT-based smart systems have been designed to initiate and manipulate cargo release based on abnormalities in physiological/environmental conditions. Several studies designed CNT systems in response to either endogenous factors (pH [151-153, 195-199], enzymatic [148, 157, 166, 200], redox gradients [162, 164, 165, 171], and temperature [201]) or exogenous factors (electric [202-204], electromagnetic radiation [145, 205-207], magnetic [175] and ultrasound [170]).

2.3.4 Active targeting of CNTs

To further augment the efficacy of CNTs as drug delivery vehicles, CNTs can be coupled with targeting moieties providing selectivity to malignant cells while minimizing the toxic

effect of therapeutic molecules on healthy tissue. Selecting the targeting (antibody or non-antibody) ligand is governed by the receptor expression, binding affinity and ligand density on the surface of CNTs.

Several CNT systems have utilized monoclonal antibodies or antibody fragments as targeting ligands. Various studies explored different receptors in ligand-receptor targeting, such as tyrosine kinase-7 [159], biotin receptors [171], HER-2 [208] , B-lymphocyte antigen CD20 [209], carcinoembryonic antigen [210], p-glycoprotein [145], lipoprotein receptor [211], transferrin [198], epidermal growth factor receptor [152, 163], folate receptor [169, 212], Integrin $\alpha_v\beta_3$ [153], hyaluronate receptor [156], lectin receptors [213] and nuclear receptor [214]. Although targeting is considered a major advancement in the field, only a few receptors have been shown to be effective for targeting. Active targeting is a complex approach where various parameters play a role, such as the binding chemistry, the Spacer arm length and physiological factors such as protein binding.

2.3.5 Thermal ablation by means of the intrinsic properties of CNTs

In addition to conveying multiple therapeutic loads to selected tissue, CNTs offer a dual therapy opportunity compared to other multifunctional drug delivery systems. The confinement of carbon atoms in nanometer sized volumes enhances electromagnetic energy absorption, thereby generating heat [215]. That unique intrinsic property can be explained in terms of the electronic transition for the first or second Van Hove singularities that result in strong optical absorbance [45]. The movement of the Van Hove-like singularity in the density of states toward the top of the valence band augments the effective density of states near the Fermi energy and enhances the electron-phonon interaction, increasing the temperature of the nanotubes [216]. In addition, CNTs are ballistic in term of thermal conductivity [217].

Both SWNTs and MWNTs have shown good promise as photothermal agents for hyperthermia. However, MWNTs have more advantages as they are activated by a broader band width of electromagnetic radiation, and more proficient in absorption of electromagnetic energy. The abolishing capacity of tubes is restricted to the cells present in the heating radial distance of the tube; therefore, MWNTs can offer better breach to cells [218]. The mode of cell death can be attuned to necrosis or apoptosis, dependent on the temperature chosen for ablation. In case of apoptosis or heat-controlled necrosis, the thermal effect triggers the activation of heat shock proteins such as the Bcl-2 family proteins [219, 220]. Ghosh *et al.* [221] showed that encapsulating MWNTs with DNA

enhanced heat emission subject to the NIR irradiation. This also endorsed a 3 fold reduction of the original MWNT concentration required to escalate 10°C in suspension.

In the advancement of ablation capacity, it is known that CNTs behave as classical dipole antennas, and the most efficient CNT agents are the tubes longer than half of the wavelength of the incident light [215]. In a study published by Torti and colleagues [218], they investigated the length effect of nitrogen doped MWNTs (N-MWNTs). They showed that N-MWNTs 700 nm and 1100 nm long showed significant cytotoxicity and cell death compared to 300 nm tubes when exposed to NIR. Moreover, the existence of structural defects in the carbon lattice caused by nitrogen dopant across the tube longitudinal axis showed an enhanced efficiency for cell destruction.

Burke *et al.* [222] showed that at 100 μg dose of MWNTs injected intratumorally, there is efficient thermal ablation of kidney cancer both *in vitro* and *in vivo*. In addition to tumor regression after a single 30 second treatment at 3 W/cm^2, they also report no tumor recurrence for ca. 3 months in 80% of the mouse population. Wang *et al.* [223] showed complete abolishment of glioblastoma xenografts targeted by antibody modified SWNTs before subcutaneous implantation. Zhou *et al.* [224, 225] showed that upon cellular uptake of PEGylated SWNTs, there was a localization in the mitochondria. The mitochondrial uptake is explained in terms of the existence of electric potential which is much higher for malignant cells compared to normal tissue. This was further interpolated as a selective mitochondrial destruction in cancerous cell after NIR stimulation. Levi *et al.* [215] showed that 10 seconds of exposure to NIR radiation leads to thermal ablation efficacy compared to those incubated with antineoplastic agents. Levi *et al.* also introduced an additional potential of NIR irradiation to act as an assisting therapy by enhancing cell permeability for treatment by chemotherapeutic agents afterward.

In a noteworthy step in the development of state-of-the-art photothermal agents, Robinson *et al.* [226] administered PEGylated SWNTs (ca. 140 nm in length) i.v. in the tail of mice bearing 4T1 murine breast tumors. The tubes accumulated in the tumor site through the enhanced permeability effect in 3 days. Subsequent to the NIR irradiation, full tumor ablation was witnessed. No tumor reoccurrence was noticed for 6 months. The study also highlighted that SWNTs are much more efficient hyperthermia agents than Au nanorods. Another intriguing study by Antaris *et al.* [227] successfully administered isolated (6,5) SWNTs i.v.. They showed that SWNT constructs accumulated in 4T1 tumor xenografts, at a very low administered dose of ~4 μg, and showed high thermal increase at the tumor site.

Similar studies investigated the surface modification chemistry of SWNTs to increase tumor accumulation and obtained similar results [228].

Gannon *et al.* [229] reported hyperthermia induction by means of radiofrequency (RF) radiation. They studied the RF ablation effects of non-covalent functionalized SWNTs injected intratumorally in rabbits bearing hepatic VX2 tumors. The study demonstrated complete tumor necrosis 48 hours post injection. The treatment was selective, noninvasive and showed concentration-dependent thermal destruction. Although RF has better tissue penetration that NIR, the study highlighted that RF treatment causes damage to surrounding normal cells and incomplete thermal ablation of malignant cells.

2.3.6 Photoacoustic abolition by means of the intrinsic properties of CNTs

A unique approach was introduced by Kang *et al.* [230] employing the photoacoustic effect of SWNTs surpassing the RF and NIR thermal therapeutic efficiency. In comparison to photothermal therapy that uses long time continuous laser irradiation with a power density of 0.5-3 W/cm^2, photoacoustic treatment requires only millisecond pulsed laser exposing the cells to 200 mW/cm^2. The rapid heat deposition and nonlinear thermal expansion generates a shock wave taking the shape of a bubble that causes the cell to explode [231, 232]. It is worth mentioning that this cell burst will lead to the release of cell content to the surrounding tissue, and it might be engulfed by neighboring cells by phagocytosis, increasing tumor reoccurrence probability.

The use of hyperthermia and photoacoustics to eradicate tumors is a thriving acknowledged application of CNTs in oncology. The transfer of such methodology to a clinical setting requires extensive exploration and optimization in irradiation parameters to provide localized heating by controlling the spatial and temporal distribution of heat [233-235]. It is also worth mentioning that the success of such treatment is not only dependent on the physiochemical characteristics of the CNTs but also upon the structural and chemical environment in the tumor and the delivery strategy to the tumor [236].

2.3.7 Carbon nanotube stealth strategies

Following the administration of CNTs as therapeutic nano-carriers, various cells of the immune system are activated. The immune cells recognize foreign CNT constructs as pathogens that must be excreted or digested to more tolerable forms [237]. As a drug delivery device or therapeutic moiety, a sufficient time window must be secured to facilitate reaching the target site. The CNT smart systems need to be retained in the blood circulation, avoiding opsonins binding/tagging. For that, CNT stealth strategies have been

developed to limit the phagocytosis by the mononuclear phagocyte system and increasing the systemic circulation time from minutes to hours or even days [238]. As deliberated in earlier biodistribution context, all forms of engineered CNT constructs show high accumulation in the liver and spleen. To improve the bioavailability and to deceive the immune system, several stealth sheltering ligands such as polysaccharides and polyvinyl-alcohol have been introduced.

In drug delivery systems, polyethylene glycol (PEG) and PEG derivatives are known to be the golden standard imparting stealth characteristics [239]. In addition, PEG is nontoxic and FDA approved for human clinical use, which reduces the complexity when considering clinical transfer for such smart delivery systems. PEG is comprised of a chemically inert polyether backbone with flanges of hydroxyl functional groups. The hydroxyl terminal can be altered to bind another functional group of interest or can be used directly for conjugation with other entities including imaging, targeting, therapeutic or further surface modification [238]. PEGylation of CNTs can be engrafted through chemical conjugation and, in the case of amphiphilic PEG derivatives, physical surface adsorption can be an alternative modification strategy. PEG endures spatial conformations inducing steric hindrance, preventing opsonization of the CNTs. This was explained as hydrogen bonding being established between the water molecules and the oxygen present in the PEG chains, forming a hydrated cloud that resists plasma protein interaction [239]. Jeon *et al.* [240, 241] showed through a mathematical model that long chain and high surface densities are desirable to induce steric repulsion upon the compression of PEG layers induced by the protein diffusion. The effect of van der Waals attraction between the hydrophobic surface of the nanoparticle and the plasma proteins was also studied and found to be negligible compared to the steric repulsion. Another motive for a thicker PEG layer is to overcome the van der Waals attraction, which is strong below 100 Å [242].Yamaoka and colleagues [243] demonstrated experimentally that the increase of PEG molecular weight from 6k to 190k increased the halftime of nanoparticles in circulation from 18 min to 24 hours. In addition to increased retention time, pharmacokinetic studies showed that PEG molecular weight is a vital parameter when the nano-constructs translocate from circulation to extravascular tissue. It is also important to mention that beside molecular weight, PEG structural conformations (branched or linear) play a dynamic role in effective stealth and avoiding undesirable binding.

Yang *et al.* [244] reported that covalent attachment of SWNTs with PEG is much more effective than the physical adsorption of PEG derivatives of the same molecular weight as it

increases blood retention time (ca. 15 hours) and reduces hepatic uptake. Robinson *et al.* [245] investigated the use of a PEG derivative consisting of poly(maleic anhydride-alt-1-octadecene) as a hydrophobic ligand for physical modification of SWNTs. His results showed an enormous increase in blood circulation time of the SWNT constructs - up to 30 hours. Moreover, a lower hepatic uptake and tumor accumulation was noticed upon surface modification with the PEG derivative.

2.3.7.1 Parameters affecting stealth

Another consideration to be taken into account to obtain a high stealth efficiency is the physicochemical nature of the CNTs. Sund *et al.* [246] showed that SWNTs bind less cellular protein compared to spherical nanoparticles, detailing that the high radius of curvature of SWNTs is not thermodynamically favorable for binding plasma proteins. Several research groups have experimentally demonstrated that having an extremely high radius of curvature might lead to high impediment of uptake [247], and this was confirmed by defined mathematical models [248]. In addition, the agglomeration geometry or shape in terms of bundle diameter or size plays a role in how the CNT is recognized by the opsonins [249]. Shape effect on stealth is a more complex issue, because even though the tubes can be a target for plasma proteins they are yet not successfully phagocytosed. The shape governs the point of initial contact angle with the cellular membrane; an angle > 45^{o} will not initiate cellular uptake [249]. Shi *et al.* [250] demonstrated that cellular uptake of nano-tubular structure arises from the tip contact point.

CNT surface charge plays a vital role in escaping the innate immune system. In a recent study, Fleischer *et al.* [251] show that surface charge does not define the selection of adsorbed proteins, yet it primes the same protein to different binding status conformations on the nanoparticle surface. However, the different structural conformations influence the CNT stealth efficiency and the cellular uptake mechanism [138]. Another valuable factor to consider when designing stealth approach is the surface lipophilicity. The more hydrophobic the nature of the CNTs, the more they are vulnerable to plasma protein binding [252] which in turn affects the tissue distribution and excretion profile. The criteria for stealth design should be compromised to adapt the increased blood retention while still maintaining the hydrophobic nature to carry out drug loading or other required functionalities.

2.4 NANOTOXICOLOGY: TOXICITY ASSESSMENT OF CARBON NANOTUBES

Nanotoxicology is the study of the adverse effects of nanomaterials on living organisms [253, 254]. Nanomaterials render a different toxicity profile compared to bulk material. With the prompt increase of CNT production for various nanotechnology applications, it became necessary to study how this class of fibers will interact with humans. Safety assessment of CNTs for nanotechnology and nanomedicine has gained a lot of attention [255, 256]. In studies of CNT toxicity, there are conflicting reports concerning exposure of CNTs to different cell lines. The inconsistency of these findings may be explained in terms of the intrinsic properties of the CNT itself.

2.4.1 CNT Toxicity derived from physico-chemical characteristics

2.4.1.1 Length & shape of CNTs

Due to the morphological similarities with asbestos, the scientific community questioned if CNTs should own additional hazardous effects compared to compact shape nanoparticles [257-259]. The hypothesis was semi-acknowledged by the research conducted by Sato *et al.* [260], who revealed that 220 nm long MWNTs injected subcutaneously showed slight inflammatory responses such as degeneration, necrosis, or neutrophil infiltration compared to 825 nm long MWNTs. A similar study by Poland *et al.* [261] showed that only long needle shapes of MWNTs (i.e. longer than about 15 μm) administered intraperitoneally showed similar mesothelial inflammogenicity to that of asbestos. However, they also showed that short and tangled MWNTs did not induce any pathogenic effect. Both studies [261, 262] pinpoint that long tubes might induce proinflammatory conditions due to the frustrated phagocytosis hindering CNT clearance. Yamashita *et al.* [262] highlighted that long MWNTs induce DNA damage compared to smaller ones. Other studies also reported that a long needle shape activates NLRP3 cascade secreting cytokine, i.e. IL-1R and IL-1β [263]

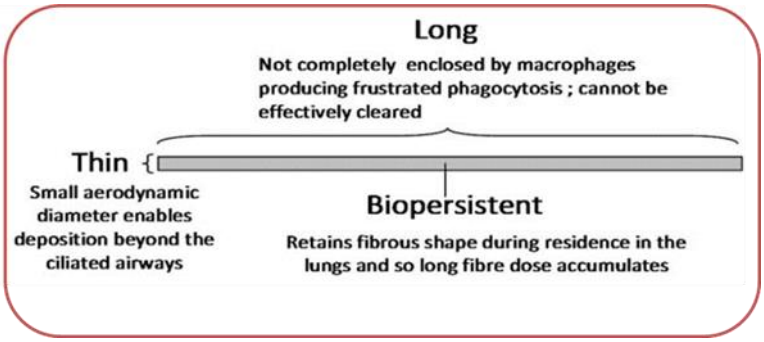

Figure 4. The role of carbon nanotube physical characterization in pathogenicity. Reproduced from ref. [259] with permission from BioMed Central.

2.4.1.2 Agglomeration of CNTs

The aggregation state of CNTs affects the shape and the surface area available for molecular interaction [264]. Belyanskaya and coworkers [265] investigated the influence of SWNTs with different degrees of agglomeration on primary cell cultures. They showed that large agglomerations decrease the DNA content in the cells compared to better dispersed SWNT bundles. Another interesting observation reported by Wick *et al.* [266] is that big agglomerations induced a higher pathogenic effect than asbestos fibers at the same concentrations in primary cell cultures. A similar observation was reported by Murray *et al.* [264] showing that collagen deposition and granulomatous lesions were linked to SWNT agglomerates while no granulomas were associated with exposure to asbestos. Moreover, SWNTs showed a signature of oxidative stress evidenced by accumulations of carbonylated and 4-HNE proteins [264]. Murray and colleagues [264] introduced a novel perspective of how CNT dose should be presented, showing that effective surface area along with mass dose is by far more important than specific surface area or particle number in influencing the toxicological responses.

2.4.1.3 Number of CNT layers and layer rigidity

The number of graphitic layers in the tube has been shown to play a prominent role in activating proinflammatory cascades and showing signs of necrosis, apoptosis or degeneration. Jia *et al.* [267] showed that SWNTs hindered phagocytosis of alveolar macrophages at a low dose of 0.38 mg/cm^2 compared to MWNTs that showed similar toxicity but at a higher dose of 3.06 mg/cm^2. Muller and colleagues [268] demonstrated that MWNTs (< 1 μm in length) injected i.p. in Wistar rats displayed no carcinogenic response after 24 months.

Nagai *et al.* [269] showed that highly crystalline thin MWNTs (ca. 50 nm in diameter) were more efficient in mesothelial piercing of cell membranes than highly crystalline thicker MWNTs (ca. 150 nm). More importantly, they report that mesothelioma was induced by a similar mechanism of asbestos, which is deletion of Cdkn2a/2b tumor suppressor genes.

2.4.1.4 Catalytic impurities derived toxicity

The inconsistency of available toxicity data can be elucidated in terms of the selected transient metal catalyst used during the manufacturing process. Metal catalyst containments such as Co, Mo, Fe, Ni [270] are usually present in the nanomaterials even after applying rigorous purification techniques. The residual metal catalyst is usually protected by a

graphitic sheath or located in the tube channel [271]. Transient metal residues influence the toxicity and biocompatibility of CNTs.

Pulskamp *et al.* [272] showed that there is a proportional relationship between the amount of metal contaminants and the toxicity profile. A higher metal residue leads to increased intracellular reactive oxygen species and reduced mitochondrial membrane potential. Kagan *et al.* [273] showed that metal contaminants alter the redox responses of macrophages. They showed that Fe-rich SWNTs lead to a significant reduction of intracellular glutathione and increased accumulation of lipid hydroperoxides in both PMA and zymosan stimulated RAW 264.7 macrophages. An interesting observation was noted by Guo *et al.* [274] , demonstrating that sample aging introduces a dramatic variation in Fe oxidation over the course of 1 year of atmospheric exposure due to progressive oxidation.

2.5 BIODEGRADATION OF CARBON NANOTUBES

Application of CNTs as a therapeutic nano-carrier was acknowledged with biodegradation findings. Allen *et al.* [275] reported the first study showing that SWNTs can be biodegraded through natural enzymatic catalysis. They showed that horseradish peroxidase is able to degrade oxSWNTs in the presence of low hydrogen peroxide concentrations (ca. 40 μM) at static conditions. Horseradish peroxidase is a monomeric enzyme that contains a noncovalent bound ferriprotoporphyrin IX prosthetic heme group as an active site attached to the enzyme at the proximal histidine residue. The heme center is converted into a porphyrin π cation radical (Compound I) and an oxo-ferryl iron via a protein-assisted mechanism upon reaction with hydrogen peroxide [276]. Getting a deeper insight into how horseradish peroxidase degrades only oxSWNTs, Star and colleagues [277] reported a mechanistic study including molecular docking modelling. They raised several hypotheses on why p-SWNTs are not susceptible to enzymatic degradation which include 1) the intrinsic hydrophobic nature of the CNTs lead to aggregations and bundle formation that further leads to sedimentation and loss of suspension stability and thus no enzymatic interaction; 2) the presence of oxygen bearing negatively charged groups presented on the CNT surface enhances the interaction with enzymes through electrostatic interaction with positively charged residues. Through molecular modelling, they suggested that chemically oxidized SWNTs are oriented toward a positively charged arginine residue (Arg178) which acts as a binding stabilizer [277]. Molecular docking data showed that oxSWNTs are in 5Å distance to residues that are vital for catalysis of oxidation reaction, while p-SWNTs interact at the distal end of the enzyme placing it opposite from the heme moiety [275, 277]. Russier *et al.* [278], showed that biodegradation increased with the introduction of

functional groups in a proportional approach. Horseradish peroxidase showed 100% degradation in at least 30 days of incubation [277, 278].

Following the discovery that a plant enzyme is capable of degradation, Kagen *et al.* [279], investigated if similar human peroxidase is also proficient in CNT degradation. They showed that human neutrophils and macrophage enzyme myeloperoxidase catalyze the biodegradation of SWNTs. Human myeloperoxidase generates strong reactive radical intermediates and hypochlorous acid in the presence of hydrogen peroxide. A complete absence of oxSWNT structure was reported after 24 hours of incubation with myeloperoxidase or sodium hypochlorite. The study systematically proves that a radical-driven mechanism is the driving force of biodegradation. Myeloperoxidase is predominately expressed in granules of neutrophils and is released upon bacterium phagocytosis [280]. *In vivo* incubation of IgG-propped oxSWNTs with myeloperoxidase-rich neutrophils demonstrated 100% degradation of oxidized SWNTs. p-SWNT degradation was also reported with myeloperoxidase enzyme, to a lesser extent [279]. Moreover, they also proposed, through docking simulation, the bindings sites for both oxidized and pristine SWNTs [279]. It is worth mentioning that the modelling data of myeloperoxidase enzyme lacks relevant consideration with respect to the morphology of the oxSWNTs and the enzyme capacity to bind to such a big molecule. The reported model shows that the enzyme binds to the tip/cap of the oxSWNTs which is thermodynamically not favorable due to the formation of protein corona.

In the case of finding more peroxide enzymes that play a role in SWNT degradation Andon *et al.* [281] showed that eosinophil peroxidase is also capable of degrading oxSWNTs. In another *in vitro* setup, Neves *et al.* [282] reported that the RNA-coated oxidized MWNTs internalized by human prostate adenocarcinoma cells showed structural induced defects after 18 hours. However, the degradation mechanism was not discussed.

Through an *in vivo* model, Shvedova *et al.* [283] provided direct evidence for the participation of myeloperoxidase in the biodegradation of oxSWNTs by using myeloperoxidase knockout mice. They showed that the degradation and clearance of SWNTs from the lungs of knockout mice subsequent to pharyngeal aspiration was significantly more robust than in wild-type mice. In another interesting study, Nunes *et al.* [284] investigated the fate of amine-functionalized MWNTs stereo-tactically injected into the motor cortex of a murine brain. They noticed cellular transport to different types of brain cells including neurons that underwent severe structural deformation, yielding amorphous debris 2 days post injection.

The discovery of biodegradation of carbon based nanomaterial is indeed a remarkable milestone on the path to controlled and targeted spatiotemporal degradation of CNTs. Moreover, it opens up for the utilization of such a phenomenon to serve as a controlled therapeutic release mechanism.

2.6 NANOPARTICLE-PROTEIN CORONA

When nanoparticles as part of different formulations for biomedical applications come into contact with physiological media or blood, a spontaneous nanoparticle-protein interaction occurs. Blood serum is a complex body fluid that comprises more than 1500 proteins ranging in concentration over at least 9 orders of magnitude [285, 286]. The formation of protein corona is governed by the exposure time, the nature of the physiological environment and the physiochemical properties of the nanoparticle including size, surface charge, composition and surface functional groups [287, 288].

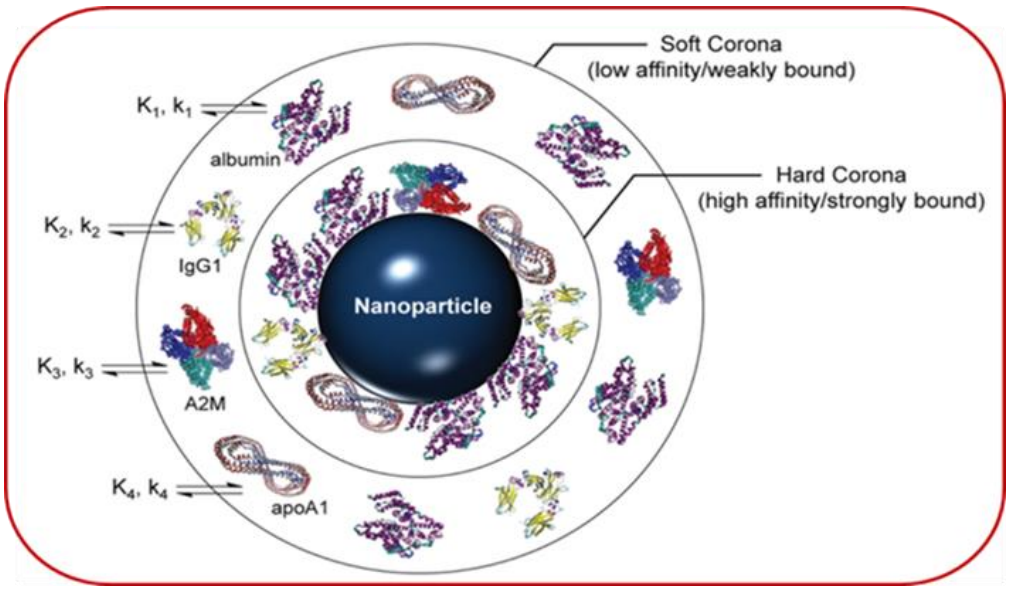

Figure 5. Schematic of protein corona formation on a nanoparticle surface. Protein adsorption is a kinetic (k) and thermodynamic (K) function of both the individual proteins and NP properties, such as composition, diameter, and surface modification. Reproduced from ref. [251] with permission from American Chemical Society.

The initial interaction of nanoparticles is governed by the migration of the most abundant proteins that occur through concentration gradient or by potential energy gradient [289]. Spontaneous adsorption occurs if it is thermodynamically favorable. Proteins may undergo structural conformational change during adsorption to facilitate interaction with the nanoparticle surface [287, 290]. Alteration of protein structural conformation is irreversible, even after desorption from the nanoparticle surface [291]. Shang *et al.* [292] demonstrated that proteins adsorbed to highly curved nanoparticles tend to undergo fewer changes in conformation than those adsorbed to less curved surfaces.

Biocorona is a complex phenomenon that is dynamic with time. Rapidly adsorbed proteins are exchanged with ones that have a higher affinity dominated by the Vroman effect [293]. The biomolecular corona is formed of two main strata, the *hard corona* and the *soft corona.* The hard corona is composed of tightly bound proteins that do not easily desorb, while the soft corona is composed of loosely bound proteins that adsorb with low affinity [294]. Walkey *et al.* [289] suggested that only the hard corona is due to the protein interaction directly with the surface of the nanoparticle, while the soft corona is formed as a consequence of interaction with the hard corona.

Shannahan *et al.* [295] examined the formation of protein corona on oxidized SWNTs, oxidized MWNTs and polyvinylpyrrolidone functionalized MWNTs, showing that all types were associated with a subset of proteins including apolipoproteins, titin, and albumin. Both oxidized types of CNTs are found to bind more proteins than polyvinylpyrrolidone functionalized MWNTs, demonstrating the importance of surface charge.

Protein corona creates a new biological identity for the nanoparticles that define physiological response such as cellular uptake, circulation lifetime, accumulation, agglomeration, kinetics, and toxicity [296]. Hard corona plays an important role in the *in vivo* fate of nanoparticles. Furthermore, changes in the hard corona might occur when the particles are transferred to another biological compartment upon internalization [297]. Ge *et al.* [298] showed that π-π stacking interactions between the aromatic residues of the proteins and the SWNTs play a vital role in protein adsorption. Moreover, protein coated SWNTs alter their cellular interaction pathways and result in a much reduced cytotoxicity profile [298].

3 AIM OF THE STUDIES

In 2008, the Food and Drug Administration and The Alliance for NanoHealth [299] declared a vision to facilitate the translation of leading nanomedicine into clinical use. In order to actualize a part of this vision, the present thesis aimed to assist the integration of single walled carbon nanotubes (SWNT) into the medical field.

The main aim would be achieved via specific aims

- To develope a novel imaging modality to facilitate real time imaging in order to study the biodistribution of the SWNTs.

- To investigate the effect of SWNTs on cytochrome P450 enzyme CYP3A4, using an *in vitro* model system of human CYP3A4 and human CYP reductase.

- To study the degradation of oxidized and pristine SWNTs by CYP 3A4. In addition, to understand the role of SWNT surface chemistry in degradation.

- To study the degradation of oxSWNTs by lactoperoxidase, a secreted peroxidase enzyme, and whether pulmonary surfactant hampers biodegradation.

- To investigate the degradation of SWNTs coated or chemically functionalized with PEG and to assess their propensity to undergo biodegradation *in vitro* using recombinant myeloperoxidase (MPO) and *ex vivo* using primary human neutrophils.

4 MATERIALS AND METHODS

Detailed description of the materials and technique utilized in the studies can be found in appended publications included in the thesis. The sections below provide a summary of the methods and their basic principles.

- ***Oxidation and shortening of SWNTs***

In paper I, II, III, IV and V: p-SWNTs were dispersed using a tip probe sonicator (9 sec×6 times) in a mixture of H_2SO_4 and HNO_3 at a ratio of 3:1 respectively in a round bottom flask. The flask was then equipped with a condenser and the dispersion was refluxed. The resulting dispersion was then quenched by placing the flask in ice until the temperature decreased to 15˚C, then diluted by deionized water followed by filtration on a 100 nm pore size hydrophilic PTFE membrane disc. The filtrate was washed and not allowed to dry until it reached the pH of deionized water. The sample was then dried in vacuum at 80˚C overnight. The oxidized/carboxylated SWNTs (ox/c-SWNTs) were then suspended in PBS buffer pH 7.4 using bath sonication (Branson 2510) to obtain ox/c-SWNT suspension. The ox/c-SWNT suspension was ultra-centrifuged for 6 hours at 21000 g, the upper 70% was collected and another round of centrifugation was performed to ensure that any large bundles or impurities were removed from the solution. A calibration curve for the thus obtained ox/c-SWNT concentration was determined based on an absorption peak of 280 nm, which is attributable to the surface π plasmon excitation due to the aromatic structure of the nanotubes [300].

- ***Bioconjugation reactions to (ox/c-SWNTs)***

Chemical conjugation of biomolecules with *ox/c-SWNTs* was achieved using carbodiimide chemistry. Carbodiimides are one of the most important classes of compounds in organic chemistry [301]. They are widely used to mediate the attachments of biomarkers to polypeptides. Carbodiimide agents are used to activate carboxylic acids towards ester or amide formation. *N*-hydroxybenzotriazole or *N*-hydroxysuccinimide are often added to increase yields and decrease side reactions [302].

In paper I: EDC, a water-soluble carbodiimide was used in presence of *N*-hydroxysuccinimide to form an amide bond with the enzyme. Non-covalent binding was also completed via a physical adsorption process between the protein and SWNTs through π–π interactions, hydrophobic interactions and van der Waals force.

In papers II & V: DCC, an organic soluble carbodiimide, was used to facilitate covalent conjugation of ox/c-SWNTs with methyl terminated linear PEG of different molecular weights. The organic solvent was extracted by rotary evaporator.

4.1 PHYSICAL AND CHEMICAL CHARACTERIZATION METHODS

In order to investigate the SWNT size and size distribution and morphology, electron microscopy was used.

- **Transmission electron microscopy (TEM)**

TEM is a microscopy technique in which a ray of electrons is transmitted thought an ultra-thin sample. The images are formed due to the interaction of the electron beam with the specimen. The analysis was performed with a Joel JEM-2000EX at 200 KV. The specimen was prepared by dropping the suspension of SWNTs on a carbon coated 200 mesh copper grid followed by drying at ambient conditions.

- **Scanning electron microscopy (SEM)**

SEM is a microscopy technique in which an image of the specimen is formed by scanning it with a focused beam of electrons in two perpendicular directions covering a square/rectangular area of the sample. The analysis was preformed using GEMINI Zeiss ultra 55.

- **Fourier transform infrared spectroscopy (FTIR)**

The study of the surface chemistry of the particles was performed using FTIR analysis. The basic theory of FTIR is that most molecules absorb light in the infra-red region of the electromagnetic spectrum (0.8 μm to 1 mm wavelength) [303]. The SWNT constructs are irradiated with a broad spectrum of IR light and the absorbance frequencies are plotted. The FTIR spectrum is a fingerprint of a sample. The analysis was performed using Thermo Scientific Nicolet iS10 FT-IR Spectrometer.

- **Thermogravimetric analysis (TGA)**

TGA is a thermal analysis method which studies the change in weight of the materials against temperature variation in a controlled atmosphere. TGA analysis was completed using TGA Q500.

- **Zeta potential measurements (ζ-potential)**

ζ-potential is a physical property that determines the colloidal stability. In suspension, the liquid layer surrounding the nanoparticle is constituted of two parts. The first inner layer referred to as the Stern layer is associated with the ions that are bound strongly to the solid surface of the nanoparticle. An outer layer formed of weakly bound ions constitutes the slipping plane. The potential at the slipping boundary is the ζ-potential.

- **Ultraviolet – visible spectroscopy (UV–Vis)**

UV-Vis absorption spectroscopy measures the attenuation of a beam of light after it passes through a sample. Ultraviolet and visible light are energetic enough to excite outer electrons of molecules containing non-bonding electrons or π-electrons to higher anti-bonding molecular orbitals [304]. UV-Vis is an informative method of empirically determining concentrations and of confirming successful conjugation or adsorption of molecules. LAMBDA 750 UV/Vis/NIR Spectrophotometer was used for this measurement.

- **Electrophoresis mobility shift assay (EMSA)**

EMSA is a very sensitive technique for the study of the binding properties of proteins [305]. In our work, we used it to confirm the binding of biomacromolecules to functionalized SWNTs. We also utilized the technique to study the different binding modes.

- **Bioluminescence measurements**

This is a robust method for determining the bioluminescence activity in a controlled temperature environment for a predetermined period of time. BioOrbit 1251 luminometer was used (collaboration with Biothema AB, Sweden).

- ***In vivo* imaging**

All animal experiments were conducted under the protocol approved by the Institutional Animal Care of Karolinska Institutet. Imaging was conducted on the IVIS™ system (Xenogen Corp., Alameda, CA) coupled to a data acquisition PC running Living Image™ software (Xenogen Corp.). During image acquisition, isoflurane anesthesia was maintained using a nose cone delivery system and animal body temperature was regulated using a digitally thermostated bed integrated within the IVIS system.

- **High-performance liquid chromatography (HPLC)**

HPLC is an analytical chemistry technique used to identify, separate and quantify chemical components in a mixture. The mixture is forced under high pressure in a column packed with functionalized particles. Interactions between the packing materials and the flowing solvent containing the chemical mixture lead to separation of the components. The separated components leave the column at different time points and are identified and quantified by means of attached detectors. There is a wide range of detector types including UV-Vis absorption spectrometer, Mass spectrometer, and fluorescence spectrometer [306]. The HPLC system used was Waters alliance.

- **Confocal Raman spectroscopy (CRS)**

CRS is spectroscopic technique that couples a standard optical microscope to a Raman spectrometer. CRS refers to the ability to spatially analyze the sample in lateral and depth coordinates. The spatial resolution is defined by the microscope objective selected, laser wavelength, and the laser quality. Typical spatial resolution is about 0.5-1 μm. The measurements were performed with a WITec alpha300 system in combination with a 785 nm laser for excitation and a 100x objective. CRS was employed to determine the structural integrity and defects of CNTs in paper III, IV and V.

- **Atomic force microscope (AFM)**

AFM is a scanning probe microscope utilizing a probe to measure the physical properties such as sample surface roughness, morphology, sample length, width, and height. The vertical resolution is up to 0.1 nm and the lateral resolution is in the order of 30 nm [307].

- **X-ray photoelectron spectroscopy (XPS)**

XPS is a surface chemical spectroscopic technique. XPS can measure the chemical state, elemental composition, and electronic state of the elements within a material. In brief, the material is radiated by a beam of x-rays while simultaneously measuring the electrons and kinetic energy emitted from the top of the materials. Peaks appear in the photoelectron spectrum from atoms emitting electrons of a particular characteristic energy. These peaks enable quantification and identification of all surface elements (except hydrogen) [308].

- **Lactate dehydrogenase cytotoxicity assay (LDH)**

LDH is a biomarker for cytotoxicity. LDH assay is a colorimetric assay to quantify LDH release into media from damaged cells. It is the most reliable assay for nanomaterials. Wörle-Knirsch *et al.* [309] demonstrated that other cytotoxicity assays can yield misleading results due to the interference of nanomaterials with the detection dye.

5 RESULTS: SUMMARY OF THE MAJOR FINDINGS

Paper I. THERMOSTABLE LUCIFERASE FOR *IN VIVO* IMAGING OF OXSWNTS

***All figures reproduced with permission of the American Chemical Society.*

In this study, we introduced a novel method for visualizing the biodistribution of oxSWNTs loaded with a chemotherapeutic drug. The study showed that thermostable green fluorescent proteins (Luciferase from Luciola cruciate, LcL) can be a powerful method to determine the biodistribution subsequent to administration. Luciferase protein permitted imaging at a depth of a few centimeters which made it possible to visualize at an organ resolution.

SWNTs were subjected to an oxidation treatment by means of an acid treatment (H_2SO_4+HNO_3) which resulted in generation of oxygen bearing functional groups on the surface of SWNTs (oxSWNTs). The acid treatment also shortened the SWNTs. Material characterization was made by FTIR to confirm the presence of a carboxylic functional group. TEM imaging of oxSWNTs showed the pristine tubes were shortened and defects were introduced to the surface of the tubes.

We investigated the mode of attachment on the LcL fluorescence intensity. Chemical binding of LcL to the oxSWNTs was validated by electrophoresis assay. We observed that the bioluminescence intensity is in the order LcL (control)> physically adsorbed LcL-CNT> chemical conjugated LcL-CNT (Figure 6).

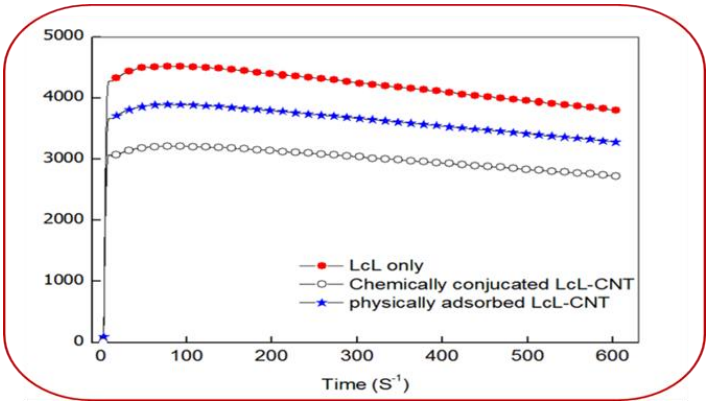

Figure 6. Chemiluminescence intensity of LcL-CNT, chemically conjugated (empty circles), physically adsorbed (stars), and only LcL (filled circles).*

We assessed the effect of physical adsorption and chemical conjugation. oxSWNTs were first reacted with BSA protein to block possible conjugating sites or adsorbing sites on oxSWNT walls before adding LcL. The chemiluminescence intensity as shown in figure 7 was in the order of LcL+ BSA alone < LcL + physically adsorbed BSA-oxSWNTs = LcL + chemically conjugated BSA-oxSWNTs.

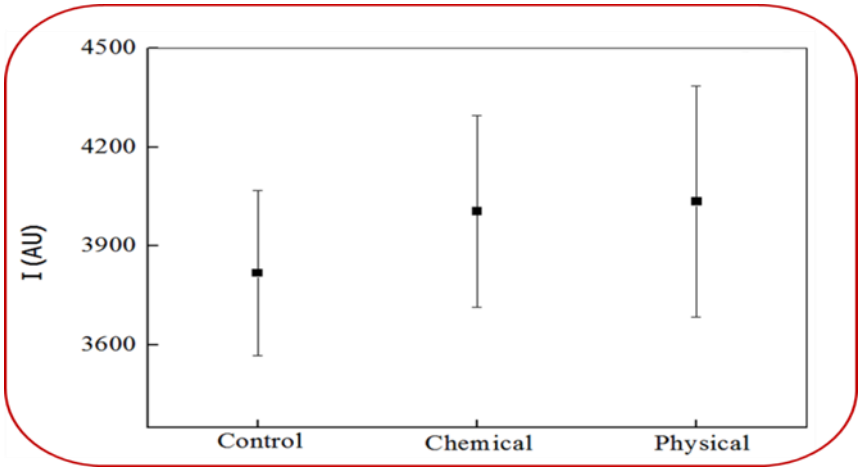

Figure 7. Chemiluminescence intensity of LcL physically adsorbed to CNT, chemically conjugated BSA to SWNT, and a control experiment with only BSA.*

The effect of physical adsorption and chemical conjugation of LcL to oxSWNTs on the bioluminescence decay rate and half-life was also studied. The plot of luminescence intensity expressed as ln(I) against time gives a linear relationship indicating a first order reaction. The bioluminescence of non-bound, chemically conjugated, and physically adsorbed LcL was investigated. In these three cases, the initial luminescence intensity was proportional to the LcL concentration and the bioluminescence decays following a first order reaction kinetics. No clear correlation between the LcL concentration or the coupling method and the decay kinetics was found.

The LcL-CNTs conjugate biological activity after loading doxorubicin as a chemotherapeutic molecule was evaluated. We showed clearly that LcL remains *in vivo* biologically active. Distribution to liver, spleen, and inguinal lymph nodes was observed 20 min after i.v. administration of LcL-CNTs (figure 8).

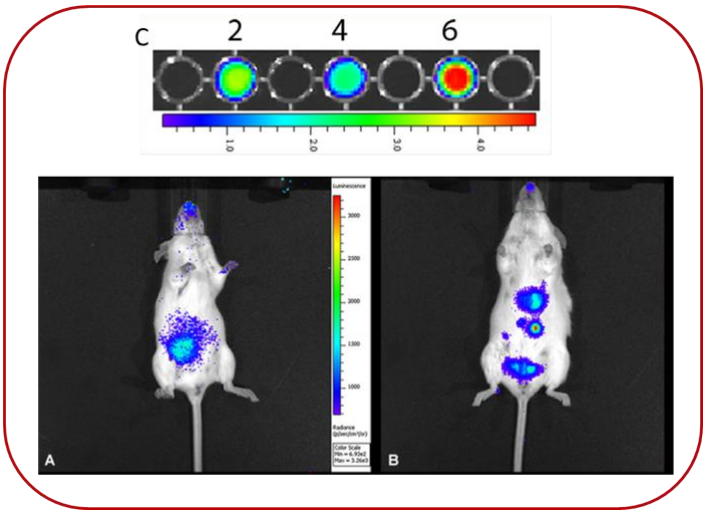

Figure 8. Biodistribution of LcL-CNT-DOX (A) and LcL-CNT (B) 20 min after IV administration. (A) Distribution of LcL-CNT DOX to the lymphoid, cecum, and mesenteric lymph nodes. (B) Distribution of LcL-CNT to spleen, liver, and inguinal lymph nodes. (C) In vitro chemiluminescence intensity of LcL-CNT and LcL-CNT- DOX. Well 2 and 4 contain 10 and 5 µL of LcL-CNT-DOX, respectively, well 6 contains 10 µL of LcL-CNT. ATP and D-luciferin were added to all wells.*

Finally, we studied the biodistribution of LcL and chemically conjugated LcL-CNTs in FVB mice using IVIS spectrum at two different epochs subsequent to i.v. and intraperitoneal

(i.p.) administration. Imaging was performed at time t = 0 min, that is forthwith subsequent to the administration, and at time t = 180 min after administration. Following i.v. administration, it was evident that free LcL is swiftly taken up and distributed to the mucosal membrane of the mouth, the ventriculus, and the vulva mucosal membrane while the LcL conjugate is rapidly taken up and distributed to the liver, thymus, jejunum, and the vulva mucosal membrane. Three hours post i.v. injection LcL-oxSWNTs were redistributed to the jejunum site and to the vulva mucosal membrane. We also observed a strong bioluminescence from the subiliac lymph node within the left hind leg of the mouse. The uptake of LcL and LcL-CNTs was confirmed by imaging harvested organs obtained after sacrificing the mice. Subsequent to i.p. injection of LcL and LCL-oxSWNTs, the signal remained localized in the peritoneal cavity of the mouse even after 3 hours post injection as shown in figure 9.

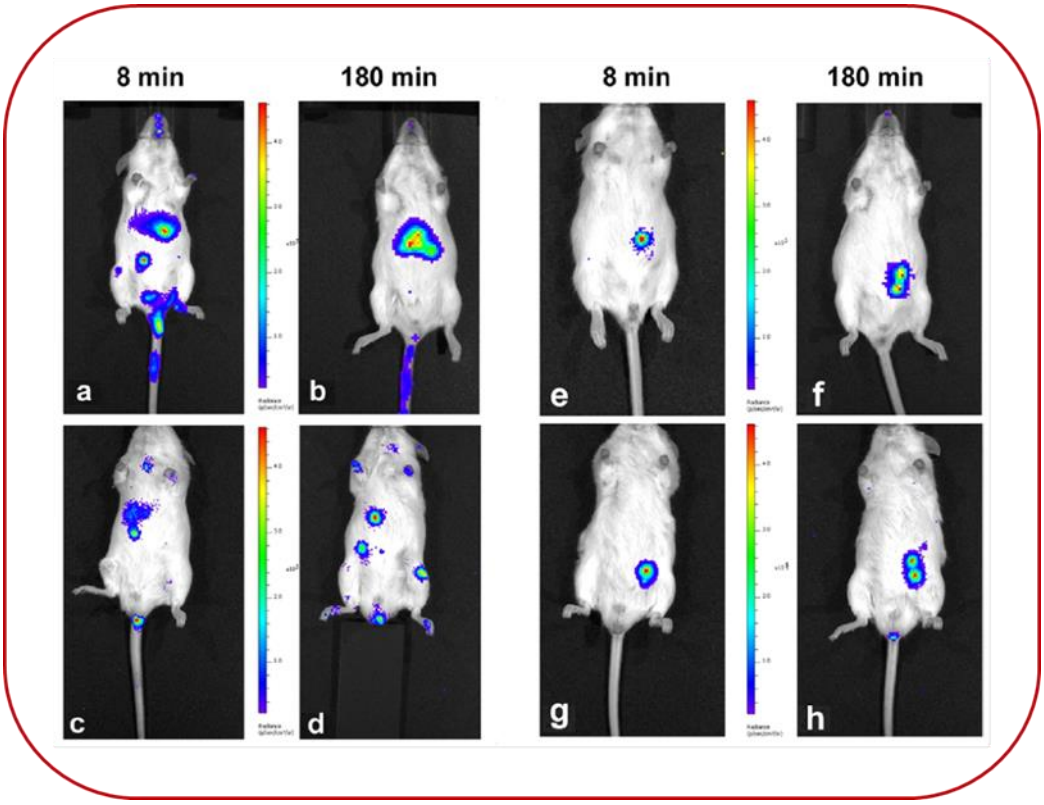

Figure 9. (a) The 8 min post i.v. administration of LcL only; (b) 180 min post i.v. administration of LcL only; (c) 8 min post i.v. administration of LcL-CNT; (d) 180 min after i.v. administration of LcL-CNT; (e) 8 min post i.p. administration of LcL only; (f) 180 min after i.p. administration of LcL only; (g) 8 min post i.p. administration of LcL-CNT; and (h) 180 min after i.p. administration of LcL-CNT.*

PAPER II. SINGLE-WALLED CARBON NANOTUBES INHIBIT THE CYTOCHROME P450 ENZYME -CYP3A4-

In this study, we turned our attention to CYP3A4, the most prominent cytochrome P450 isoenzyme in the liver. Using a combination of computational and experimental approaches, we investigated the interaction between oxSWNTs and CYP3A4 which is vital for progressing *in vivo* applications involving SWNTs.

SWNTs synthesized by chemical vapor deposition were subjected to a chemical oxidation treatment that resulted in the generation of oxygen-containing functional groups on the surface of the SWCNTs. This yielded short oxSWNTs with a length distribution of (178.7 ± 100 nm) and a zeta potential of -61.2 mV (Paper II & III).

HPLC was used to quantify the conversion of testosterone to 6β-hydroxy testosterone, as an indicator of CYP3A4 activity. Our results demonstrated that there is a dose-dependent inhibition of CYP3A4 as shown in Figure 10a. We also validated this result under the present experimental conditions ruling out that inhibition can be a potential artifact due to SWNT physicochemical characteristics (Figure 10b).

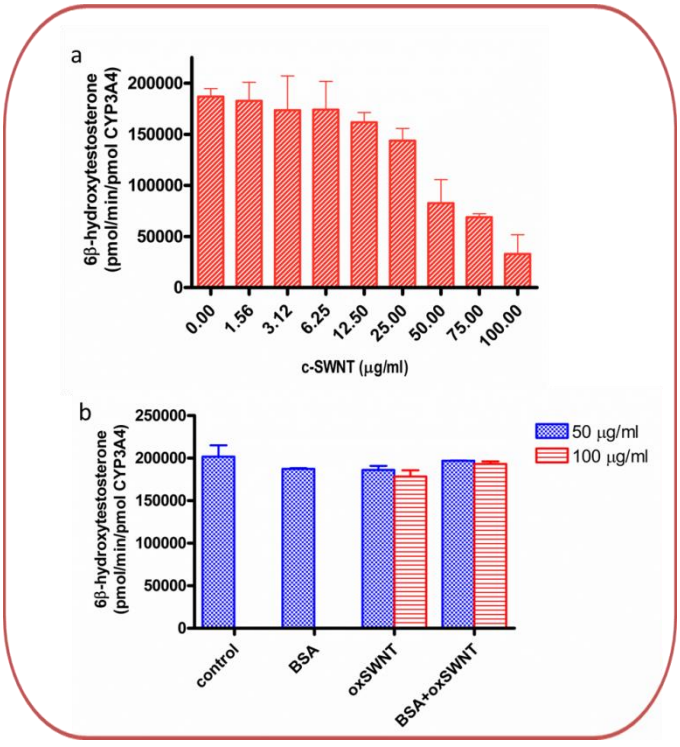

Figure 10. oxSWNTs dose-dependently inhibit CYP3A4. (a) The conversion of testosterone, to 6β-hydroxy testosterone as a measurement of the enzymatic activity of CYP3A4. (b) The addition of oxSWNTs or oxSWNTs with a corona of bovine serum albumin (BSA) to the reaction mixture after completion of the enzymatic reaction demonstrated that c-SWCNTs do not interfere with the assay.

Moreover, we investigated the potential role of the protein corona on the inhibition of CYP3A4 activity, by creating a synthetic protein corona with bovine serum albumin (BSA). We clearly demonstrated that the protein corona prevented the enzyme inhibition by the oxSWNTs (Figure 11).

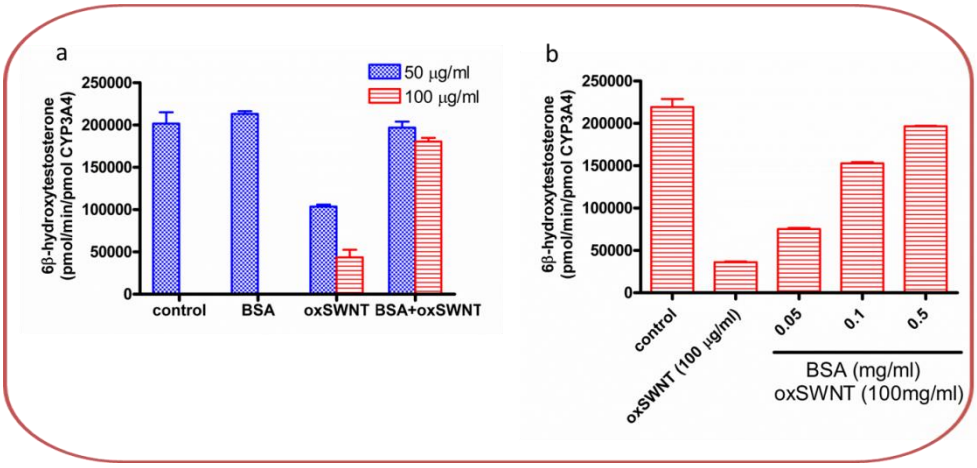

Figure 11. Mitigation of CYP3A4 inhibition by a protein corona. (a) The effect of bovine serum albumin (BSA) adsorbed onto oxSWNTs on the enzymatic activity of CYP3A4. (b) The protein corona effect is dependent upon the amount of BSA adsorbed onto the oxSWNTs.

PEG is known as the gold standard surface modification to extend the circulation time in the blood stream. In this part of the studies, we examined the potential role of PEG functionalization and compared constructs with different grafting of linear PEG chains of various molecular weights (750 Da, 5 KDa, and 10 KDa). The results showed that there is a proportional relation between the molecular weight of the linear PEG chain mediating inhibition (Figure 12).

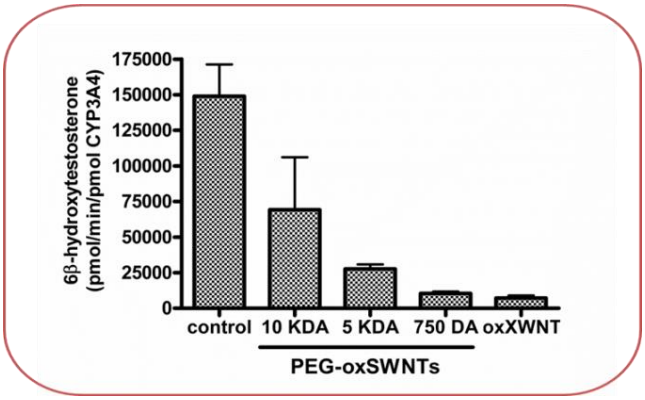

Figure 12. PEG-functionalization mitigates CYP3A4 inhibition. The effect of different molecular weight (MW) polyethylene glycol (PEG) chains (750Da, 5kDa, 10kDa) on the oxSWNT-mediated inhibition of enzymatic activity of CYP3A4.

Last, we tried to shed light on the inhibition mechanism employing molecular dynamics simulations and docking simulations. The analysis showed that CYP3A4 unfolding/misfolding is not the cause of enzymatic activity reduction. Moreover, we uncovered a novel finding, namely that oxSWNTs could potentially block the access channel to the active site of the enzyme. We showed that oxSWNTs adsorb onto the exit of the 2e channel of CYP3A4 through a complex binding mechanism, with hydrophobic, π–π stacking and van der Waals interactions playing a

dominant role, while the Coulomb and hydrogen bond interactions also promoted this interaction.

PAPER III. DEGRADATION OF PRISTINE AND OXIDIZED SINGLE WALL CARBON NANOTUBES BY CYP 3A4

In this investigation, we report for the first time the capacity of CYP450 (CYP3A4 isozyme) to degrade pristine SWNTs (p-SWNTs) and oxSWNTs by means of the monooxygenase cycle in an *in vitro* setup. CYP3A4 was shown to be more proficient in degrading p-SWNTs than oxSWNTs.

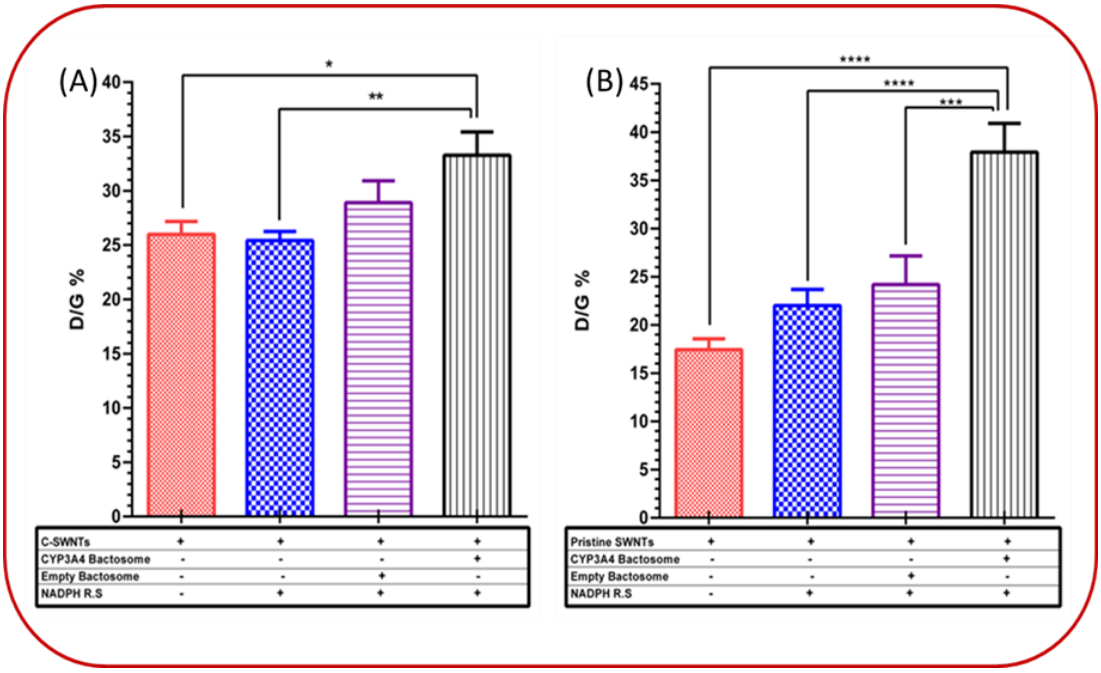

*Figure 13. Raman spectroscopy was used for the analysis of oxSWNTs. (A), p-SWNTs (B), incubated with 30 pmol of CYP3A4, 7 µg of p-SWNTs or c-SWNTs, 40 µl of NADPH-generating system. The CYP3A4 content in the system was refurbished every 12 hours. Statistical analysis performed using one-way ANOVA followed by Tukey's post hoc test. *P < 0.05*

We developed further insight on why CYP3A4 degrades p-SWNTs more proficiently than oxSWNTs by employing molecular dynamics and docking assessment. The analysis demonstrated clearly that p-SWNTs are packed more tightly into the CYP binding site, whereas the oxSWNT nanoparticle tends to protrude outside the binding cavity (figure 14). p-SWNTs were found to be bound strongly to the CYP enzyme with a minimal MolDock Score of −186.34 kcal/mol (ERY as reference control has MolDock Score = −141 kcal/mol), while oxSWNTs have a weaker affinity to the CYP 3A4 receptor and a higher binding energy profile (MolDock Score = −111.47 kcal/mol).

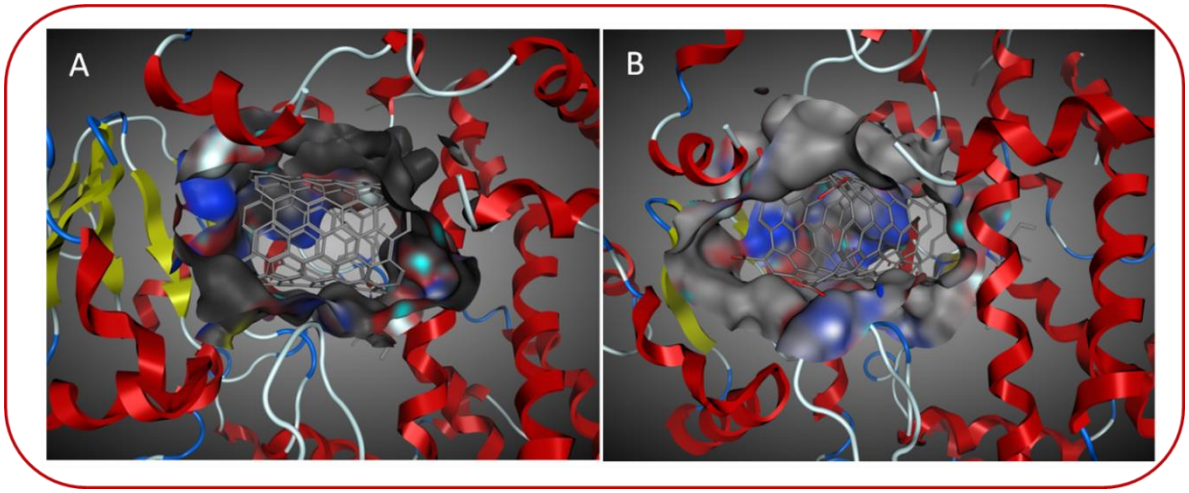

Figure 14. Molecular docking 3D patterns of the p-SWNT (A) and oxSWNT (B) molecules docked to the CYP3A4 binding cavity. Molecular surface is reconstructed within 4.5 Å from the CNT atoms to visualize the carbon nanotube interaction with the CYP450 3A4 protein.

We also investigated the potential of transfected HEK293 cell lines to degrade oxSWNTs. Raman analysis showed that there is no significant deterioration of oxSWNT structures after 96 hours of incubation. These findings raise more questions regarding the protein corona and how this can hamper cellular degradation.

PAPER IV. THE ROLE OF LACTOPEROXIDASE IN THE DEGRADATION OF SINGLE-WALLED CARBON NANOTUBES

***All figures reproduced with permission from Elsevier.*

The degradation of oxSWNTs in the airways was discussed. In the present investigation we studied the role of lactoperoxidase (LPO), a secreted peroxidase present in the airways, and whether pulmonary surfactant affects the biodegradation of oxSWNTs.

Pristine SWNTs with low metal content (4-8%) were subjected to chemical oxidation treatment to induce surface defects rich with oxygen bearing functional groups; oxygen content was quantified by means of XPS showing an increase of 3.1%. TEM imaging showed a length biodistribution of 1254 ± 479 nm while SEM images revealed the average diameter of the oxSWNT bundles to be 90 ± 42 nm.

We assessed the biodegradation of oxSWNTs in an *in vitro* system using recombinant LPO supplemented with physiologically relevant concentrations of both cofactors SCN^- and H_2O_2. Degradation was assessed primarily by means of Raman spectroscopy. We found a significant time dependent degradation and the efficiency of degradation of ox-SWCNTs

was found to be bLPO + H_2O_2+NaSCN> bLPO+H_2O_2 > bLPO + NaSCN > bLPO (figure 15). No degradation was observed for p-SWNTs in the presence of bLPO + H_2O_2+NaSCN.

We also studied the effect of Curosurf, which is a natural surfactant derived from porcine lung, to analyze the possible impact that lung surfactant can have on the degradation competence of LPO. Raman analysis showed comparable time dependent structural integrity damage of Curosurf-coated oxSWNTs in the presence of bLPO + H_2O_2 + NaSCN as shown in figure 15.

In order to assess whether biodegradation of oxSWNTs would occur in a more complex and physiologically more relevant medium, biodegradation of oxSWNTs was determined in cell-free bronchoalveolar lavage fluid (BALF). The magnitude of degradation shown by Raman analysis in the mBALF + H_2O_2 + NaSCN system was much lower when compared with the bLPO + H2O2 + NaSCN system as shown in figure 15.

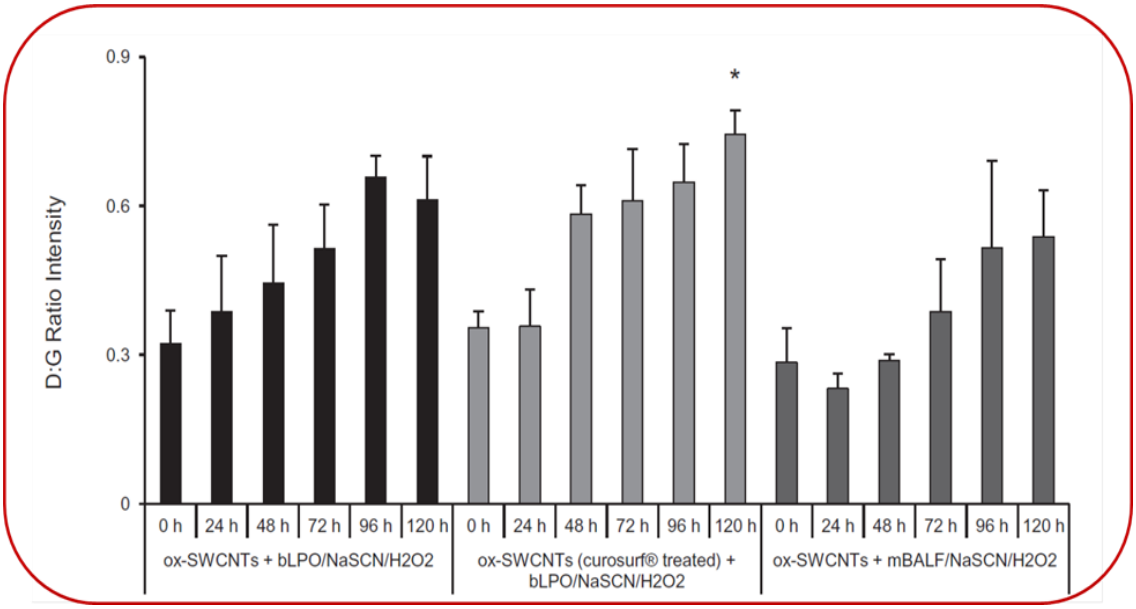

*Figure 15**. Raman spectroscopy was used for the analysis of ox-SWCNTs incubated with bLPO + H2O2 + NaSCN in the presence or absence of pulmonary surfactant (Curosurf), or in the presence of cell-free murine bronchoalveolar lavage fluid (mBALF) with H2O2 + NaSCN. A time-dependent increase in the D:G ratio intensity was observed, and comparable results were obtained for ox-SWCNT samples incubated in the presence or absence of Curosurf. Statistical analysis was performed using one-way ANOVA followed by Tukey's post hoc test of 0 h vs. 24 h, 48 h, 72 h, 96 h and 120 h. *P < 0.05.*

PAPER V. ENZYMATIC 'STRIPPING' AND DEGRADATION OF PEGYLATED CARBON NANOTUBES

****All figures reproduced with permission of The Royal Society of Chemistry.*

PEGylation is known to be a gold standard for chemical modification of nanomaterials including SWNTs. In this study, we investigated the effect of PEGylation on the inhibition of SWNTs biodegradation in natural conditions. Furthermore, we examined the role of PEG chain molecular weight and type of modification [non-covalent PEG coating (cPEG-SWNTs) vs. covalent PEG-functionalization (fPEG-SWNTs)] on the myeloperoxidase (MPO)-driven degradation of PEG-modified SWNTs (PEG-SWNTs).

The oxSWNTs were functionalized with PEG by means of carbodiimide chemistry. The surface PEG densities for cPEG-SWNTs and fPEG-SWNTs were equal to ~0.1 and 0.4 mmol per gram of nanotube material, quantified by Kaiser test. AFM showed that the average height of cPEG-SWNTs and fPEG-SWNTs was ~1 nm and ~7 nm.

Moreover, PEG-SWNT biodegradation *in vitro* with recombinant human MPO supplemented with H_2O_2 and NaCl in the presence of the metal chelator DTPA over a period of 7 days was investigated. Raman analysis (figure 16) showed that structural damage is induced to the sidewall of fPEG-SWNTs. More interestingly, MPO-driven degradation of fPEG-SWNTs decreased with PEG chain MW. fPEG-SWNT biodegradation was also confirmed by measuring the intensity of the semiconductor S22 band at 999 nm wavelength in the UV-Vis-NIR absorption spectrum. Both 2 kDa and 5 kDa fPEG-SWNTs showed a decrease of ca. 20% in the intensity of the S22 band. The degradation of 10 kDa fPEG-SWNTs was less evident. p-SWNT and cPEG-SWNTs did not undergo *in vitro* degradation.

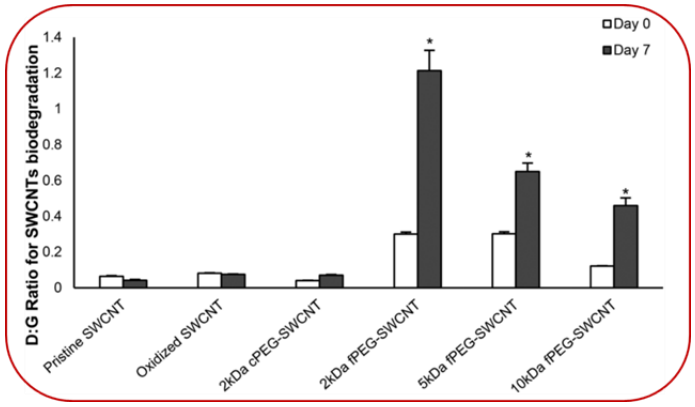

*Figure 16***. Raman spectroscopy was used for the analysis of MPO-driven in vitro degradation of SWCNTs. p values * ≤ 0.05 by 2-tailed t-test*

We investigated whether biodegradation of PEG-modified SWCNTs occurs in a natural system of *ex vivo* activated primary human neutrophils (Immune cells enclosing MPO). Neutrophils were activated by agonists fMLP and cytochalasin B to release intracellular MPO followed by addition of oxSWNTs, 2 kDa cPEG-SWNTs and 2, 5 and 10 kDa fPEG-SWNTs. Raman analysis (figure 16) revealed a time-dependent increase in the D:G band intensity ratio for all the SWNTs, indicative of enzymatic degradation, with the exception of the p-SWNTs.

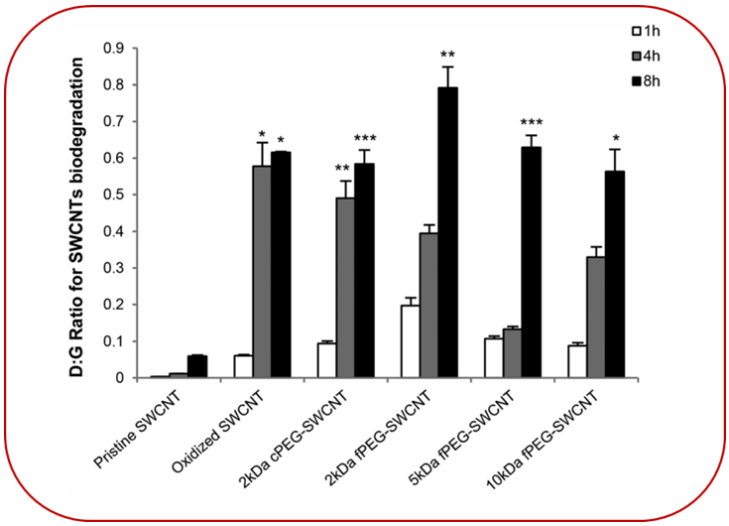

*Figure 17***. Raman spectroscopy was used for the analysis of* ex vivo *degradation of SWCNTs by primary human neutrophils. p values * ≤ 0.05, ** ≤ 0.01, *** ≤ 0.001 by one-way ANOVA*

The finding that an *ex vivo* system of activated neutrophils is so much more efficient than the *in vitro* system based on recombinant MPO raised the question if other factors that human neutrophil azurophilic granules contain could play a role in that enhancement. We reasoned that assisting factors could remove some or all of the PEG chains on the surface of the SWNTs, thereby permitting the contact of peroxidase to the SWNTs. Evaluating if neutrophil elastase (NE), a well-studied neutrophil protease, can be involved, it was evident that NE is able to remove ~2.5% and ~58% PEG chains from the surface of the 5 kDa fPEG-SWNTs following 6 hours and 6 days exposure as determined by TGA analysis.

6 DISCUSSION

Nanomedicine promises a revolution in better health care, personalized medicine and health economics. The Food and Drug Administration (FDA) listed nanomedicine as a priority field in a 2006 report entitled "*The Critical Path Opportunities List and Report*". With this fascinating field evolving, scientists and researchers exert joined efforts to unravel the full potential and create a working path for a fast and efficient bench-to-clinic translation. In 2008, the FDA and the Alliance for Nano-Health identified 7 key hurdles that need to be addressed to facilitate the nanoengineered products [299]:

1- Determination of the biodistribution of nanocarriers subsequent to systemic administration.
2- Development of imaging modalities for visualizing the biodistribution over time.
3- Understanding of nanoparticle transport across different boundaries ranging from cell membrane and different cell organelles to enzymatic boundaries.
4- Developing reference bench marking nanoparticles.
5- Developing mathematical models to predict risk and toxicological behaviors of nanoparticles.
6- Developing computer models that predict the behavior of nanoparticles in a biological environment.
7- Developing an analytical toolkit for nanopharmaceutical manufacturers.

This thesis framework was designed to contribute in fulfilling some of the aforementioned challenges and to facilitate the transfer of CNTs from the bench to the clinical setting.

Carbon-derived nanomaterials constitute one of the technologically most imperative classes of nanomaterials. CNTs have shown enormous potential for nanotechnology in general and nanomedicine in particular. Biodistribution of CNTs could be imaged by conjugation to a fluorescent molecule such as quantum dots (QDs) or fluorophores (FPs). QDs have a high quantum efficiency and high photo stability [310, 311] yet they have several drawbacks for imaging. For instance, QDs require an external excitation source. The technical challenges are difficult to overcome when imaging at non-superficial locations (typically larger than 1 cm) within the tissue [312]. Also, the proclivity of the CNT-QD complex toward electron and/or energy transfer (Förster resonant energy transfer) from QD to CNT results in quenching the fluorescence response of QDs [313]. Furthermore, numerous QDs comprise cytotoxic ions such as Cd and Se even when they are encapsulated in a biocompatible shell; there is a considerable risk of ion release with time [314].

Tracing of CNTs can also be achieved by Radiotracers such as ^{125}I ,^{111}In, ^{14}C , and ^{86}Y [315]. Radionucleotides offer higher detection sensitivity and no limit for imaging depth, yet safety issues are of concern. They are also considerably more expensive than other imaging moieties [312]. Recently, bioluminescent proteins emerged as a promising imaging moiety posing a higher spatial resolution of 1 mm. Additionally, bioluminescent proteins permit imaging at a depth of few centimeters within biological tissue [312] which makes it possible to visualize at an organ resolution [316].

Luciferase plasmids are commonly used as reporter genes in biological *in vitro* assays [317]. Scarce luciferase proteins are proper for *in vivo* imaging applications, because their biological tissue attenuates electromagnetic radiation signals over the "absorption" wavelength range. One of the most auspicious kinds of luciferase proteins is those which catalyze the oxidation of D-luciferin molecules via a two stage process in the presence of ATP. This process is accompanied by the emission of light over a range of wavelengths from 540 to 615 nm, which lies outside the absorption wavelength range of tissue [318]. A thermostable form of luciferase (LcL) made it possible to achieve a designed chemical construct (LcL+CNT) that remains sustainable long enough to image and investigate the biodistribution phase post injection and its accumulation in tissues/organs.

The coupling of luciferase to SWNTs was reached by two different strategies. In the first system, LcL was conjugated to oxSWNTs via chemical bonding by means of carbodiimide chemistry. In the second system, LcL was attached to the oxSWNTs via a physical adsorption process by means of van der Waals force and $\pi-\pi$ interactions. The chemical conjugate was done through the primary amine groups present on the *N*-terminus of the polypeptide chain, or on the lysine side chain of the LcL. The existence of such functional groups on the outer surface of the protein structure offers readily accessible sites for chemical conjugation to oxSWNTs, minimizing major LcL-structure alteration that can lead to protein denaturation rendering a non-active protein.

We observed a higher a higher fluorescence quenching for oxSWNTs chemically conjugated to LcL compared to oxSWNTs physically functionalized with LcL. A valid argument could be based in terms of energy transfer mechanism. LcL acts as an acceptor for photoexcited electrons from the oxSWNTs. Photoexcited electrons from the oxSWNT conduction band tunnel to the lowest unoccupied molecular orbitals of the LcL molecules, thus reducing the fluorescence intensity [319]. The fluorescence reduction in case of oxSWNTs with LcL physically adsorbed is expected due to the partial overlapping between the π-orbitals of the LcL and those of the oxSWNTs.

The observed bioluminescence intensity, in the order LcL (control) > physically adsorbed LcL-CNTs > chemically conjugated LcL-CNTs, can be explained in terms of the LcL protein structural change during the catalysis process. It is acknowledged that light emission during the oxidation of luciferin by LcL is initiated by proton abstraction at the carbon 4 position [320] plus large conformational change of the enzyme [321].The chemiluminescence intensity for the chemically conjugated complex was lowest because LcL is conjugated directly to the CNTs, which limits the conformational modifications. This is not the case in physical adsorption, where the protein has a higher degree of freedom for conformational changes on the CNT walls. These findings are in line with the findings of Tu *et al.* [322], who reported that chemical conjugation influences the conformational changes, such as the transformation of the original spherical shape to an elongated form.

To further confirm that LcL chemiluminescence declination was due to the effect of chemical conjugation but not physical adsorption, a synthetic corona utilizing BSA protein was formed to block possible conjugating sites or adsorbing sites on oxSWNT walls. BSA was selected due to its isoelectric point, ca. 5.64, which is lower than that of LcL (6.4), offering a higher affinity to oxSWNTs. Moreover, BSA has 60 amino moieties in lysine residues facilitating its chemical conjugation. The insignificant enhancement of intensity for LcL + physically adsorbed BSA-CNTs and LcL + chemically conjugated BSA-CNTs might be attributed to the adsorption of oxy-luciferin either on the side walls and/or inside the oxSWNTs, precluding it from jamming the protein activity.

Biodistribution in FVB mice of the chemical conjugate showed a different uptake pattern compared to free luciferase. The chemical construct was rapidly taken up and distributed to the thymus, the liver, the jejunum, and the vulva mucosal membrane. After three hours, LcL-CNTs were redistributed to the jejunum site and to the vulva mucosal membrane. Furthermore, we observed a strong bioluminescence from the subiliac lymph node within the left hind leg of the mouse. It is worth mentioning that nanoparticles (size <100 nm) have been reported to accumulate in the lymphoid organs [123]. This finding opens the frontier to questions of how the length of the CNTs can play an important role in affecting the biodistribution and in targeting the lymphoid system.

In pursuing a multifunctional theranostic agent, we showed that loading doxorubicin (16% loading efficiency) did not hamper the activity of the LcL-CNT chemical construct. The biodistribution of the theranostic agent showed an uptake in the spleen, liver, and inguinal lymph nodes. It was evident that the liver had the highest accumulation of the oxSWNTs. It

is also quite acknowledged that the liver is the main accumulation site for many other nanoparticles. This leads to a question that has to be investigated: Do nanomaterials, namely CNTs, interfere with liver functions?

Notably, the liver is a key organ involved in detoxification, metabolism, secretion of cytokines, and growth factor synthesis of proteins and lipids and immune/inflammatory responses. The cytochrome P450 (CYP450) enzyme family is a diverse group of proteins which are responsible for the initial biotransformation of xenobiotic compounds and drug metabolism. CYP450 plays a vital role in the determining the ultimate toxicological and pharmacological activity of 80% of available drugs. In addition, many substances (prodrugs) are bio-activated by CYPs to form their active compounds [323].

The impact of oxSWNTs on CYP450 function was evaluated using commercially available bactosomes, i.e., human hepatic cytochrome P450 isoenzymes (namely CYP3A4) coexpressed functionally in Escherichia coli with human NADPH-P450 reductase. E. coli-expressed CYPs have been validated as surrogates to their counterparts in human liver microsomes [324]. CYP3A4 was chosen as it is the most prominent isozyme and responsible for more than 40% of drug biotransformation in drugs such as paclitaxel, doxorubicin, and docetaxel. CYP3A4 activity was determined utilizing the conversion of its substrate, testosterone, to its metabolite, 6β-hydroxy testosterone, by means of HPLC. HPLC evades the drawbacks of available fluorescence-based assays; it is acknowledged that carbon based nanomaterials interfere with dye based assays [309]. We revealed that oxSWNTs suppress the conversion of testosterone to 6β-hydroxy testosterone in a dose dependent manner.

Xia *et al.* [325] anticipated and presented experimental evidence for the adsorption of small molecules, including steroid hormones, onto multi-walled CNTs. This observation led us to question whether the perceived inhibition of CYP3A4 conversion of testosterone to 6β-hydroxy testosterone could be illuminated by adsorption of the parent compound or its metabolites. To rule out this possible artifact, we designed an experiment in which CYP3A4 activity was assessed with or without the addition of oxSWNTs to the solution after the enzymatic reaction ran to completion. We showed that the 6β-hydroxy testosterone concentration, determined by HPLC, was similar to that of the control (without oxSWNTs).

Validating that inhibition in an *in vitro* setup, we turned our attention to mimicking the physiological experimental conditions. In biological fluids, proteins adsorb to the surface of nanoparticles, which can critically alter the interaction of nanoparticles with biological entities [326]. Dutta *et al.* [327] identified albumin as the major plasma protein that adsorbs to SWNTs, demonstrating the influence of protein corona in influencing the molecular targeting and biological activity of nanomaterials. We questioned if albumin protein corona would mediate CYP3A4 inhibition? The design of BSA corona would be reasonable due to the physiochemical nature of both SWNTs and albumin. BSA point of zero net charge is ca. 5.64, giving a high affinity of BSA adsorption to the walls of oxSWNTs. Moreover, BSA had no counter action on the CYP3A4 enzymatic activity as the HPLC analysis revealed. Our results showed that a BSA corona was indeed successful in preventing the enzymatic inhibition caused by oxSWNTs. The results also showed that protein corona has a positive potential and can be exploited to mediate toxicity profiles based on nanoparticle interactions.

In recent years, many researchers have tried to design nanoparticles with chemical entities such as polyethylene glycol (PEG) to evade the corona formation in order to enhance circulation time, efficacy and site targeting. Our results have shown that PEGylated oxSWNTs can prevent the CYP3A4 inhibition and the enzymatic activity was proportional to the molecular weight of the PEG chains. PEGylation induces steric hindrance and repulsion between the oxSWNTs and the CYP3A4 bactosomes. These findings support the evidence that points to the inhibition being due to a direct interaction between CYP3A4 isozyme and the oxSWNTs. In addition, it is in agreement with our AFM images showing the enzyme binding to the walls of oxSWNTs.

To elucidate more of the potential inhibitory mechanisms, we employed computational and molecular dynamics simulations to understand the docking and further the interaction. The CYP3A4 active site is positioned at the hydrophobic core of the protein. The proximity of the enzyme is linked to the surface of the enzyme through access channels. Enzyme gates prevent solvent access to specific regions of the protein and contribute to enzyme selectivity by controlling substrate access to the active site [328]. Fishelovitch *et al.* [329] identified six distinct channels (2a, 2b, 2c, 2e, 3, and S). Through computing preferred channel path for substrate/product and their gating mechanism, we identified two specific channels (2e and 3) that best suit the departure of the 6β-hydroxy testosterone. To investigate the 2e egress conduit, we studied different model simulations altering the

orientation of oxSWNTs relative to the enzyme 2e gate. In all the models, oxSWNTs could effectively block the 2e channel via direct sidewall binding stabilized by hydrophobic and π–π stacking interactions. In addition, the analysis revealed that oxygen bearing groups do not integrate in the channel blocking it, yet the functional groups interact with the charged/polar groups. The data showed that the interaction of CYP3A4 with oxSWNTs is sustained primarily by the dispersive components of hydrogen bonding interactions and hydrophobic, π–π stacking. However, adsorption is driven in part by early electrostatic attraction. Despite the considerable number of contacts that are formed between the protein and the nanotube, the enzyme's structure deforms only slightly.

CYP3A4 catalyzes numerous reactions of endogenous and exogenous substrates by means of the monooxygenation cycle. CYP3A4 catalyzes a variety of reactions including aromatic hydroxylation [330], Baeyer–Villiger oxidation [331], epoxidation of C=C double bonds [332] and cleavage of C–C bonds ring formation [333]. From this perspective we questioned if CYP3A4 also can cause a chemical structural alteration to the walls of the pristine CNTs or oxSWNTs. The finding that CYP3A4 is proficient at digesting oxSWNTs and p-SWNTs by promoting the defect sites on the CNT structure was determined by Raman spectroscopy. Raman spectroscopy measures the relative ratio between the G and D bands. These bands are fingerprints for CNTs and represent the in plane vibration of the C-C bond and the presence of disordered carbon, respectively [334]. These results support the fact that other families of enzymes operating by a different mechanism than peroxidase are capable of degradation of CNTs. It is known that some peroxidases exhibit homologous similarities up to 70% with CYP450; however, there are major chemical and structural alterations [335].

The fact that CYP3A4 degradation was observable for 5 days in both oxSWNTs and p-SWNTs compared to 16 days in other reported studies based on peroxidase enzymes such as myeloperoxidase and eosinophil peroxidase can be illuminated in terms of the chemical nature of CYP3A4. All peroxidases have histidine as a proximal ligand to the heme iron, while in CYP450 the proximal ligand is cysteine thiolate [336]. The chemical nature of CYP allows a higher metal-oxo complex redox potential of 1.5-2 V compared to 1 V in peroxidase (for reference a robust hydroxyl radical is 2.3 V [337]). Moreover, in peroxidases the oxygen complex created by the catalytic turnover acts as an electron sink while in CYP450 the catalytic mechanism is orchestrated by two oxidation equivalents, in which electron transfer precedes the oxygen transfer [338]. Another parameter that might

assist CYP adequate degradation compared to peroxidases is the structural complexity. The CYP3A4 heme binding region and substrate oxidation site is defined by 4 α-helix forming a depression in the protein surface that allows a close approach to the redox partner to the heme group [339]. Contrary to the peroxidase enzymes, the structure is an irregular packing of α helices to form ellipsoids and no organized β sheet structure forming a frame over the heme pocket [337].

It was surprising to find that the p-SWNT degradation was more significant compared to oxSWNTs when incubated with the same reaction conditions in CYP degradation for 5 days. By employing molecular dynamics and docking simulations, we were able to show that p-SWNTs bind strongly to the CYP3A4 enzyme compared to the oxSWNTs. p-SWNTs bind to the enzyme primarily through hydrophobic interactions, permitting a larger surface area for interaction compared to ox-SWNTs.
Our finding that degradation of ox-SWNTs was not successful in an *in vivo* setup utilizing transfected Hek293 cell line in Paper III can be explained in terms of protein corona formation. The cellular uptake was confirmed and eliminated the notion that ox-SWNTs did not come in close contact with the enzyme located endoplasmic reticulum.

Many concerns have been raised regarding the adverse effect on human health and environmental safety in terms of the persistence/clearance and degradation of pristine CNTs and functionalized CNTs. Previous reports showed that both pristine and functionalized CNTs can prompt fibrosis and pulmonary inflammation as well as carcinogenic effects upon pharyngeal aspiration or inhalation [340, 341]. Through further exploration of the notion of protein corona influence on the degradation of CNTs, Tabi *et al.* [342] discovered that CNTs were present in bronchoalveolar lavage fluid samples taken from the airways of 64 asthmatic Parisian children. An earlier report by Murr *et al.* [343] reported the existence of CNTs, CNT aggregates and other graphitic nanostructures created in the combustion of Texas piñon pine wood chips in air. Similar observations were also reported in India [344]. These findings support the fact that humans are routinely exposed to CNTs. How much CNTs infiltrate the lower respiratory tract is unknown. Pulmonary exposure to CNTs and other nanostructured carbons is neither avoidable nor controlled.

Degradation of oxSWNTs by means of various human peroxidase enzymes including myeloperoxidase (MPO) and Eosinophil peroxidase upon activation of innate immune cells has been reported [281]. Lactoperoxidase (LPO) is known as the third largest peroxidase

family which is expressed and excreted by goblet cells present in the epithelial lining of the respiratory tract and other mucosal surfaces and exocrine secretions [345]. The LPO system is known as a major contributor to airway defenses against bacteria.

Our findings show that LPO can proficiently break down the carbon back bone of oxSWNTs in the presence of the halogen substrates in an *in vitro* setup. To mimic physiological conditions, we also investigated the role of pulmonary surfactants and found that protein corona did not cause any interference with the LPO catalyzed-oxidization reaction nor with the degradation of oxSWNTs. Furthermore, we were able to show that the presence of biomolecules did not mask the assessment of degradation. These findings were contrary to the suggestions of Kagan *et al.* [279], showing that coating SWNTs with phosphatidylcholine, a major phospholipid component of pulmonary surfactant, prevented MPO driven biodegradation.

We complemented our findings showing that degradation occurs in murine BALF containing peroxidase activity combing both MPO and LPO. Although LPO and MPO were detected in lower concentrations compared to the *in vitro* setup, our data do not identify LPO (or MPO) as being solely responsible for oxSWNT degradation in mBALF. These findings are of importance in highlighting the possibility of oxSWNT clearance, yet they also shed light on possible implications that defense mechanisms against bacteria are compromised due to the preoccupation of LPO with oxSWNTs. These hypotheses are also in line with the findings of Shvedova et *al.* [346], showing that subsequent to oxSWNTs, bacteria exposure resulted in decreased bacterial clearance. This was found to be associated with decreased phagocytosis of bacteria by macrophages.

It is evident that theranostic agents including CNTs are usually administered after being coated or functionalized with PEG as a stealth moiety, evading the reticuloendothelial system. We questioned if PEG availability and PEG binding mode on the outer side walls of the CNT can affect biodegradation. Using an established Myeloperoxidase (MPO) model for biodegradation of oxSWNTs, our findings concluded degradation of PEG (M_w: 2k and 5k) covalently functionalized SWNTs (f-SWNTs). PEG molecular weight was proportional with the time needed to achieve noticeable degradation. This can be explained as being due to the fact that covalent bonding leads to an intense coverage of the surface of SWNTs, forming a mushroom brush transition conformation. The higher molecular weight of PEG induces steric repulsion upon the compression of the PEG layer caused by the protein diffusion [240, 241]. Moreover, a longer chain of PEG overcomes the van der Waals

attraction which is strong below 100 Å [242]. SWNTs bound to PEG by means of a non-covalent bond (a-SWNTs) did not show any degradation behavior in the presence of MPO and needed biodegradation cofactors. It is worth stating that that the degree of MPO-driven degradation of f-SWNTs in our present study was relatively low when compared to the earlier study by Vlasova *et al.* [347]. This can be attributed to the fact that Vlasova and colleagues utilized a lower molecular weight of PEG (600 Da) and permitted only (10–25%) grafting intensity.

Questioning whether the enzymatic stripping of PEG and degradation of f-SWNTs is possible in an *ex vivo* setup, we found that f-SWNTs were not able to simulate MPO release when incubated with primary human neutrophils, proposing absence of endotoxin contamination. To facilitate the biodegradation study, primary human neutrophils were simulated by cytochalasin B to release MPO from the intracellular compartments. Addition of exogenous cofactors such as H_2O_2, compulsory to activate the peroxidase cycle, was not needed as f-SWNTs activate the NADPH oxidase. Our results showed that both a-SWNTs and f-SWNTs were degraded proportionally with time with no clear dependence on either PEG molecular weight (2k, 5k, and 10k) or binding method. *Ex vivo* degradation studies were only permitted for 8 hours as neutrophils show significant spontaneous cell death with time in cell culture [348]. Tracking the SWNTs by means of confocal microscopy showed that in 6 hours both a-SWNT and f-SWNT agglomerates were present outside the neutrophils, probably due to cell death or cellular exocytosis. This observation combined with the fact that the carbon back bone defect intensity increases in 8 hours suggests that degradation is taking place both intra- and extra-cellularly.

All of these findings lead us to conclude that the presence of PEG does not hinder the digestion of SWNTs and also raises an important question as to how MPO evades the presence of PEG and physically attaches to the surface of SWNTs to start digesting the graphic structure. We reasoned that other factors released from the neutrophils may play an intermediate role in cleaving the PEG chains from the surface of SWNTs. Human neutrophil azurophilic granules enclose large amounts of three antibacterial serine proteases, cathepsin G, neutrophil elastase (NE), and proteinase [349]. We explored whether recombinant human NE can cleave the PEG from the surface in an *in vitro* setup. Our findings clearly showed that NE was successful in removing 2.5% of the PEG chains after 6 hours and 58% of the PEG chains after 6 days. With these findings we demonstrate

that the degradation in neutrophils is orchestrated by a combined action of MPO and other proteases released during degranulation.

7 CONCLUSION

The present thesis contributes to the development of CNTs as a theranostic carrier by exploring the CNT biodistribution post systemic administration, developing biocompatible imaging modalities for visualization of CNTs, and most of all understanding the biological fate and interaction with different enzymatic boundaries.

Paper I:

- Thermostable Luciferase from Luciola cruciate is an effective imaging modality for CNT nanocarriers.
- Loading doxorubicin as a chemo-therapeutic agent did not impair the chemiluminescent activity of Luciola cruciate Luciferase.
- The liver has the highest share of accumulation of the LcL-CNT complex.

Paper II:

- We present a potential route of inhibition to the CYP3A4 enzyme by oxSWNTs as it blocks the access to the active sites.
- Synthetic BSA Protein corona and PEGylation of oxSWNTs mitigated the inhibition of CP3A4.
- These findings suggest that oxSWNTs may alter the metabolism of xenobiotic compounds by CYP450 enzymes in a clinical setting.

Paper III:

- CYP3A4 is proficient in degrading/metabolizing the p-SWNTs and to a lesser extent oxSWNTs.
- A direct interaction between CNTs and CYP3A4 is required for the degradation to occur.

Paper IV:

- Lactoperoxidase (LPO) is capable of degrading oxSWNTs in an *in vitro* system.
- Formation of bio-corona from porcine lung surfactant on oxSWNTs does not restrain LPO degradation capacity.
- Cell-free biodegradation of oxSWNTs was also observed *ex vivo* in murine bronchoalveolar lavage fluid.

Paper V:

- PEGylation of oxSWNTs may obstruct myeloperoxidase degradation capacity in an *in vitro* setup.
- Using activated human neutrophils as *ex vivo* setup, oxSWNTs were degraded independently of PEG binding chemistry and PEG chain molecular weight.
- Degradation is a complex phenomenon where striping of the PEG chain occurs by means of proteases followed by digestion of the graphitic backbone of oxSWNTs.

8 ACKNOWLEDGEMENTS

I am overwhelmingly grateful to both Prof. Mustapha Hassan and Prof. Mamoun Muhammad for coaching my academic pathway and adjusting my personal life perception. I was very lucky to have both of you in my life and to be trained in your Labs.

My sincere gratefulness to Prof. Mustapha Hassan, whom without his consistent assistance and support I would have never reached this point of my career. He taught me that professorship is not only related to scientific merits but should also consist of great human nature. He assisted me when I needed help the most and guided me throughout the PhD. He is humble, honest (exquisitely) and very cheerful imprinting that in his lab. His talent lays in giving the student their ultimate freedom in their projects; he supports different ideas and demands for further work and development. He achieves success for himself when his team succeeds. He taught me to always step an extra mile to assist all "*folks*". Scientifically, he taught me persistence, patience, research independency, and introduced me to new medical technologies, giving me new perspectives about novel possibilities. His memorable on-door quotes are "honesty is very expensive, don't expect to find it in cheap people" & "Life is too short, enjoy the ride".

I would like to express my sincere appreciation to Prof. Mamoun Muhammed who introduced me to nanotechnology and research. He supported me since we first met in 2009. I was deeply impressed that he never focused only on science achievements, yet he always considered the notion of life in the students he supervised generating not only a lead scientists but successful and happy persons that are able to carry on a successful life. His support to me in 2009 and encouragement to explore the possibilities of life and science was tremendous. He supported my decision to discover new areas of research in new continents and even supported my decision to come back to start over the PhD in 2011. He embraces the talent of winning people's hearts and consequently reaching the highest level of achievements in his students. He taught me how to perform research and how to live with four key rules: 1-with a smile you can cross a thousand miles, 2- in science, novelty is the key and you will publish or perish, 3- there is always a room for improvement in all matters, 4- there is nothing called wrong, it is just a different perspective. Prof. Mamoun is a unique person & has an astonishing character.

I am also thankful to Prof. Bengt Fadeel for introducing me to Nanotoxicology.

I am profoundly thankful to Prof. Andreas Nyström for his support and for being a distinctive person in his principles. I wish you the best of success and happiness ahead in your life.

Many thanks are also due to Dr. Fei Ye for sharing his polymer and chemistry knowledge. He was also a great help when I needed assistance in my projects and a great mind when we were collaborating.

I am also indebted to thank Jennifer Usterud, Kathrin Reiser and Hanna Gador, LabMed Administrators, for all the cooperative administrative effort they put in handling my paper work and friendly attitude.

I am very grateful to my current and formal group member and friends in laboratory medicine department, Karolinska Institutet: Fadwa Benkassou, Manuchehr Abedi-Valugerdi, Wenyi Zheng, Åsa Barrefelt, Ying Zhou, Maria Cardona, José Arteaga, Ibrahim El-Serafi, Ahmed El-Serafi, Sulaiman Al-Hashmi, Mona Fares, Risul Amin, Eman Zaghloul, Kariem Ezzat (amazingly I have known him for 28 years, the most ancient friend I have), Abdulrahman Hamasy, Dara Mohammed, Sylvian Geny, Mei Lim, Sebastian Sjöqvist, and Dr. Rainer Heuchel .

I would like to thank Functional Nanomaterials Division (Royal Institute of Technology), formal group members and friends, I would like to thank Wubshet Sahle and Hans Bergqvist (for their time, patience and kindness introducing me to and teaching me different electron microscopy techniques), Dr. Salam Uhedia, Himanshu Jain, prof. Abd El-Hady Kayshout, Prof. Muhammed Toprak, Radwa Mahmoud, Martia Avila, Carmen Vogt, Terrance Bucks, Mohsin Salemi, Mohsen Tafti, Najmeh Najmoddin, Heba Assem, Adrine Melick, Kaouther Abderrazek, Faisal Aziz, Rabia Akan, Robina Shahid, Mazhar Yar & Sverker. I was very lucky to meet both Milad Ghadami and Aleksandrs Marinins as master students and very glad to see them achieving their goals.

I am very thankful for IMM group members and friends, mainly Malahat Mousavi; she was a great support for me during the desperate times, without her presence I would have never got this far. I would like to thank Neus Feliu, Xiaoli Feng**,** Fernando Andón, Consol Farrera, Lucian Farcal, Clara, Teresa Hollund, Hanna Karlsson, Olesja Bondarenko, Parisa Far, Sebastiano Di Bucchianico, Yuning Zhang, Ali Imran, Aram Ghalali, Prof. Ulla Stenius, Prof. Ralf Morgenstern, and Prof. Bengt Jernström. I was very blessed sharing the office with Katha Klöditz, Beatrice Lazzaretto, Aki Maeda, Lucie Valero, Anda Gliga, and Ines Smit. My special thanks in IMM go to Maria Sandelin, for whom I am very grateful in assisting me in pulling through the tough situations; I wish you a great happy life.

I am very grateful to all international & national collaborators; without them this thesis would have not been completed. Special thanks to Arne Lundin & Michael Voice.

My special appreciation to my Gang, family and friends in Sweden, Burcu Bestas (The Sister), Shiva (The Philosopher), Alicjia Bejger (The Lady), Beata Serwacinska (The Boss), Aida Zamanzad, Shole Habibi, Mahitab Ismail, Sara Elkhabiry, Mae Abo El Makarem, Reham El-Babtain, Kariem El Gammal , Mahmoud Ismail, Rami Mansour, Abubakrelsedik KaraliTumeng Mao, Mohamed Saad, Edgard Batista, Cihan Selvi, Ahmed Waraky, Thaer Morsi, Mina Safwat, Nancy Barakat, Amira Soliman, Amir Shalaby, Rania Mansour, Jihad Boufus, Medhat Lofty, Hien Tran, Zeynep Aslan, Sally AbdelMoaty, Mohamed Yousry, Atwa, Askalany, Ahmed Sallam, Hesham Omran, Athina Genaridou, Salman Niazi, and Kholod Salman. I would also like to express my sincere gratitude to Madam Lobna, Madam Cherine, Madam Marion, and Mr. Mansour.

A special thanks to my friend and brother Ralph Stephan (The German Shepherd) the cheerful guy who always assisted me on my way to my PhD by making amazing breakfast, amazing steaks and most of all chocolate rolls. You were never forgotten and I wish you the best of luck and success.

My great appreciation to my friends in Egypt who supported me to finish the PhD, Mohammed Serag, Mouhamed Haitham (Brother in arms), Omar Haitham, Ramy Essam, Omar Ishak, Sarah Nabil, Mennat-Allah Ismail, Hassan Yehia, Mohammad Omar Abuelnaga, Mohamed Faisal Elbatran, Ahmed Shaboon, Kareem Ahmad Abdel Fattah, Mohamed Kahoul, and Sherief Mohamed.

Now it is time to express my deep respect and gratitude to the people whom I owe most of my success and achievements in life. They are also my prevalent supporters, Hala Labib (mother), Sayed Helal (Father), Amr Helal & Hazem Helal (brothers). I am also indebted to express my gratitude to all my family members in Egypt for their continuous support and care.

Finally, I would like to apologies to those that by any chance I have forgotten to mention.

9 REFERENCES

1. Muhammed, M., *Engineering of Nanostructured Materials*, in *Nanostructures: Synthesis, Functional Properties and Applications*, T. Tsakalakos, I. Ovid'ko, and A. Vasudevan, Editors. 2003, Springer Netherlands. p. 37-79.
2. Horikoshi, S. and N. Serpone, *Introduction to Nanoparticles*, in *Microwaves in Nanoparticle Synthesis*. 2013, Wiley-VCH Verlag GmbH & Co. KGaA. p. 1-24.
3. Commission, E., *Scientific Basis for the Definition of the Term "Nanomaterial"* 2010.
4. Freestone, I., et al., *The Lycurgus Cup — A Roman nanotechnology.* Gold Bulletin, 2007. **40**(4): p. 270-277.
5. Heiligtag, F.J. and M. Niederberger, *The fascinating world of nanoparticle research.* Materials Today, 2013. **16**(7–8): p. 262-271.
6. Yong, Z.H., *Solar-Powered Nanotech-Purified Air In Medieval Churches*. 2008.
7. Sciau, P., *Nanoparticles in Ancient Materials: The Metallic Lustre Decorations of Medieval Ceramics*. 2012: INTECH Open Access Publisher.
8. Walter, P., et al., *Early Use of PbS Nanotechnology for an Ancient Hair Dyeing Formula.* Nano Letters, 2006. **6**(10): p. 2215-2219.
9. Williams, D. and C.B. Carter, *The Transmission Electron Microscope*, in *Transmission Electron Microscopy*. 1996, Springer US. p. 3-17.
10. Commission, E., *Nanotechnology: the invisible giant tackling Europe's future challenges*, R.a. Innovation, Editor. 2013: Belgium.
11. Kreuter, J., *Nanoparticles—a historical perspective.* International Journal of Pharmaceutics, 2007. **331**(1): p. 1-10.
12. apos, J. Silva, and G. van Calster, *Taking Temperature — A Review of European Union Regulation in Nanomedicine.* European Journal of Health Law, 2009. **16**(3): p. 249-269.
13. Wagner, V., et al., *The emerging nanomedicine landscape.* Nat Biotech, 2006. **24**(10): p. 1211-1217.
14. Commission, E., *European Technology Platform on NanoMedicine Nanotechnology for Health*. 2005: Belgium.
15. Moghimi, S.M., A.C. Hunter, and J.C. Murray, *Nanomedicine: current status and future prospects.* The FASEB Journal, 2005. **19**(3): p. 311-330.
16. Bao, G., S. Mitragotri, and S. Tong, *Multifunctional Nanoparticles for Drug Delivery and Molecular Imaging.* Annual Review of Biomedical Engineering, 2013. **15**(1): p. 253-282.
17. Xu, S., et al., *Assembly of micro/nanomaterials into complex, three-dimensional architectures by compressive buckling.* Science, 2015. **347**(6218): p. 154-159.

18. Wang, R., P.S. Billone, and W.M. Mullett, *Nanomedicine in action: an overview of cancer nanomedicine on the market and in clinical trials.* J. Nanomaterials, 2013. **2013**: p. 1-1.

19. Gu, Z., et al., *Tailoring nanocarriers for intracellular protein delivery.* Chemical Society Reviews, 2011. **40**(7): p. 3638-3655.

20. Mehra, N.K., V. Mishra, and N.K. Jain, *A review of ligand tethered surface engineered carbon nanotubes.* Biomaterials, 2014. **35**(4): p. 1267-1283.

21. Thess, A., et al., *Crystalline Ropes of Metallic Carbon Nanotubes.* Science, 1996. **273**(5274): p. 483-487.

22. Hata, K., et al., *Water-Assisted Highly Efficient Synthesis of Impurity-Free Single-Walled Carbon Nanotubes.* Science, 2004. **306**(5700): p. 1362-1364.

23. Charlier, J.C., *Defects in Carbon Nanotubes.* Accounts of Chemical Research, 2002. **35**(12): p. 1063-1069.

24. Collins, P.G., *Defects and Disorder in Carbon Nanotubes*. 2010.

25. Fan, Y., B.R. Goldsmith, and P.G. Collins, *Identifying and counting point defects in carbon nanotubes.* Nat Mater, 2005. **4**(12): p. 906-911.

26. Hiura, H., et al., *Role of sp3 defect structures in graphite and carbon nanotubes.* Nature, 1994. **367**(6459): p. 148-151.

27. Ebbesen, T.W. and T. Takada, *Topological and SP3 defect structures in nanotubes.* Carbon, 1995. **33**(7): p. 973-978.

28. Zhou, O., et al., *Defects in Carbon Nanostructures.* Science, 1994. **263**(5154): p. 1744-1747.

29. Zhu, H.W., et al., *Direct Synthesis of Long Single-Walled Carbon Nanotube Strands.* Science, 2002. **296**(5569): p. 884-886.

30. Green, A.A. and M.C. Hersam, *Properties and Application of Double-Walled Carbon Nanotubes Sorted by Outer-Wall Electronic Type.* ACS Nano, 2011. **5**(2): p. 1459-1467.

31. Shen, C., A.H. Brozena, and Y. Wang, *Double-walled carbon nanotubes: Challenges and opportunities.* Nanoscale, 2011. **3**(2): p. 503-518.

32. Pfeiffer, R., et al., *Double-Wall Carbon Nanotubes*, in *Carbon Nanotubes*, A. Jorio, G. Dresselhaus, and M. Dresselhaus, Editors. 2008, Springer Berlin Heidelberg. p. 495-530.

33. Moore, K.E., et al., *Separation of Double-Walled Carbon Nanotubes by Size Exclusion Column Chromatography.* ACS Nano, 2014. **8**(7): p. 6756-6764.

34. Hirschmann, T.C., et al., *Characterization of Bundled and Individual Triple-Walled Carbon Nanotubes by Resonant Raman Spectroscopy.* ACS Nano, 2013. **7**(3): p. 2381-2387.

35. Wen, Q., et al., *100 mm Long, Semiconducting Triple-Walled Carbon Nanotubes.* Advanced Materials, 2010. **22**(16): p. 1867-1871.

36. Muramatsu, H., et al., *Bulk Synthesis of Narrow Diameter and Highly Crystalline Triple-Walled Carbon Nanotubes by Coalescing Fullerene Peapods.* Advanced Materials, 2011. **23**(15): p. 1761-1764.

37. Baliyan, A., et al., *Synthesis of an Ultradense Forest of Vertically Aligned Triple-Walled Carbon Nanotubes of Uniform Diameter and Length Using Hollow Catalytic Nanoparticles.* Journal of the American Chemical Society, 2014. **136**(3): p. 1047-1053.

38. Andrews, R., et al., *Multiwall Carbon Nanotubes: Synthesis and Application.* Accounts of Chemical Research, 2002. **35**(12): p. 1008-1017.

39. Zhao, X., et al., *Smallest Carbon Nanotube is 3 Å in Diameter.* Physical Review Letters, 2004. **92**(12): p. 125502.

40. Qin, L.-C., et al., *Materials science: The smallest carbon nanotube.* Nature, 2000. **408**(6808): p. 50-50.

41. Truong, V., et al. *Multi-walled carbon nanotubes of 200 nm diameter and carbon micro-balloons*. in *Nanoscience and Nanotechnology (ICONN), 2010 International Conference on*. 2010.

42. Terrones, M., *SCIENCE AND TECHNOLOGY OF THE TWENTY-FIRST CENTURY: Synthesis, Properties, and Applications of Carbon Nanotubes.* Annual Review of Materials Research, 2003. **33**(1): p. 419-501.

43. Tu, X., et al., *DNA sequence motifs for structure-specific recognition and separation of carbon nanotubes.* Nature, 2009. **460**(7252): p. 250-253.

44. Rossouw, D., et al., *Metallic and Semiconducting Single-Walled Carbon Nanotubes: Differentiating Individual SWCNTs by Their Carbon 1s Spectra.* ACS Nano, 2012. **6**(12): p. 10965-10972.

45. Bachilo, S.M., et al., *Structure-Assigned Optical Spectra of Single-Walled Carbon Nanotubes.* Science, 2002. **298**(5602): p. 2361-2366.

46. Avouris, P., M. Freitag, and V. Perebeinos, *Carbon-nanotube photonics and optoelectronics.* Nat Photon, 2008. **2**(6): p. 341-350.

47. O'Connell, M.J., et al., *Band Gap Fluorescence from Individual Single-Walled Carbon Nanotubes.* Science, 2002. **297**(5581): p. 593-596.

48. Dai, H., *Carbon Nanotubes: Synthesis, Integration, and Properties.* Accounts of Chemical Research, 2002. **35**(12): p. 1035-1044.

49. Wilder, J.W.G., et al., *Electronic structure of atomically resolved carbon nanotubes.* Nature, 1998. **391**(6662): p. 59-62.

50. Miyata, Y., et al., *Optical Evaluation of the Metal-to-Semiconductor Ratio of Single-Wall Carbon Nanotubes.* The Journal of Physical Chemistry C, 2008. **112**(34): p. 13187-13191.

51. Krupke, R., et al., *Separation of Metallic from Semiconducting Single-Walled Carbon Nanotubes.* Science, 2003. **301**(5631): p. 344-347.

52. Rao, R., et al., *Insights into carbon nanotube nucleation: Cap formation governed by catalyst interfacial step flow.* Sci. Rep., 2014. **4**.

53. Chen, Y., et al., *State of the Art of Single-Walled Carbon Nanotube Synthesis on Surfaces.* Advanced Materials, 2014. **26**(34): p. 5898-5922.

54. Dresselhaus, M.S., et al., *Carbon Nanotubes*, in *The Physics of Fullerene-Based and Fullerene-Related Materials*, W. Andreoni, Editor. 2000, Springer Netherlands: Dordrecht. p. 331-379.

55. Prasek, J., et al., *Methods for carbon nanotubes synthesis—review.* Journal of Materials Chemistry, 2011. **21**(40): p. 15872-15884.

56. Novoselova, I.A., N.F. Oliynyk, and S.V. Volkov, *ELECTROLYTIC PRODUCTION OF CARBON NANO-TUBES IN CHLORIDE-OXIDE MELTS UNDER CARBON DIOXIDE PRESSURE*, in *Hydrogen Materials Science and Chemistry of Carbon Nanomaterials*, T.N. Veziroglu, et al., Editors. 2007, Springer Netherlands. p. 459-465.

57. Chen, G. and D. Fray, *Recent development in electrolytic formation of carbon nanotubes in molten salts.* Journal of Mining and Metallurgy, Section B: Metallurgy, 2003. **39**(1-2): p. 309-342.

58. Park, H.S., et al., *Ionic-Liquid-Assisted Sonochemical Synthesis of Carbon-Nanotube-Based Nanohybrids: Control in the Structures and Interfacial Characteristics.* Small, 2009. **5**(15): p. 1754-1760.

59. Jeong, S.-H., et al., *A Sonochemical Route to Single-Walled Carbon Nanotubes under Ambient Conditions.* Journal of the American Chemical Society, 2004. **126**(49): p. 15982-15983.

60. Katoh, R., et al., *Sonochemical production of a carbon nanotube.* Ultrasonics Sonochemistry, 1999. **6**(4): p. 185-187.

61. Ganesh, E., *Single walled and multi walled carbon nanotube structure, synthesis and applications.* International Journal of Innovative Technology and Exploring Engineering, 2013. **2**(4): p. 311-320.

62. Rafique, M.M.A. and J. Iqbal, *Production of carbon nanotubes by different routes-a review.* Journal of encapsulation and adsorption sciences, 2011. **1**(02): p. 29.

63. Niyogi, S., et al., *Chemistry of Single-Walled Carbon Nanotubes.* Accounts of Chemical Research, 2002. **35**(12): p. 1105-1113.

64. Hirsch, A., *Functionalization of single-walled carbon nanotubes.* Angewandte Chemie International Edition, 2002. **41**(11): p. 1853-1859.

65. Hirsch, A. and O. Vostrowsky, *Functionalization of Carbon Nanotubes*, in *Functional Molecular Nanostructures*, A.D. Schlüter, Editor. 2005, Springer Berlin Heidelberg. p. 193-237.

66. Dementev, N., et al., *Purification of carbon nanotubes by dynamic oxidation in air.* Journal of Materials Chemistry, 2009. **19**(42): p. 7904-7908.

67. Bradley, R.H., et al., *Surface studies of hydroxylated multi-wall carbon nanotubes.* Applied Surface Science, 2012. **258**(11): p. 4835-4843.

68. Datsyuk, V., et al., *Chemical oxidation of multiwalled carbon nanotubes.* Carbon, 2008. **46**(6): p. 833-840.

69. Weydemeyer, E.J., A.J. Sawdon, and C.-A. Peng, *Controlled cutting and hydroxyl functionalization of carbon nanotubes through autoclaving and sonication in hydrogen peroxide.* Chemical Communications, 2015. **51**(27): p. 5939-5942.

70. Shi, X., et al., *Fabrication of porous ultra-short single-walled carbon nanotube nanocomposite scaffolds for bone tissue engineering.* Biomaterials, 2007. **28**(28): p. 4078-4090.

71. Donkor, D.A. and X.S. Tang, *Tube length and cell type-dependent cellular responses to ultra-short single-walled carbon nanotube.* Biomaterials, 2014. **35**(9): p. 3121-3131.

72. Pastorin, G., *Crucial Functionalizations of Carbon Nanotubes for Improved Drug Delivery: A Valuable Option?* Pharmaceutical Research, 2009. **26**(4): p. 746-769.

73. Liu, L., et al., *Ultrashort single-walled carbon nanotubes in a lipid bilayer as a new nanopore sensor.* Nat Commun, 2013. **4**.

74. Chen, Z., et al., *Soluble Ultra-Short Single-Walled Carbon Nanotubes.* Journal of the American Chemical Society, 2006. **128**(32): p. 10568-10571.

75. Gao, G., M. Pan, and C.D. Vecitis, *Effect of the oxidation approach on carbon nanotube surface functional groups and electrooxidative filtration performance.* Journal of Materials Chemistry A, 2015. **3**(14): p. 7575-7582.

76. Jhi, S.-H., S.G. Louie, and M.L. Cohen, *Electronic Properties of Oxidized Carbon Nanotubes.* Physical Review Letters, 2000. **85**(8): p. 1710-1713.

77. Chen, J., et al., *Solution properties of single-walled carbon nanotubes.* Science, 1998. **282**(5386): p. 95-98.

78. Lim, J.K., et al., *Selective thiolation of single-walled carbon nanotubes.* Synthetic Metals, 2003. **139**(2): p. 521-527.

79. Hsu, M.-H., et al., *Simple and highly efficient direct thiolation of the surface of carbon nanotubes.* RSC Advances, 2014. **4**(28): p. 14777-14780.

80. Haddon, R.C., *.pi.-Electrons in three dimensiona.* Accounts of Chemical Research, 1988. **21**(6): p. 243-249.

81. Diederich, F. and C. Thilgen, *Covalent fullerene chemistry.* Science, 1996. **271**(5247): p. 317.

82. Diederich, F. and M. Gómez-López, *Supramolecular fullerene chemistry.* Chemical Society Reviews, 1999. **28**(5): p. 263-277.

83. Banerjee, S., T. Hemraj-Benny, and S.S. Wong, *Covalent Surface Chemistry of Single-Walled Carbon Nanotubes.* Advanced Materials, 2005. **17**(1): p. 17-29.

84. Georgakilas, V., et al., *Organic Functionalization of Carbon Nanotubes.* Journal of the American Chemical Society, 2002. **124**(5): p. 760-761.

85. Holzinger, M., et al., *Sidewall functionalization of carbon nanotubes.* Angewandte Chemie International Edition, 2001. **40**(21): p. 4002-4005.

86. Ying, Y., et al., *Functionalization of Carbon Nanotubes by Free Radicals.* Organic Letters, 2003. **5**(9): p. 1471-1473.

87. Tagmatarchis, N. and M. Prato, *Functionalization of carbon nanotubes via 1, 3-dipolar cycloadditions.* Journal of materials chemistry, 2004. **14**(4): p. 437-439.

88. Chen, Z., W. Thiel, and A. Hirsch, *Reactivity of the Convex and Concave Surfaces of Single-Walled Carbon Nanotubes (SWCNTs) towards Addition Reactions:*

Dependence on the Carbon-Atom Pyramidalization. ChemPhysChem, 2003. **4**(1): p. 93-97.

89. Moore, V.C., et al., *Individually suspended single-walled carbon nanotubes in various surfactants.* Nano Letters, 2003. **3**(10): p. 1379-1382.

90. Wang, H., *Dispersing carbon nanotubes using surfactants.* Current Opinion in Colloid & Interface Science, 2009. **14**(5): p. 364-371.

91. Tummala, N.R. and A. Striolo, *SDS surfactants on carbon nanotubes: aggregate morphology.* Acs Nano, 2009. **3**(3): p. 595-602.

92. Yan, L.Y., et al., *Individually dispersing single-walled carbon nanotubes with novel neutral pH water-soluble chitosan derivatives.* The Journal of Physical Chemistry C, 2008. **112**(20): p. 7579-7587.

93. Star, A., et al., *Preparation and properties of polymer-wrapped single-walled carbon nanotubes.* Angewandte Chemie International Edition, 2001. **40**(9): p. 1721-1725.

94. Numata, M., et al., *Inclusion of Cut and As-Grown Single-Walled Carbon Nanotubes in the Helical Superstructure of Schizophyllan and Curdlan (β-1,3-Glucans).* Journal of the American Chemical Society, 2005. **127**(16): p. 5875-5884.

95. Zhao, Y.-L. and J.F. Stoddart, *Noncovalent Functionalization of Single-Walled Carbon Nanotubes.* Accounts of Chemical Research, 2009. **42**(8): p. 1161-1171.

96. Zhu, J., et al., *Dispersing Carbon Nanotubes in Water: A Noncovalent and Nonorganic Way.* The Journal of Physical Chemistry B, 2004. **108**(31): p. 11317-11320.

97. Chen, R.J., et al., *Noncovalent sidewall functionalization of single-walled carbon nanotubes for protein immobilization.* Journal of the American Chemical Society, 2001. **123**(16): p. 3838-3839.

98. Guldi, D.M., et al., *Carbon nanotubes in electron donor-acceptor nanocomposites.* Accounts of Chemical Research, 2005. **38**(11): p. 871-878.

99. Ehli, C., et al., *Interactions in single wall carbon nanotubes/pyrene/porphyrin nanohybrids.* Journal of the American Chemical Society, 2006. **128**(34): p. 11222-11231.

100. Guldi, D.M., et al., *Integrating Single-Wall Carbon Nanotubes into Donor–Acceptor Nanohybrids.* Angewandte Chemie, 2004. **116**(41): p. 5642-5646.

101. Baskaran, D., J.W. Mays, and M.S. Bratcher, *Noncovalent and Nonspecific Molecular Interactions of Polymers with Multiwalled Carbon Nanotubes.* Chemistry of Materials, 2005. **17**(13): p. 3389-3397.

102. Naito, M., et al., *Stiffness-and conformation-dependent polymer wrapping onto single-walled carbon nanotubes.* Journal of the American Chemical Society, 2008. **130**(49): p. 16697-16703.

103. Ikeda, A., et al., *Solubilization of Single-Walled Carbon Nanotubes by Supramolecular Complexes of Barbituric Acid and Triaminopyrimidines.* Langmuir, 2007. **23**(22): p. 10913-10915.

104. Kim, O.-K., et al., *Solubilization of Single-Wall Carbon Nanotubes by Supramolecular Encapsulation of Helical Amylose.* Journal of the American Chemical Society, 2003. **125**(15): p. 4426-4427.

105. Rouse, J.H. and P.T. Lillehei, *Electrostatic assembly of polymer/single walled carbon nanotube multilayer films.* Nano Letters, 2003. **3**(1): p. 59-62.

106. Kim, J.B., et al., *A Facile Approach to Single-Wall Carbon Nanotube/Poly (allylamine) Nanocomposites.* Macromolecular rapid communications, 2007. **28**(3): p. 276-280.

107. Huang, S.-C.J., et al., *Persistence Length Control of the Polyelectrolyte Layer-by-Layer Self-Assembly on Carbon Nanotubes.* Journal of the American Chemical Society, 2005. **127**(41): p. 14176-14177.

108. Barone, P.W. and M.S. Strano, *Reversible control of carbon nanotube aggregation for a glucose affinity sensor.* Angewandte Chemie, 2006. **118**(48): p. 8318-8321.

109. Star, A., et al., *Starched carbon nanotubes.* Angewandte Chemie International Edition, 2002. **41**(14): p. 2508-2512.

110. Ishibashi, A. and N. Nakashima, *Individual Dissolution of Single-Walled Carbon Nanotubes in Aqueous Solutions of Steroid or Sugar Compounds and Their Raman and Near-IR Spectral Properties.* Chemistry – A European Journal, 2006. **12**(29): p. 7595-7602.

111. Wang, D. and L. Chen, *Temperature and pH-Responsive Single-Walled Carbon Nanotube Dispersions.* Nano Letters, 2007. **7**(6): p. 1480-1484.

112. Najeeb, C.K., et al., *Highly efficient individual dispersion of single-walled carbon nanotubes using biocompatible dispersant.* Colloids and Surfaces B: Biointerfaces, 2013. **102**: p. 95-101.

113. Farvadi, F., et al., *Micellar stabilized single-walled carbon nanotubes for a pH-sensitive delivery of doxorubicin.* Research in pharmaceutical sciences, 2014. **9**(1): p. 1.

114. Karchemsky, F., et al., *Diameter-selective dispersion of carbon nanotubes by β-lactoglobulin whey protein.* Colloids and Surfaces B: Biointerfaces, 2013. **112**: p. 16-22.

115. Caneba, G., et al., *Novel ultrasonic dispersion of carbon nanotubes.* Journal of Minerals and Materials Characterization and Engineering, 2010. **9**(03): p. 165.

116. Heister, E., et al., *Higher dispersion efficacy of functionalized carbon nanotubes in chemical and biological environments.* Acs Nano, 2010. **4**(5): p. 2615-2626.

117. Etika, K.C., et al., *Temperature Controlled Dispersion of Carbon Nanotubes in Water with Pyrene-Functionalized Poly(N-cyclopropylacrylamide).* Journal of the American Chemical Society, 2009. **131**(38): p. 13598-13599.

118. McDevitt, M.R., et al., *PET imaging of soluble yttrium-86-labeled carbon nanotubes in mice.* Plos one, 2007. **2**(9): p. e907.

119. Singh, R., et al., *Tissue biodistribution and blood clearance rates of intravenously administered carbon nanotube radiotracers.* Proceedings of the National Academy of Sciences of the United States of America, 2006. **103**(9): p. 3357-3362.

120. Guo, J., et al., *Biodistribution of functionalized multiwall carbon nanotubes in mice.* Nuclear Medicine and Biology, 2007. **34**(5): p. 579-583.

121. Liu, Z., et al., *In vivo biodistribution and highly efficient tumour targeting of carbon nanotubes in mice.* Nature nanotechnology, 2007. **2**(1): p. 47-52.

122. Singh, R.P., et al., *Functionalization density dependent toxicity of oxidized multiwalled carbon nanotubes in a murine macrophage cell line.* Chemical research in toxicology, 2012. **25**(10): p. 2127-2137.

123. Moghimi, S.M., A.C. Hunter, and J.C. Murray, *Long-circulating and target-specific nanoparticles: theory to practice.* Pharmacological reviews, 2001. **53**(2): p. 283-318.

124. Zhan, L., et al., *Biodistribution of co-exposure to multi-walled carbon nanotubes and graphene oxide nanoplatelets radiotracers.* Journal of Nanoparticle Research, 2011. **13**(7): p. 2939-2947.

125. Kang, B., et al., *Biodistribution and accumulation of intravenously administered carbon nanotubes in mice probed by Raman spectroscopy and fluorescent labeling.* Carbon, 2009. **47**(4): p. 1189-1192.

126. Liu, Z., et al., *Circulation and long-term fate of functionalized, biocompatible single-walled carbon nanotubes in mice probed by Raman spectroscopy.* Proceedings of the National Academy of Sciences, 2008. **105**(5): p. 1410-1415.

127. Choi, H.S., et al., *Renal clearance of quantum dots.* Nature biotechnology, 2007. **25**(10): p. 1165-1170.

128. Yang, S.-t., et al., *Biodistribution of Pristine Single-Walled Carbon Nanotubes In Vivo†.* The Journal of Physical Chemistry C, 2007. **111**(48): p. 17761-17764.

129. Al Faraj, A., et al., *In Vivo Imaging of Carbon Nanotube Biodistribution Using Magnetic Resonance Imaging.* Nano Letters, 2009. **9**(3): p. 1023-1027.

130. Cherukuri, P., et al., *Mammalian pharmacokinetics of carbon nanotubes using intrinsic near-infrared fluorescence.* Proceedings of the National Academy of Sciences, 2006. **103**(50): p. 18882-18886.

131. Iverson, N.M., et al., *In vivo biosensing via tissue-localizable near-infrared-fluorescent single-walled carbon nanotubes.* Nature nanotechnology, 2013. **8**(11): p. 873-880.

132. Welsher, K., et al., *A route to brightly fluorescent carbon nanotubes for near-infrared imaging in mice.* Nat Nano, 2009. **4**(11): p. 773-780.

133. Al-Jamala, K.T. and K. Kostarelosb, *Imaging carbon nanotubes in vivo: A vignette of imaging modalities at the nanoscale.* Nanoimaging, 2011: p. 251.

134. Chen, K.G. and B.I. Sikic, *Molecular pathways: regulation and therapeutic implications of multidrug resistance.* Clinical Cancer Research, 2012. **18**(7): p. 1863-1869.

135. Gottesman, M.M., T. Fojo, and S.E. Bates, *Multidrug resistance in cancer: role of ATP–dependent transporters.* Nature Reviews Cancer, 2002. **2**(1): p. 48-58.

136. Heldin, C.-H., et al., *High interstitial fluid pressure [mdash] an obstacle in cancer therapy.* Nat Rev Cancer, 2004. **4**(10): p. 806-813.

137. Al-Jamal, K.T., et al., *Cellular uptake mechanisms of functionalised multi-walled carbon nanotubes by 3D electron tomography imaging.* Nanoscale, 2011. **3**(6): p. 2627-2635.

138. Kostarelos, K., et al., *Cellular uptake of functionalized carbon nanotubes is independent of functional group and cell type.* Nat Nano, 2007. **2**(2): p. 108-113.

139. Lacerda, L., et al., *Translocation mechanisms of chemically functionalised carbon nanotubes across plasma membranes.* Biomaterials, 2012. **33**(11): p. 3334-3343.

140. Shi Kam, N.W., et al., *Nanotube Molecular Transporters: Internalization of Carbon Nanotube−Protein Conjugates into Mammalian Cells.* Journal of the American Chemical Society, 2004. **126**(22): p. 6850-6851.

141. Chen, X., et al., *A cell nanoinjector based on carbon nanotubes.* Proceedings of the National Academy of Sciences, 2007. **104**(20): p. 8218-8222.

142. Lopez, C.F., et al., *Understanding nature's design for a nanosyringe.* Proceedings of the National Academy of Sciences of the United States of America, 2004. **101**(13): p. 4431-4434.

143. Pantarotto, D., et al., *Functionalized carbon nanotubes for plasmid DNA gene delivery.* Angewandte Chemie, 2004. **116**(39): p. 5354-5358.

144. Jin, H., et al., *Size-Dependent Cellular Uptake and Expulsion of Single-Walled Carbon Nanotubes: Single Particle Tracking and a Generic Uptake Model for Nanoparticles.* ACS Nano, 2009. **3**(1): p. 149-158.

145. Li, R., et al., *P-Glycoprotein Antibody Functionalized Carbon Nanotube Overcomes the Multidrug Resistance of Human Leukemia Cells.* ACS Nano, 2010. **4**(3): p. 1399-1408.

146. Prabhakar, U., et al., *Challenges and key considerations of the enhanced permeability and retention effect for nanomedicine drug delivery in oncology.* Cancer research, 2013. **73**(8): p. 2412-2417.

147. Iyer, A.K., et al., *Exploiting the enhanced permeability and retention effect for tumor targeting.* Drug Discovery Today, 2006. **11**(17–18): p. 812-818.

148. Wu, W., et al., *Covalently Combining Carbon Nanotubes with Anticancer Agent: Preparation and Antitumor Activity.* ACS Nano, 2009. **3**(9): p. 2740-2750.

149. Tian, Z., et al., *Supramolecular assembly and antitumor activity of multiwalled carbon nanotube–camptothecin complexes.* Journal of nanoscience and nanotechnology, 2011. **11**(2): p. 953-958.

150. Sahoo, N.G., et al., *Functionalized carbon nanomaterials as nanocarriers for loading and delivery of a poorly water-soluble anticancer drug: a comparative study.* Chemical Communications, 2011. **47**(18): p. 5235-5237.

151. Tripisciano, C., et al., *Multi-wall carbon nanotubes–a vehicle for targeted Irinotecan drug delivery.* physica status solidi (b), 2010. **247**(11-12): p. 2673-2677.

152. Chen, C., et al., *EGF-functionalized single-walled carbon nanotubes for targeting delivery of etoposide.* Nanotechnology, 2012. **23**(4): p. 045104.

153. Liu, Z., et al., *Supramolecular Chemistry on Water-Soluble Carbon Nanotubes for Drug Loading and Delivery.* ACS Nano, 2007. **1**(1): p. 50-56.

154. Ali-Boucetta, H., et al., *Multiwalled carbon nanotube–doxorubicin supramolecular complexes for cancer therapeutics.* Chemical Communications, 2008(4): p. 459-461.

155. Heister, E., et al., *Drug loading, dispersion stability, and therapeutic efficacy in targeted drug delivery with carbon nanotubes.* Carbon, 2012. **50**(2): p. 622-632.

156. Datir, S.R., et al., *Hyaluronate tethered,"smart" multiwalled carbon nanotubes for tumor-targeted delivery of doxorubicin.* Bioconjugate chemistry, 2012. **23**(11): p. 2201-2213.

157. Chaudhuri, P., S. Soni, and S. Sengupta, *Single-walled carbon nanotube-conjugated chemotherapy exhibits increased therapeutic index in melanoma.* Nanotechnology, 2010. **21**(2): p. 025102.

158. Chen, Z., et al., *Adsorption behavior of epirubicin hydrochloride on carboxylated carbon nanotubes.* International Journal of Pharmaceutics, 2011. **405**(1–2): p. 153-161.

159. Taghdisi, S.M., et al., *Reversible Targeting and controlled release delivery of daunorubicin to cancer cells by aptamer-wrapped carbon nanotubes.* European Journal of Pharmaceutics and Biopharmaceutics, 2011. **77**(2): p. 200-206.

160. Chen, G., et al., *In vitro and in vivo studies of pirarubicin-loaded SWNT for the treatment of bladder cancer.* Brazilian Journal of Medical and Biological Research, 2012. **45**(8): p. 771-776.

161. Risi, G., et al., *In vitro study of multiwall carbon nanotubes (MWCNTs) with adsorbed mitoxantrone (MTO) as a drug delivery system to treat breast cancer.* RSC Advances, 2014. **4**(36): p. 18683-18693.

162. Feazell, R.P., et al., *Soluble single-walled carbon nanotubes as longboat delivery systems for platinum (IV) anticancer drug design.* Journal of the American Chemical Society, 2007. **129**(27): p. 8438-8439.

163. Bhirde, A.A., et al., *Targeted Killing of Cancer Cells in Vivo and in Vitro with EGF-Directed Carbon Nanotube-Based Drug Delivery.* ACS Nano, 2009. **3**(2): p. 307-316.

164. Li, J., et al., *Platinum(iv) prodrugs entrapped within multiwalled carbon nanotubes: Selective release by chemical reduction and hydrophobicity reversal.* Chemical Science, 2012. **3**(6): p. 2083-2087.

165. Dhar, S., et al., *Targeted Single-Wall Carbon Nanotube-Mediated Pt(IV) Prodrug Delivery Using Folate as a Homing Device.* Journal of the American Chemical Society, 2008. **130**(34): p. 11467-11476.

166. Samorì, C., et al., *Enhanced anticancer activity of multi-walled carbon nanotube–methotrexate conjugates using cleavable linkers.* Chemical Communications, 2010. **46**(9): p. 1494-1496.

167. Das, M., et al., *Augmented anticancer activity of a targeted, intracellularly activatable, theranostic nanomedicine based on fluorescent and radiolabeled, methotrexate-folic acid-multiwalled carbon nanotube conjugate.* Molecular pharmaceutics, 2013. **10**(7): p. 2543-2557.

168. Yang, D., et al., *Hydrophilic multi-walled carbon nanotubes decorated with magnetite nanoparticles as lymphatic targeted drug delivery vehicles.* Chemical Communications, 2009(29): p. 4447-4449.

169. Singh, R., et al., *Gemcitabine-loaded smart carbon nanotubes for effective targeting to cancer cells.* Journal of drug targeting, 2013. **21**(6): p. 581-592.

170. Dillon, E., M.S. Bhutani, and A.R. Barron, *Small molecule capture and release from PEI-functionalized single walled carbon nanotubes with endoscopic ultrasound.* Journal of Materials Chemistry B, 2013. **1**(10): p. 1461-1465.

171. Chen, J., et al., *Functionalized single-walled carbon nanotubes as rationally designed vehicles for tumor-targeted drug delivery.* Journal of the American Chemical Society, 2008. **130**(49): p. 16778-16785.

172. Arora, S., et al., *Translocation and Toxicity of Docetaxel Multi-Walled Carbon Nanotube Conjugates in Mammalian Breast Cancer Cells.* Journal of biomedical nanotechnology, 2014. **10**(12): p. 3601-3609.

173. Liu, Z., et al., *Drug delivery with carbon nanotubes for in vivo cancer treatment.* Cancer research, 2008. **68**(16): p. 6652-6660.

174. Lay, C.L., et al., *Delivery of paclitaxel by physically loading onto poly (ethylene glycol)(PEG)-graftcarbon nanotubes for potent cancer therapeutics.* Nanotechnology, 2010. **21**(6): p. 065101.

175. Wu, C.-H., et al., *Trojan-horse nanotube on-command intracellular drug delivery.* Nano letters, 2012. **12**(11): p. 5475-5480.

176. Cross, D. and J.K. Burmester, *Gene Therapy for Cancer Treatment: Past, Present and Future.* Clinical Medicine and Research, 2006. **4**(3): p. 218-227.

177. Weichselbaum, R.R. and D. Kufe, *Gene therapy of cancer.* The Lancet, 1997. **349, Supplement 2**: p. S10-S12.

178. Bates, K. and K. Kostarelos, *Carbon nanotubes as vectors for gene therapy: Past achievements, present challenges and future goals.* Advanced drug delivery reviews, 2013. **65**(15): p. 2023-2033.

179. Liu, Y., et al., *Polyethylenimine-grafted multiwalled carbon nanotubes for secure noncovalent immobilization and efficient delivery of DNA.* Angewandte Chemie, 2005. **117**(30): p. 4860-4863.

180. Paul, A., et al., *The attenuation of restenosis following arterial gene transfer using carbon nanotube coated stent incorporating TAT/DNAAng1+Vegf nanoparticles.* Biomaterials, 2012. **33**(30): p. 7655-7664.

181. Nunes, A., et al., *Hybrid Polymer-Grafted Multiwalled Carbon Nanotubes for In vitro Gene Delivery.* Small, 2010. **6**(20): p. 2281-2291.

182. Crinelli, R., et al., *Oxidized ultrashort nanotubes as carbon scaffolds for the construction of cell-penetrating NF-κB decoy molecules.* ACS nano, 2010. **4**(5): p. 2791-2803.

183. Jia, N., et al., *Intracellular delivery of quantum dots tagged antisense oligodeoxynucleotides by functionalized multiwalled carbon nanotubes.* Nano letters, 2007. **7**(10): p. 2976-2980.

184. Al-Jamal, K.T., et al., *Functional motor recovery from brain ischemic insult by carbon nanotube-mediated siRNA silencing.* Proceedings of the National Academy of Sciences, 2011. **108**(27): p. 10952-10957.

185. Wang, L., et al., *Synergistic anticancer effect of RNAi and photothermal therapy mediated by functionalized single-walled carbon nanotubes.* Biomaterials, 2013. **34**(1): p. 262-274.

186. Zhang, Z., et al., *Delivery of Telomerase Reverse Transcriptase Small Interfering RNA in Complex with Positively Charged Single-Walled Carbon Nanotubes Suppresses Tumor Growth.* Clinical Cancer Research, 2006. **12**(16): p. 4933-4939.

187. Mohammadi, M., et al., *Single-walled carbon nanotubes functionalized with aptamer and piperazine–polyethylenimine derivative for targeted siRNA delivery into breast cancer cells.* International Journal of Pharmaceutics, 2015. **485**(1–2): p. 50-60.

188. Dong, H., et al., *The use of polyethylenimine-grafted graphene nanoribbon for cellular delivery of locked nucleic acid modified molecular beacon for recognition of microRNA.* Biomaterials, 2011. **32**(15): p. 3875-3882.

189. Van den Bossche, J., et al., *Efficient receptor-independent intracellular translocation of aptamers mediated by conjugation to carbon nanotubes.* Chemical Communications, 2010. **46**(39): p. 7379-7381.

190. Zhang, H., et al., *In vitro and in vivo evaluation of antitumor drug-loaded aptamer targeted single-walled carbon nanotubes system.* Current pharmaceutical biotechnology, 2013. **14**(13): p. 1105-1117.

191. Bartholomeusz, G., et al., *In vivo therapeutic silencing of hypoxia-inducible factor 1 alpha (HIF-1α) using single-walled carbon nanotubes noncovalently coated with siRNA.* Nano Research, 2009. **2**(4): p. 279-291.

192. Albertorio, F., et al., *Base dependent DNA–carbon nanotube interactions: activation enthalpies and assembly–disassembly control.* Nanotechnology, 2009. **20**(39): p. 395101.

193. Johnson, R.R., A.C. Johnson, and M.L. Klein, *Probing the structure of DNA-carbon nanotube hybrids with molecular dynamics.* Nano Letters, 2008. **8**(1): p. 69-75.

194. Zheng, M., et al., *DNA-assisted dispersion and separation of carbon nanotubes.* Nat Mater, 2003. **2**(5): p. 338-342.

195. Zhang, X., et al., *Targeted delivery and controlled release of doxorubicin to cancer cells using modified single wall carbon nanotubes.* Biomaterials, 2009. **30**(30): p. 6041-6047.

196. Huang, H., et al., *A new family of folate-decorated and carbon nanotube-mediated drug delivery system: Synthesis and drug delivery response.* Advanced Drug Delivery Reviews, 2011. **63**(14–15): p. 1332-1339.

197. Li, R., et al., *Folate and iron difunctionalized multiwall carbon nanotubes as dual-targeted drug nanocarrier to cancer cells.* Carbon, 2011. **49**(5): p. 1797-1805.

198. Chen, M.-L., et al., *Quantum dots conjugated with Fe3O4-filled carbon nanotubes for cancer-targeted imaging and magnetically guided drug delivery.* Langmuir, 2012. **28**(47): p. 16469-16476.

199. Ji, Z., et al., *Targeted therapy of SMMC-7721 liver cancer in vitro and in vivo with carbon nanotubes based drug delivery system.* Journal of Colloid and Interface Science, 2012. **365**(1): p. 143-149.

200. Sobhani, Z., et al., *Increased paclitaxel cytotoxicity against cancer cell lines using a novel functionalized carbon nanotube.* Int J Nanomedicine, 2011. **6**: p. 705-719.

201. Mashat, A., et al., *Zippered release from polymer-gated carbon nanotubes.* Journal of Materials Chemistry, 2012. **22**(23): p. 11503-11508.

202. Luo, X., et al., *Carbon nanotube nanoreservior for controlled release of anti-inflammatory dexamethasone.* Biomaterials, 2011. **32**(26): p. 6316-6323.

203. Spizzirri, U.G., et al., *Spherical gelatin/CNTs hybrid microgels as electro-responsive drug delivery systems.* International journal of pharmaceutics, 2013. **448**(1): p. 115-122.

204. Im, J.S., B.C. Bai, and Y.-S. Lee, *The effect of carbon nanotubes on drug delivery in an electro-sensitive transdermal drug delivery system.* Biomaterials, 2010. **31**(6): p. 1414-1419.

205. Fujigaya, T., T. Morimoto, and N. Nakashima, *Isolated single-walled carbon nanotubes in a gel as a molecular reservoir and its application to controlled drug release triggered by near-IR laser irradiation.* Soft Matter, 2011. **7**(6): p. 2647-2652.

206. Guven, A., et al., *Cisplatin@ US-tube carbon nanocapsules for enhanced chemotherapeutic delivery.* Biomaterials, 2012. **33**(5): p. 1455-1461.

207. Raoof, M., et al., *Remotely triggered cisplatin release from carbon nanocapsules by radiofrequency fields.* Biomaterials, 2013. **34**(7): p. 1862-1869.

208. Xiao, Y., et al., *Anti-HER2 IgY antibody-functionalized single-walled carbon nanotubes for detection and selective destruction of breast cancer cells.* Bmc Cancer, 2009. **9**(1): p. 351.

209. McDevitt, M.R., et al., *Tumor targeting with antibody-functionalized, radiolabeled carbon nanotubes.* Journal of Nuclear Medicine, 2007. **48**(7): p. 1180-1189.

210. Heister, E., et al., *Triple functionalisation of single-walled carbon nanotubes with doxorubicin, a monoclonal antibody, and a fluorescent marker for targeted cancer therapy.* Carbon, 2009. **47**(9): p. 2152-2160.

211. Ren, J., et al., *The targeted delivery of anticancer drugs to brain glioma by PEGylated oxidized multi-walled carbon nanotubes modified with angiopep-2.* Biomaterials, 2012. **33**(11): p. 3324-3333.

212. Meng, L., et al., *Single walled carbon nanotubes as drug delivery vehicles: targeting doxorubicin to tumors.* Biomaterials, 2012. **33**(6): p. 1689-1698.

213. Pruthi, J., N.K. Mehra, and N.K. Jain, *Macrophages targeting of amphotericin B through mannosylated multiwalled carbon nanotubes.* Journal of drug targeting, 2012. **20**(7): p. 593-604.

214. Lodhi, N., N.K. Mehra, and N.K. Jain, *Development and characterization of dexamethasone mesylate anchored on multi walled carbon nanotubes.* Journal of drug targeting, 2013. **21**(1): p. 67-76.

215. Levi-Polyachenko, N.H., et al., *Rapid Photothermal Intracellular Drug Delivery Using Multiwalled Carbon Nanotubes.* Molecular Pharmaceutics, 2009. **6**(4): p. 1092-1099.

216. Kim, P., et al., *Electronic Density of States of Atomically Resolved Single-Walled Carbon Nanotubes: Van Hove Singularities and End States.* Physical Review Letters, 1999. **82**(6): p. 1225-1228.

217. Berber, S., Y.-K. Kwon, and D. Tománek, *Unusually High Thermal Conductivity of Carbon Nanotubes.* Physical Review Letters, 2000. **84**(20): p. 4613-4616.

218. Torti, S.V., et al., *Thermal ablation therapeutics based on CNx multi-walled nanotubes.* International journal of nanomedicine, 2007. **2**(4): p. 707.

219. Bhayani, K., J. Rajwade, and K. Paknikar, *Radio frequency induced hyperthermia mediated by dextran stabilized LSMO nanoparticles: in vitro evaluation of heat shock protein response.* Nanotechnology, 2013. **24**(1): p. 015102.

220. Ito, A., H. Honda, and T. Kobayashi, *Cancer immunotherapy based on intracellular hyperthermia using magnetite nanoparticles: a novel concept of "heat-controlled necrosis" with heat shock protein expression.* Cancer Immunology, Immunotherapy, 2006. **55**(3): p. 320-328.

221. Ghosh, S., et al., *Increased heating efficiency and selective thermal ablation of malignant tissue with DNA-encased multiwalled carbon nanotubes.* ACS nano, 2009. **3**(9): p. 2667-2673.

222. Burke, A., et al., *Long-term survival following a single treatment of kidney tumors with multiwalled carbon nanotubes and near-infrared radiation.* Proceedings of the National Academy of Sciences, 2009. **106**(31): p. 12897-12902.

223. Wang, C.-H., et al., *Photothermolysis of glioblastoma stem-like cells targeted by carbon nanotubes conjugated with CD133 monoclonal antibody.* Nanomedicine: nanotechnology, biology and medicine, 2011. **7**(1): p. 69-79.

224. Zhou, F., et al., *Mitochondria-targeting single-walled carbon nanotubes for cancer photothermal therapy.* Small, 2011. **7**(19): p. 2727-2735.

225. Zhou, F., et al., *New Insights of Transmembranal Mechanism and Subcellular Localization of Noncovalently Modified Single-Walled Carbon Nanotubes.* Nano Letters, 2010. **10**(5): p. 1677-1681.

226. Robinson, J.T., et al., *High performance in vivo near-IR (> 1 μm) imaging and photothermal cancer therapy with carbon nanotubes.* Nano research, 2010. **3**(11): p. 779-793.

227. Antaris, A.L., et al., *Ultra-Low Doses of Chirality Sorted (6,5) Carbon Nanotubes for Simultaneous Tumor Imaging and Photothermal Therapy.* ACS Nano, 2013. **7**(4): p. 3644-3652.

228. Liu, X., et al., *Optimization of surface chemistry on single-walled carbon nanotubes for in vivo photothermal ablation of tumors.* Biomaterials, 2011. **32**(1): p. 144-151.

229. Gannon, C.J., et al., *Carbon nanotube-enhanced thermal destruction of cancer cells in a noninvasive radiofrequency field.* Cancer, 2007. **110**(12): p. 2654-2665.

230. Kang, B., et al., *Cancer-cell targeting and photoacoustic therapy using carbon nanotubes as "Bomb" agents.* Small, 2009. **5**(11): p. 1292-1301.

231. Beveridge, A.C., et al., *Photoacoustic shock generation in carbon suspensions.* Applied Physics Letters, 1999. **75**(26): p. 4204-4206.

232. Kang, B., et al., *Explosion of single-walled carbon nanotubes in suspension induced by a large photoacoustic effect.* Carbon, 2008. **46**(6): p. 978-981.

233. Picou, L., et al., *Spatio-temporal thermal kinetics of in situ MWCNT heating in biological tissues under NIR laser irradiation.* Nanotechnology, 2010. **21**(43): p. 435101.

234. Huang, N., et al., *Single-wall carbon nanotubes assisted photothermal cancer therapy: Animal study with a murine model of squamous cell carcinoma.* Lasers in Surgery and Medicine, 2010. **42**(9): p. 798-808.

235. Xie, B., et al., *Heat localization for targeted tumor treatment with nanoscale near-infrared radiation absorbers.* Physics in medicine and biology, 2012. **57**(18): p. 5765.

236. Singh, R. and S.V. Torti, *Carbon nanotubes in hyperthermia therapy.* Advanced drug delivery reviews, 2013. **65**(15): p. 2045-2060.

237. Dobrovolskaia, M.A. and S.E. McNeil, *Immunological properties of engineered nanomaterials.* Nat Nano, 2007. **2**(8): p. 469-478.

238. van Vlerken, L.E., T.K. Vyas, and M.M. Amiji, *Poly (ethylene glycol)-modified nanocarriers for tumor-targeted and intracellular delivery.* Pharmaceutical research, 2007. **24**(8): p. 1405-1414.

239. Gref, R., et al., *The controlled intravenous delivery of drugs using PEG-coated sterically stabilized nanospheres.* Advanced drug delivery reviews, 2012. **64**: p. 316-326.

240. Jeon, S.I., et al., *Protein—surface interactions in the presence of polyethylene oxide.* Journal of Colloid and Interface Science, 1991. **142**(1): p. 149-158.

241. Jeon, S. and J. Andrade, *Protein—Surface interactions in the presence of polyethylene oxide: II. Effect of protein size.* Journal of Colloid and Interface Science, 1991. **142**(1): p. 159-166.

242. Guo, Y. and S.W. Hui, *Poly(ethylene glycol)-conjugated surfactants promote or inhibit aggregation of phospholipids.* Biochimica et Biophysica Acta (BBA) - Biomembranes, 1997. **1323**(2): p. 185-194.

243. Yamaoka, T., Y. Tabata, and Y. Ikada, *Distribution and tissue uptake of poly (ethylene glycol) with different molecular weights after intravenous administration to mice.* Journal of pharmaceutical sciences, 1994. **83**(4): p. 601-606.

244. Yang, S.-T., et al., *Covalently PEGylated Carbon Nanotubes with Stealth Character In Vivo.* Small, 2008. **4**(7): p. 940-944.

245. Robinson, J.T., et al., *In Vivo Fluorescence Imaging in the Second Near-Infrared Window with Long Circulating Carbon Nanotubes Capable of Ultrahigh Tumor Uptake.* Journal of the American Chemical Society, 2012. **134**(25): p. 10664-10669.

246. Sund, J., et al., *Proteomic characterization of engineered nanomaterial–protein interactions in relation to surface reactivity.* Acs Nano, 2011. **5**(6): p. 4300-4309.

247. Moghimi, S.M. and J. Szebeni, *Stealth liposomes and long circulating nanoparticles: critical issues in pharmacokinetics, opsonization and protein-binding properties.* Progress in lipid research, 2003. **42**(6): p. 463-478.

248. Li, X., *Size effects of carbon nanotubes and graphene on cellular uptake.* EPL (Europhysics Letters), 2012. **100**(4): p. 46002.

249. Champion, J.A. and S. Mitragotri, *Role of target geometry in phagocytosis.* Proceedings of the National Academy of Sciences of the United States of America, 2006. **103**(13): p. 4930-4934.

250. Shi, X., et al., *Cell entry of one-dimensional nanomaterials occurs by tip recognition and rotation.* Nature nanotechnology, 2011. **6**(11): p. 714-719.

251. Fleischer, C.C. and C.K. Payne, *Nanoparticle–cell interactions: molecular structure of the protein corona and cellular outcomes.* Accounts of chemical research, 2014. **47**(8): p. 2651-2659.

252. Zhang, X., et al., *Tuning the cellular uptake and cytotoxicity of carbon nanotubes by surface hydroxylation.* Journal of Nanoparticle Research, 2011. **13**(12): p. 6941-6952.

253. Oberdörster, G., E. Oberdörster, and J. Oberdörster, *Nanotoxicology: an emerging discipline evolving from studies of ultrafine particles.* Environmental health perspectives, 2005: p. 823-839.

254. Haynes, C., *The emerging field of nanotoxicology.* Analytical and Bioanalytical Chemistry, 2010. **398**(2): p. 587-588.

255. Oberdörster, G., *Safety assessment for nanotechnology and nanomedicine: concepts of nanotoxicology.* Journal of internal medicine, 2010. **267**(1): p. 89-105.

256. Yanamala, N., V.E. Kagan, and A.A. Shvedova, *Molecular modeling in structural nano-toxicology: Interactions of nano-particles with nano-machinery of cells.* Advanced Drug Delivery Reviews, 2013. **65**(15): p. 2070-2077.

257. Kane, A., J. Macdonald, and P. Moalli. *Acute injury and regeneration of mesothelial cells produced by crocidolite asbestos fibers*. in *American Review Of Respiratory Disease*. 1986. AMER LUNG ASSOC 1740 BROADWAY, NEW YORK, NY 10019.

258. Boutin, C., et al., *Black spots concentrate oncogenic asbestos fibers in the parietal pleura. Thoracoscopic and mineralogic study.* American journal of respiratory and critical care medicine, 1996. **153**(1): p. 444-449.

259. Donaldson, K., et al., *Asbestos, carbon nanotubes and the pleural mesothelium: a review of the hypothesis regarding the role of long fibre retention in the parietal pleura, inflammation and mesothelioma.* Part Fibre Toxicol, 2010. **7**(5): p. 5.

260. Sato, Y., et al., *Influence of length on cytotoxicity of multi-walled carbon nanotubes against human acute monocytic leukemia cell line THP-1 in vitro and subcutaneous tissue of rats in vivo.* Molecular BioSystems, 2005. **1**(2): p. 176-182.

261. Poland, C.A., et al., *Carbon nanotubes introduced into the abdominal cavity of mice show asbestos-like pathogenicity in a pilot study.* Nature nanotechnology, 2008. **3**(7): p. 423-428.

262. Yamashita, K., et al., *Carbon Nanotubes Elicit DNA Damage and Inflammatory Response Relative to Their Size and Shape.* Inflammation, 2010. **33**(4): p. 276-280.

263. Palomäki, J., et al., *Long, Needle-like Carbon Nanotubes and Asbestos Activate the NLRP3 Inflammasome through a Similar Mechanism.* ACS Nano, 2011. **5**(9): p. 6861-6870.

264. Murray, A.R., et al., *Factoring-in agglomeration of carbon nanotubes and nanofibers for better prediction of their toxicity versus asbestos.* Part Fibre Toxicol, 2012. **9**(10): p. 1-19.

265. Belyanskaya, L., et al., *Effects of carbon nanotubes on primary neurons and glial cells.* Neurotoxicology, 2009. **30**(4): p. 702-711.

266. Wick, P., et al., *The degree and kind of agglomeration affect carbon nanotube cytotoxicity.* Toxicology Letters, 2007. **168**(2): p. 121-131.

267. Jia, G., et al., *Cytotoxicity of carbon nanomaterials: single-wall nanotube, multi-wall nanotube, and fullerene.* Environmental science & technology, 2005. **39**(5): p. 1378-1383.

268. Muller, J., et al., *Absence of carcinogenic response to multi-wall carbon nanotubes in a 2-year bioassay in the peritoneal cavity of the rat.* Toxicological Sciences, 2009: p. kfp100.

269. Nagai, H., et al., *Diameter and rigidity of multiwalled carbon nanotubes are critical factors in mesothelial injury and carcinogenesis.* Proceedings of the National Academy of Sciences, 2011. **108**(49): p. E1330-E1338.

270. Hoyos-Palacio, L., et al. *Catalytic effect of Fe, Ni, Co and Mo on the CNTs production*. in *IOP Conference Series: Materials Science and Engineering*. 2014. IOP Publishing.

271. Pumera, M., *Carbon nanotubes contain residual metal catalyst nanoparticles even after washing with nitric acid at elevated temperature because these metal nanoparticles are sheathed by several graphene sheets.* Langmuir, 2007. **23**(11): p. 6453-6458.

272. Pulskamp, K., S. Diabaté, and H.F. Krug, *Carbon nanotubes show no sign of acute toxicity but induce intracellular reactive oxygen species in dependence on contaminants.* Toxicology Letters, 2007. **168**(1): p. 58-74.

273. Kagan, V.E., et al., *Direct and indirect effects of single walled carbon nanotubes on RAW 264.7 macrophages: Role of iron.* Toxicology Letters, 2006. **165**(1): p. 88-100.

274. Guo, L., et al., *Iron bioavailability and redox activity in diverse carbon nanotube samples.* Chemistry of materials, 2007. **19**(14): p. 3472-3478.

275. Allen, B.L., et al., *Biodegradation of single-walled carbon nanotubes through enzymatic catalysis.* Nano Letters, 2008. **8**(11): p. 3899-3903.

276. Veitch, N.C., *Horseradish peroxidase: a modern view of a classic enzyme.* Phytochemistry, 2004. **65**(3): p. 249-259.

277. Allen, B.L., et al., *Mechanistic investigations of horseradish peroxidase-catalyzed degradation of single-walled carbon nanotubes.* Journal of the American Chemical Society, 2009. **131**(47): p. 17194-17205.

278. Russier, J., et al., *Oxidative biodegradation of single- and multi-walled carbon nanotubes.* Nanoscale, 2011. **3**(3): p. 893-896.

279. Kagan, V.E., et al., *Carbon nanotubes degraded by neutrophil myeloperoxidase induce less pulmonary inflammation.* Nat Nano, 2010. **5**(5): p. 354-359.

280. Metzler, Kathleen D., et al., *A Myeloperoxidase-Containing Complex Regulates Neutrophil Elastase Release and Actin Dynamics during NETosis.* Cell Reports, 2014. **8**(3): p. 883-896.

281. Andón, F.T., et al., *Biodegradation of Single-Walled Carbon Nanotubes by Eosinophil Peroxidase.* Small, 2013. **9**(16): p. 2721-2729.

282. Neves, V., et al., *Uptake and release of double-walled carbon nanotubes by mammalian cells.* Advanced Functional Materials, 2010. **20**(19): p. 3272-3279.

283. Shvedova, A.A., et al., *Impaired clearance and enhanced pulmonary inflammatory/fibrotic response to carbon nanotubes in myeloperoxidase-deficient mice.* PLoS one, 2012. **7**(3): p. e30923.

284. Nunes, A., et al., *In vivo degradation of functionalized carbon nanotubes after stereotactic administration in the brain cortex.* Nanomedicine, 2012. **7**(10): p. 1485-1494.

285. Adkins, J.N., et al., *Toward a Human Blood Serum Proteome: Analysis By Multidimensional Separation Coupled With Mass Spectrometry.* Molecular & Cellular Proteomics, 2002. **1**(12): p. 947-955.

286. Anderson, L. and N.G. Anderson, *High resolution two-dimensional electrophoresis of human plasma proteins.* Proceedings of the National Academy of Sciences of the United States of America, 1977. **74**(12): p. 5421-5425.

287. Lacerda, S.H.D.P., et al., *Interaction of Gold Nanoparticles with Common Human Blood Proteins.* ACS Nano, 2010. **4**(1): p. 365-379.

288. Cedervall, T., et al., *Understanding the nanoparticle–protein corona using methods to quantify exchange rates and affinities of proteins for nanoparticles.* Proceedings of the National Academy of Sciences, 2007. **104**(7): p. 2050-2055.

289. Walkey, C.D. and W.C. Chan, *Understanding and controlling the interaction of nanomaterials with proteins in a physiological environment.* Chemical Society Reviews, 2012. **41**(7): p. 2780-2799.

290. Chakraborty, S., et al., *Contrasting Effect of Gold Nanoparticles and Nanorods with Different Surface Modifications on the Structure and Activity of Bovine Serum Albumin.* Langmuir, 2011. **27**(12): p. 7722-7731.

291. Norde, W. and C.E. Giacomelli, *BSA structural changes during homomolecular exchange between the adsorbed and the dissolved states.* Journal of Biotechnology, 2000. **79**(3): p. 259-268.

292. Shang, W., et al., *Cytochrome c on silica nanoparticles: influence of nanoparticle size on protein structure, stability, and activity.* Small, 2009. **5**(4): p. 470-476.

293. Vroman, L., et al., *Interaction of high molecular weight kininogen, factor XII, and fibrinogen.* Blood, 1980. **55**(1): p. 156-9.

294. Monopoli, M.P., et al., *Physical−Chemical Aspects of Protein Corona: Relevance to in Vitro and in Vivo Biological Impacts of Nanoparticles.* Journal of the American Chemical Society, 2011. **133**(8): p. 2525-2534.

295. Shannahan, J.H., et al., *Comparison of Nanotube–Protein Corona Composition in Cell Culture Media.* Small, 2013. **9**(12): p. 2171-2181.

296. Nel, A.E., et al., *Understanding biophysicochemical interactions at the nano–bio interface.* Nature materials, 2009. **8**(7): p. 543-557.

297. Lundqvist, M., et al., *The Evolution of the Protein Corona around Nanoparticles: A Test Study.* ACS Nano, 2011. **5**(9): p. 7503-7509.

298. Ge, C., et al., *Binding of blood proteins to carbon nanotubes reduces cytotoxicity.* Proceedings of the National Academy of Sciences, 2011. **108**(41): p. 16968-16973.

299. Sanhai, W.R., et al., *Seven challenges for nanomedicine.* Nat Nano, 2008. **3**(5): p. 242-244.

300. Hirano, A., et al., *Arginine Side Chains as a Dispersant for Individual Single-Wall Carbon Nanotubes.* Chemistry-A European Journal, 2014. **20**(17): p. 4922-4930.

301. Mikoz.xl, et al., *Recent developments in the carbodiimide chemistry.* Tetrahedron, 1981. **37**(2): p. 233-284.

302. Nozaki, S., *Effects of amounts of additives on peptide coupling mediated by a water-soluble carbodiimide in alcohols.* The Journal of peptide research, 1999. **54**(2): p. 162-167.

303. Griffiths, P.R. and J.A. De Haseth, *Fourier transform infrared spectrometry*. Vol. 171. 2007: John Wiley & Sons.

304. Weckhuysen, B.M., *Ultraviolet-visible spectroscopy.* In situ Spectroscopy of Catalysts, American Scientific Publishers, Stevenson Ranch, 2004: p. 255-270.

305. Hellman, L.M. and M.G. Fried, *Electrophoretic mobility shift assay (EMSA) for detecting protein–nucleic acid interactions.* Nature protocols, 2007. **2**(8): p. 1849-1861.

306. Swartz, M., *HPLC detectors: a brief review.* Journal of Liquid Chromatography & Related Technologies, 2010. **33**(9-12): p. 1130-1150.

307. Binnig, G., C.F. Quate, and C. Gerber, *Atomic force microscope*. Physical review letters, 1986. **56**(9): p. 930.

308. Hollander, J.M. and W.L. Jolly, *X-ray photoelectron spectroscopy.* Accounts of chemical research, 1970. **3**(6): p. 193-200.

309. Wörle-Knirsch, J.M., K. Pulskamp, and H.F. Krug, *Oops They Did It Again! Carbon Nanotubes Hoax Scientists in Viability Assays.* Nano Letters, 2006. **6**(6): p. 1261-1268.

310. Bottini, M., et al., *Full-Length Single-Walled Carbon Nanotubes Decorated with Streptavidin-Conjugated Quantum Dots as Multivalent Intracellular Fluorescent Nanoprobes.* Biomacromolecules, 2006. **7**(8): p. 2259-2263.

311. Zrazhevskiy, P., M. Sena, and X. Gao, *Designing multifunctional quantum dots for bioimaging, detection, and drug delivery*. Chemical Society Reviews, 2010. **39**(11): p. 4326-4354.

312. Park, C.-W., et al., *Advances in microscopy and complementary imaging techniques to assess the fate of drugs ex vivo in respiratory drug delivery: An invited paper.* Advanced Drug Delivery Reviews, 2012. **64**(4): p. 344-356.

313. Zhu, Z., et al., *Single-walled carbon nanotube as an effective quencher.* Analytical and Bioanalytical Chemistry, 2010. **396**(1): p. 73-83.

314. Derfus, A.M., W.C.W. Chan, and S.N. Bhatia, *Probing the Cytotoxicity of Semiconductor Quantum Dots.* Nano Letters, 2004. **4**(1): p. 11-18.

315. Kostarelos, K., A. Bianco, and M. Prato, *Promises, facts and challenges for carbon nanotubes in imaging and therapeutics.* Nat Nano, 2009. **4**(10): p. 627-633.

316. Sadikot, R.T. and T.S. Blackwell, *Bioluminescence imaging.* Proceedings of the American Thoracic Society, 2005. **2**(6): p. 537-540.

317. Paddison, P.J., A.A. Caudy, and G.J. Hannon, *Stable suppression of gene expression by RNAi in mammalian cells.* Proceedings of the National Academy of Sciences, 2002. **99**(3): p. 1443-1448.

318. Weissleder, R., *A clearer vision for in vivo imaging.* Nature biotechnology, 2001. **19**(4): p. 316-316.

319. Cherukuri, P., et al., *Near-Infrared Fluorescence Microscopy of Single-Walled Carbon Nanotubes in Phagocytic Cells.* Journal of the American Chemical Society, 2004. **126**(48): p. 15638-15639.

320. White, E.H., et al., *The chemi- and bioluminescence of firefly luciferin: An efficient chemical production of electronically excited states.* Bioorganic Chemistry, 1971. **1**(1): p. 92-122.

321. DeLuca, M. and W.D. McElroy, *Kinetics of the firefly luciferase catalyzed reactions.* Biochemistry, 1974. **13**(5): p. 921-925.

322. Tu, S.-C., C.-W. Wu, and J.W. Hastings, *Structural studies on bacterial luciferase using energy transfer and emission anisotropy.* Biochemistry, 1978. **17**(6): p. 987-993.

323. Nebert, D.W. and T.P. Dalton, *The role of cytochrome P450 enzymes in endogenous signalling pathways and environmental carcinogenesis.* Nature Reviews Cancer, 2006. **6**(12): p. 947-960.

324. McGinnity, D.F., et al., *Rapid characterization of the major drug-metabolizing human hepatic cytochrome P-450 enzymes expressed in Escherichia coli.* Drug metabolism and disposition, 1999. **27**(9): p. 1017-1023.

325. Xia, X.-R., N.A. Monteiro-Riviere, and J.E. Riviere, *An index for characterization of nanomaterials in biological systems.* Nature nanotechnology, 2010. **5**(9): p. 671-675.

326. Tenzer, S., et al., *Rapid formation of plasma protein corona critically affects nanoparticle pathophysiology.* Nature nanotechnology, 2013. **8**(10): p. 772-781.

327. Dutta, D., et al., *Adsorbed Proteins Influence the Biological Activity and Molecular Targeting of Nanomaterials.* Toxicological Sciences, 2007. **100**(1): p. 303-315.

328. Gora, A., J. Brezovsky, and J. Damborsky, *Gates of Enzymes.* Chemical Reviews, 2013. **113**(8): p. 5871-5923.

329. Fishelovitch, D., et al., *Theoretical Characterization of Substrate Access/Exit Channels in the Human Cytochrome P450 3A4 Enzyme: Involvement of Phenylalanine Residues in the Gating Mechanism.* The Journal of Physical Chemistry B, 2009. **113**(39): p. 13018-13025.

330. Dowers, T.S., et al., *An analysis of the regioselectivity of aromatic hydroxylation and N-oxygenation by cytochrome P450 enzymes.* Drug metabolism and disposition, 2004. **32**(3): p. 328-332.

331. Hollmann, F., K. Hofstetter, and A. Schmid, *Non-enzymatic regeneration of nicotinamide and flavin cofactors for monooxygenase catalysis.* TRENDS in Biotechnology, 2006. **24**(4): p. 163-171.

332. Kerr, B.M., et al., *Human liver carbamazepine metabolism: role of CYP3A4 and CYP2C8 in 10, 11-epoxide formation.* Biochemical pharmacology, 1994. **47**(11): p. 1969-1979.

333. Meunier, B., S.P. De Visser, and S. Shaik, *Mechanism of oxidation reactions catalyzed by cytochrome P450 enzymes.* Chemical reviews, 2004. **104**(9): p. 3947-3980.

334. Dresselhaus, M.S., et al., *Raman spectroscopy of carbon nanotubes.* Physics reports, 2005. **409**(2): p. 47-99.

335. Hrycay, E.G. and S.M. Bandiera, *The monooxygenase, peroxidase, and peroxygenase properties of cytochrome P450.* Archives of biochemistry and biophysics, 2012. **522**(2): p. 71-89.

336. Aldag, C., et al., *Probing the role of the proximal heme ligand in cytochrome P450cam by recombinant incorporation of selenocysteine.* Proceedings of the National Academy of Sciences, 2009. **106**(14): p. 5481-5486.

337. de Montellano, P.R.O., *Cytochrome P450: Structure, Mechanism, and Biochemistry*. 1995: Springer.

338. Rittle, J. and M.T. Green, *Cytochrome P450 compound I: capture, characterization, and CH bond activation kinetics.* Science, 2010. **330**(6006): p. 933-937.

339. Sevrioukova, I.F., et al., *Structure of a cytochrome P450–redox partner electron-transfer complex.* Proceedings of the National Academy of Sciences, 1999. **96**(5): p. 1863-1868.

340. Sargent, L.M., et al., *Promotion of lung adenocarcinoma following inhalation exposure to multi-walled carbon nanotubes.* Part Fibre Toxicol, 2014. **11**(3): p. b114.

341. Shvedova, A.A., et al., *Long-term effects of carbon containing engineered nanomaterials and asbestos in the lung: one year postexposure comparisons.* American Journal of Physiology-Lung Cellular and Molecular Physiology, 2014. **306**(2): p. L170-L182.

342. Kolosnjaj-Tabi, J., et al., *Anthropogenic Carbon Nanotubes Found in the Airways of Parisian Children.* EBioMedicine.

343. Murr, L. and P. Guerrero, *Carbon nanotubes in wood soot.* Atmospheric Science Letters, 2006. **7**(4): p. 93-95.

344. Kumar Sonkar, S., S. Tripathi, and S. Sarkar, *Activation of aerial oxygen to superoxide radical by carbon nano tube of aerosol trapped in indoor spider web.* Current Science, 2009. **97**(8): p. 1227-1230.

345. Davies, M.J., et al., *Mammalian heme peroxidases: from molecular mechanisms to health implications.* Antioxidants & redox signaling, 2008. **10**(7): p. 1199-1234.

346. Shvedova, A.A., et al., *Sequential exposure to carbon nanotubes and bacteria enhances pulmonary inflammation and infectivity.* American journal of respiratory cell and molecular biology, 2008. **38**(5): p. 579-590.

347. Vlasova, I.I., et al., *PEGylated single-walled carbon nanotubes activate neutrophils to increase production of hypochlorous acid, the oxidant capable of degrading nanotubes.* Toxicology and applied pharmacology, 2012. **264**(1): p. 131-142.

348. Farrera, C., et al., *Extracellular entrapment and degradation of single-walled carbon nanotubes.* Nanoscale, 2014. **6**(12): p. 6974-6983.

349. Brinkmann, V., et al., *Neutrophil extracellular traps kill bacteria.* science, 2004. **303**(5663): p. 1532-1535.